ADDIS ABABA UNIVERSITY

ETHIOPIA INSTITUTE OF WATER RESOURCES

MSc. Thesis On

Application of a Satellite Based Rainfall-Runoff Estimation: in Upper Omo-Gibe Basin to simulate the extreme flood event at Omorate.

***By*:**

Samuel Bekele

Feb, 2020

Addis Ababa, Ethiopia

Application of a Satellite Based Rainfall-Runoff Estimation: in Upper Omo-Gibe Basin to simulate the extreme flood event at Omorate.

BY

Samuel Bekele

This Thesis work submitted to Addis Ababa University, Ethiopian Institute of Water Resources for partial fulfillment of the required degree of Master of Science in Water Resources Engineering and Management specialization in surface water.

DECLARATION

I, Samuel Bekele, do hereby declare this thesis is my own original work and that it has not been presented and will not be presented to any University for the similar or any other degree award and also all sources of material used for this thesis work have been duly acknowledged.

Name: SAMUEL BEKELE

Signature---------- **Date**----------

Approval Page

This thesis proposal entitled with ***Application of a Satellite Based Rainfall-Runoff Estimation: in Upper Omo-Gibe Basin to simulate the extreme flood event at Omorate.*** has been approved by the Main adviser and board of examiners in partial fulfilment of the requirements for the degree of Master of Science in Water Resource Engineering and Management in Ethiopian Institute of Water Resource at Addis Ababa University.

Submitted by:

Samuel Bekele

APPROVED BY BOARD OF EXAMINERS

APPROVED BY

Dr. Elias Tedla (Main Advisor)	**signature** _____	**Date** _____
Dr. Tekaligne Ayele (Internal Examiner)	**signature** _____	**Date** _____
Dr. Adane Abebe (Internal Examiner)	**signature** _____	**Date** _____
Mr. Amanuel Abate (Chairman)	**signature** _____	**Date** _____

ACKNOWLEDGEMENTS

Above all, I thank Jesus Christ for his grace and mercy upon me during all my works and in all my life and your grace definitely did it.

Very special thanks to my advisor Dr. Elias Tedla for giving me valuable guidance, support and encouragement throughout my research work.

I am so pleased Mr. Yonnas Girma (PhD) for his immediate response to give an encouraging comment and also his understanding to answer when I faced difficulty.

I would like to express my deepest thanks for Dr.Azage Gebreyohannes Assistant Professor in transboundary Water Management and Education Coordinator Ethiopian Institute of Water Resources for his guidance, support and his willingness in many my questions and his quick answers, including moral support.

I wish to extend my appreciation to all staff members of DHI group in Denmark especially to for their cooperation in all aspect and directional comments and give me full internet license software in the journey of this research.

I would like to thank the National Meteorological Agency of Ethiopia (NMA) and Ethiopian Water, Irrigation and Electricity Ministry for their help by providing the necessary data free of charge.

I am so satisfied to my classmates in all our harmonization from start to end of this MSc Program in Ethiopian Institute of Water Resources at Addis Ababa University.

At the last, but not least, I am very proud of my family for their love, support and they are truly a special gift from God for me; and I don't forget my close friends support and encouragements.

Table of Contents

List of Abbreviations

a.m.s.l	Above mean sea level
AMSR-E	Advanced Microwave Scanning Radiometer-Earth Observing System
AMSU-B	Advanced Microwave Sounding Unit-B
AR4	Fourth Assessment report
AR5	Fifth Assessment Report
Arc GIS	Software for Geographic Information Systems
BBC	British Broadcasting Corporation
CAMS	Climate Assessment and Monitoring System
CERES	Cloud and Earth Radiant Energy Sensor
CMIP5	Coupled Model Inter comparison Project phase five
CORDEX	Coordinated Regional Climate Downscaling Experiment
CPC	Climate Prediction Centre
DEM	Digital Elevation Model
DHI	Danish Hydraulic Institute
DMSP	Defense Meteorological Satellite Program
EBC	Ethiopian Broadcasting Corporation
GOES	Geostationary Operational Environmental Satellite
GPCC	Global Precipitation Climatological Centre
GPI	Precipitation Index
GPM	Global Precipitation Measurement
JAXA	National Space Development Agency of Japan
LEO	Lightning Earth orbit
LIS	Lightning imaging sensor
MIKE 11	Professional software package for 1D simulation of flows in rivers and channels.
MIKE GIS	MIKE software with an extension to Arc GIS
MIKE View	viewing software used to view MIKE 11 model results
MIKE Zero	MIKE Zero is a software informer developed by DHI, which gives access to DHI's modelling system.
MoWIE	Ministry of Water, Irrigation and Electricity
NASA	National Aeronautics Space Agency

NMA	National Metrology Agency
NOAA	National Oceanic and Atmospheric Administration
PERSIANN	Precipitation Estimation from Remotely Sensed Imagery Using Artificial Neural Networks
PR	Precipitation Radar
RMSE	Root Mean Square Error
SNNPR	Southern Nations, Nationalities and People Region
SREs	Satellite Rainfall Estimates
SSM/I	Special Sensor Microwave Imager
SWOT	Surface Water and Ocean Topography
TMI	TRMM Microwave Imager
TRMM	Tropical Rainfall Measuring Mission
UNOCHA	United Nation Office for the Coordination of Humanitarian Affaires
USGS	United States Geological Survey
UTM	Universal Transverse Mercator
VIRS	Visible and Infrared Scanner

List of Figures

List of Tables

ABSTRACT

Satellite-rainfall products are recognized as an essential source of rainfall data, especially in the region where ground based measurements are unavailable. Therefore, the main objective of this study is to Apply a Satellite based Rainfall-Runoff estimation: in Upper Omo-Gibe Basin to simulate the extreme flood event at Omorate and with specific objective of evaluate the capabilities, applicability and limitations of satellite rainfall products such as CMORPH, TRMM 3B42v7 and PERSIANN, and inputs of hydrological models to simulate the Rainfall-Runoff by hydrological model NAM and preparing the Flood Hazard map in the lower water shed using MIKE-11,MIKE-21 and MIKE-FLOOD. These products and inputs were employed to simulate stream flow in the Great Gibe Watershed. The study period 2000-2012 was used for downloading and extracting the selected satellite rainfall estimates with daily-temporal and 0.25^0 x 0.25^0 spatial resolution.

Sensitivity and uncertainty analysis, calibration and validation of the model were done using MIKE ZERO particularly the Sequential Uncertainty Fitting (SUFI-2) algorism for all rainfall inputs independently. The calibration period was from 2001-2005 leaving one years as a-warm up period and the validation period was from 2006-2012 for satellite rainfall based simulations as well as in situ based simulations. Based on the modeling results of Mike Zero models had showed better performance when calibrated with the in situ rainfall with model performance efficiency of Mean Absolute Error, Maximum Values and Standard Deviation models respectively while, the satellite rainfall estimates (TRMM-3B42v7 and CMORPH) showed relatively good performance when calibrated on the models with Mean Absolute Error (5.21,4.24), Max.Val. (73.74,32.97) and Std. Deva.(7.46,4.24) in the case of Asendabo with relative to the ground based measurements in both satellite based product respectively. But, PERSIANN satellite rainfall estimates showed poor performance for all Mean Absolute Error (3.78), Max. Values (33.06) and Std. Deva. (4.24) before bias corrected.

The model output simulation results performance in analyzed of Rainfall-Runoff based up on the coefficient of determination and Nash-Sutcliffe coefficient, during the calibration it is found to be 0.509 and 0.64 respectively and the total water balance error during calibration is 14.75%. And during validation period 0.645 and 0.675 respectively with the total water balance error is 17.5%. Peak and low flows between observed and simulated hydrograph were found matching well. The simulated minimum and maximum runoff for 13 years' period the maximum annual runoff varies

between 1466.3 mm to 7525.4 mm. The simulated runoff was maximum for the month of August (6977.4 m3/s) and minimum for the month of April (5540.6 m3/s). The single flood event of year 100 in the upper part of Gibe confluence flood plain simulated using MIKE FLOOD, which integrated the calibrated and validated 1D MIKE-11 hydrodynamic model with 2D hydrodynamic model MIKE-21 for the flood plain.

Key words; Great-Gibe, Rainfall-Runoff, MIKE-11, MIKE-21, MIKE-FLOOD TRMM3B42v7, PERSIANN, CMORPH

INTRODUCTION

1.1 GENERAL BACKGROUND

Any rainfall-runoff modelling requires accurate rainfall data as a model input. However, accurate runoff simulations require accurate rainfall data as input (Ashenafi and Hailu, 2014). Rainfall information in many world regions is hampered by limitations of ground-based observational networks. Rain gauge networks often have inadequate coverage and density, represent only point scale estimates and suffer from problems relating to data quality and inconsistency (Sorooshian et al., 2005; Meng et al., 2014).

Satellite-based Rainfall-Runoff estimates have become available at high resolutions and are expected to offer an alternative to represent the variability in rainfall runoff estimation in data-sparse and ungagged catchments (Sawunyama and Hughes, 2008). In this regard, different products have been produced with the development of earth observation techniques. Rainfall variability is often influenced by nonlinear interactions between several factors like local variations of topography, the orientation of mountains and aspect (Haile et al., 2009). Terrain features also increases the variability of rainfall by means of processes such as rain shading and strong winds (Buytaert et al., 2006). Similarly, in large catchment, (Haile et al. 2009) revealed that the variation of rainfall is affected by topography.

Satellite-based rainfall-runoff estimation might provide information on rainfall occurrence, amount, and distribution at the highest spatial and temporal resolution (Anagnostou et al., 2010). On the other hand, land cover changes also affect the hydrology of a catchment by modifying evaporation and thereby influencing runoff generation (Cao et al., 2009).

In comparison with rain gauge, ground radar system can provide the instantaneous spatial distribution of precipitation over the basin indirectly and thus help to remove the bias of rain gauge observations partly. But, because of its problem of limited coverage area, high costs of establishing and maintaining infrastructure, etc., there is no perfect radar network in many

regions (Gu et al., 2010). It still cannot meet the requirements of study carried out on large scale basins. These sorts of drawbacks clearly show that rainfall data availability and accuracy impose a remarkable limitation on the application of distributed hydrological model.

However, recent advances in multi-satellite rainfall estimates have allowed uses of high resolution satellite rainfall products in hydrological modelling for runoff simulations (Bitew and Gebremichael, 2011a; Yong et al., 2012). Satellite rainfall products such as TRMM (Huffman et al., 2007), CMORPH (Joyce et al., 2004), PERSIANN (Sorooshian et al., 2000) with different spatial and temporal resolutions have emerged as an alternative or supplement to conventional precipitation observations (Sawunyama and Hughes, 2008;
Yong et al., 2012) due to their high spatial and temporal resolution and availability in remote areas.

The Climate Prediction Centre Morphing Method (CMORPH) is one technique which uses motion vectors derived from half-hourly interval geostationary satellite infrared imagery to propagate relatively high quality precipitation estimates derived from passive microwave data. Moreover, the shape and intensity of the precipitation features are modified (morphed) during the time between microwave sensor scans by performing a time-weighted linear interpolation. This process yields spatially and temporally complete microwave-derived precipitation analyses, independent of the infrared temperature field. CMORPH showed substantial improvements over both simple averaging of the microwave estimates and over techniques that blend microwave and infrared information but that derive estimates of precipitation from infrared data when passive microwave information is unavailable (Joyce et al., 2004).

Tropical Rainfall Measuring Mission (TRMM) Multi satellite Precipitation Analysis (Huffman et al., 2007) uses MW data to calibrate the IR-derived estimates and creates estimates that contain MW-derived rainfall estimates when and where MW data are available and the calibrated IR estimates where MW data are not available. The TMPA rainfall products are available in two versions: a near-real-time version (TMPA3B42RT, or 3B42RT for short) and a gauge-adjusted post-real-time research version (TMPA3B42, or 3B42 for short). The 3B42 products are released

10–15 days after the end of each month, while the 3B42RT are released about 9 hours after overpass. The main difference between the algorithms of the two versions is the use of monthly rain gauge data for bias adjustment in the 3B42 version.

Steam-flow simulation is carried out for various precipitation products that include in-situ gauge observation, gauge adjusted CMORPH, TRMM-3B42v7 and PERSIANN within a daily-temporal and 0.25^0x0.25^0 spatial resolutions. In this particular thesis work case, use the application satellite based rainfall-runoff estimating for Lower Omo-Gibe river basin for investigating and determining the extreme events of flood that was occurred on 21st August 2006 at Omorate and Nyangatom will be carried out in detail.

1.2 STATEMENT OF THE PROBLEM

Rainfall is the meteorological parameter-affecting people in the most direct way. Forecasting the spatial and temporal distribution of rain is therefore one of the major challenges for the meteorological services and research purposes. Accordingly, Scarcity of rainfall data for ungauged places and remote area within the basin is one of the major problem and gap for rainfall information users.

The Flooding problem according to the reported obtained from MoWR Omo-Gibe River Basin Catastrophic disaster was occurred in the year 2006. The extra ordinary over flow of Omo River in August 2006 affect about 8,000 people in Dasench and Nyangatom Woredas of south Omo zone. It has also killed 346 people and swept away 3200 cattle and destroyed other properties, including 760 traditional grain stores. This area is one of the most affected as compared with other Woredas of the country (August 2006 EBC and BBC News). As a result, the Author has to apply satellite based rainfall-runoff Estimating in the Upper Omo-Gibe catchment and simulating the cause of flood that happened in the Area and Suggesting the probable cause of the flood in the Area by Preparing Flood hazard map.

1.3 SIGNIFICANCE OF THE STUDY

Lack of data constitutes the biggest challenge to hydrological studies in developing countries, thereby limiting their capacity to predict, assess and plan for the water resources within catchments (Gebremichael and Hossain 2010). The Omo-Gibe River basin flood of 2006 which occurred in Omorate revealed that there were insufficient records of meteorological events in the upper and lower part of the basin as well as poor forecasting systems.

Estimates of satellite based accumulated rainfall have to be made to better understand the spatio-temporal relationship between extreme rainfall inputs and floods. This study is an attempt to solve the problem of data scarcity for management of large and possibly trans-boundary river basins in Africa. The researcher aims to increase understanding of the applicability of satellite based rainfall-runoff estimation products as major inputs to flood simulation for effect mitigation of the flood in the Omorate.

1.4 RESEARCH QUESTIONS

It is important rise a list of questions before setting the objectives and applying to the study sites. Because of this research question the researcher set some specific objectives.

- ✓ What is the spatial distribution of satellite based rainfall runoff estimation compared with measured rainfall?
- ✓ What are the informative Model data that used in satellite based rainfall- runoff estimation to simulate the flood happened in the area?
- ✓ Which model can be applied or adapted to carry out the Omo basin research to simulate a flood from an extreme rain event on the study area?
- ✓ What are the hydrologic implications of uncertainty of satellite rainfall data at the native (coarse) scale?

1.5 OBJECTIVE OF THE STUDY

The study aims to provide an overview of issues satellite based Estimating in the study Area to simulating the events of flooding Omorate. And Increase understanding of the applicability of satellite based rainfall estimation products as major inputs to rainfall-runoff models.

1.5.1 Main Objective

- ✓ The main objective of this study has focused on to use Satellite Based Rainfall-Runoff Estimation in upper Omo-Gibe River Basin to simulating the extreme flood event using MIKE 11, MIKE 21 and MIKE FLOOD occurred in 2006 at Omorate around Lower-Omo-Gibe River.

1.5.2 Specific Objectives

- ✓ To compare and analyze satellite based metrological data with temporal variation rain gauge data of Upper Omo-Gibe River Basin.
- ✓ To simulating Rainfall Runoff event that caused major Disaster using MIKE 11 NAM, by (SBRP and Gauge) data.
- ✓ Suggesting the probable cause of the flood in the Upper Area by Preparing Flood hazard map using MIKE FLOOD

1.6 HYPOTHESES

The hypothesis of this study is that: Forecasting the spatial and temporal distribution of rain is therefore one of the major challenges for the meteorological services and research purposes so satellite based Rainfall estimation is the accurate measurement of Rainfall in un gauged the Basin.

LITERATURE REVIEW

2.1 GENERAL

Spatial distribution and the amount of rainfall are important for water resources assessment and for establishing an effective flood prediction and warning services and drought monitoring. However, in many regions the number of ground measuring stations is very limited and unevenly distributed, making water resources assessment and flood prediction difficult. (Sagar Ratna Bajracharya et al. 2014)

Rainfall is a key climatic element considered as the most important factor that influencing the country agriculture and it is also principal cause of droughts and flood triggered by the fluctuation and excess of rainfall extreme events respectively. It is known that the pattern and distribution of rainfall in Ethiopia is highly variable. Therefore, the understanding of such situations and integration of this knowledge into planning and decision making process is not doubtful. At present, the great amount of available rainfall data does not allow to a direct access by human user to the whole content of information. (Dereje Mekonnen, 2007) As D.Grimes, professor of reading university in UK, cited in the proceeding of meteorological satellite data users conference in 1997, 'The past 30 years there has been concern about decreasing rainfall in Africa and weather this is linked to climate change'. He stressed that the problem of accurately assessing the situation are exacerbated by the sparseness of the rain gauge network, which has meant difficult to determine it without satellite applications like the lower part of the Omo-Gibe River Basin.

The development of remote sensing technology and application which are now able to manage the Satellite –based rainfall estimates by giving answer for specific complain such as - stations do not adequately reflect the various climatic zones of the country, unevenly distribution of gauge networking system, establishing dense network is not economically viable, accuracy and missing of gauge readings and records, and so on. Therefore, this problem can be improved only through the application of satellite data (OECDE, 1984-88).

The fact that satellite derived data is continuous in space and could be obtained regularly has made it very useful for early warning purposes. Most operational rainfall monitoring system in Africa including our country uses thermal infrared (TIR) imagery from MetoSat satellite. This is because of high repetitions rate of MetoSat images and the link between the rainfall and its convective source of clouds which is sensitive to TIR data. Half-hourly digital data from European Meteorological Satellite METEOSAT has been receiving at the National Meteorological Service agency since 1990(OECDE, 1984-88).

2.2 HYDROLOGICAL MODELING

A hydrologic system model is an approximation of the actual system; its input and output is measurable hydrologic variables and its structure is a set of equations linking the inputs and the outputs. Central to the model structure is the concept of a system transformation. The two categories of Hydrologic model: physical models and conceptual models. Physical models include scale models which represent the system on reduced scale, such as a hydraulic model of dam spillway; and analog models, which use another physical system having properties similar to those of the prototype (Ven Te Chow, 1988).

Conceptual models represent the system in mathematical form. The system in operation is described by set of equations linking the input and the output variables. These variables may be function of time, and they may also be probabilistic or random variables which do not have a fixed value at particular point in space and time but instead are described by probability distributions. Three basic decisions to be made for a model are:

- Will the model variables be random or not?
- Will they vary or be uniform in space?
- Will they vary or be constant in time

The hydrological analysis on the basin for this particular study extends from estimating the missing data to estimating satellite based rainfall-runoff model for the catchment and suggesting of the probable cause of August,21/2006 flood in the Area of Omorate. In hydrological analysis a phenomenon which undergoes change with respect to time may be called as a process. As

practically all hydrologic phenomenon changes with time, they are hydrologic processes. If the chance of occurrence of the variables involved in such process is ignored and the model is considered to follow definite law of certainty but not any law of probability the process and the model are described as deterministic. On the other hand, if the chance of occurrence of the variables taken into consideration and the concept of probability introduced in formulating the model, the process and its model are described as stochastic or probabilistic. In reality all hydrologic processes are more or less stochastic. They have been assumed deterministic or probabilistic only to simplify their analysis.

A hydrologic system model is an approximation of the actual system; its input and output is measurable hydrologic variables and its structure is a set of equations linking the inputs and the outputs. Rainfall-runoff model is a kind of abstract models, but its output may be parametric or nonparametric (pulse response). A hydrological model can yield information on water availability at closer space–time resolutions, where it is very hard to place gauges and also missing of relevant data. Thus, a hydrological model can bridge gaps in situ measurement. As there is a general lack of in situ meteorological data availability for forcing a hydrological model, there is often a need to use the more widely available satellite-based forcing products (Gebregiorgis et al. 2012; Gebregiorgis and Hossain 2011, 2013; Hong et al. 2004; Khan et al. 2012; Nijssen and Lettenmaier 2004; Kamal-Heikman et al. 2007).

Satellite estimated data such as precipitation, temperature, and wind are likely to be the more realistic source for forcing a hydrologic model for flood forecasting and water management. Satellite-based geodetic and remote sensing platforms are increasingly common in collecting hydrological measurements (Brakenridge et al. 1994; Birkett 1998; Al-Khudhairy et al. 2001).

The ability to collect data and monitor rivers by using satellite-based techniques is likely to become increasingly necessary. There are also satellite-based precipitation products like the Climate Prediction Centre (CPC) morphing technique (CMORPH; Joyce et al. 2004; Joyce and Xie 2011), Precipitation Estimation from Remotely Sensed Imagery Using Artificial Neural Networks (PERSIANN; Hsu et al. 1997; Hong et al. 2004; Hsu et al. 2010). Tropical Rainfall

Measuring Mission (TRMM)-based 3B42RT (Huffman et al. 2010). and there are also new satellite missions proposed for enhancing the availability of such hydrological data, such as precipitation [Global Precipitation Measurement (GPM) mission; Smith et al. 2007], stream flow [Surface Water and Ocean Topography (SWOT) mission; Alsdorf et al. 2007], and soil moisture [Soil Moisture Active and Passive (SMAP) mission; Entekhabi et al. 2010]. Fairly high spatial (0.25^0) and temporal resolution (3 hourly) satellite precipitation data are already routinely available. Applications of distributed hydrological models are often constrained by poor data availability. Models rely on distributed inputs for meteorological forcing and land surface parameterization.

2.3 RAINFALL-RUNOFF MODELLING AND ITS CLASSIFICATION

Rainfall-runoff modeling is a breed of abstract hydrological model. It determines the runoff signal which leaves the watershed basin from the rainfall signal received by the basin (van der Knijff et al. 2008).

It is a non-linear process according to the sequential and spatial distribution of the rainfall. So, it is difficult to explain the response of catchment system with the simpler models. Simulation of rainfall-runoff modeling is very important in water resource management, river engineering, flood control and utilization of surface and groundwater. Due to existence of different basin hydrological factors, response to rainfall-runoff phenomena are very complex.

Runoff depends on the basin geomorphologic (such as vegetation covering and soil type) and climate characteristics, such as rainfall, temperature, etc. (Hong et al. ,2007). The effects of these factors are not uniform in runoff production. Up to now many models such as MIKE -11 have been suggested this process.

Although there are a number of ways of producing an extended flow record for a river basin, broadly speaking the two main approaches are stochastic and deterministic models, within which there are further divisions. Within a hydrological model there are three main characteristics one can model: randomness, space and time.

The difference between stochastic and deterministic models is that a stochastic model represents the randomness of hydrologic series where as deterministic models do not. Another difference that the parameters of stochastic models are statistical measures of the randomness of the hydrological data while the deterministic models represent, in some degree, the physical nature of the river basin. A further difference and the last will mention here is that for a given series of input data deterministic models always give the same output whereas stochastic models will give different outputs. (Ven Te Chow, 1988)

2.3.1 Stochastic Models

Within stochastic models one of the main divisions is between 'space independent' models and 'space correlated' models. This distinction is critical. In the case of river basin of the size of the Omo-Gibe it is quite possible for different parts of the basin to experience different severities of flooding and draught and one of the aims of any water resource development would be to optimize the spatial distribution of water supplies.

This means that if a stochastic model were to be used, for the basin it would have to represent the aerial variation of hydrologic response. Indeed, one could go further and consider the case of hydropower. When a dam is built within the basin for hydro-electric generation it is unlikely that all the power will be used within the basin and one therefore has to be able to consider not only the variation in flow within the basin but also within other basins within Ethiopia. Given the short flow records available, and hence the uncertainty in the determining the statistical parameters needed for stochastic models, it is not thought that a suitable model of this type could be developed for the basin.

2.3.2 Deterministic Model

The first division to be considered here is between lumped and distributed models. A lumped model flow at Omo-rate gauging station at the southern end of the basin, would treat the whole of the basin as being homogeneous. That it would assume identical soils, land-use, rainfall and PET over the whole of the basin. Clearly, given the size of the basin this would not be a reasonable approach. The approach adopted therefore has been to simulate each of the sub-catchments that have measured flow. This in itself goes some way to representing the variation in

the river basin but, as will be seen later, the model developed represents some variation within each of these sub-catchments. Deterministic models can be classified according to weather the hydrologic process involved are empirical, conceptual or distributed.

Three main classes can be discerned:

- Empirical models (black box)
- Lumped conceptual models (Grey box)
- Distributed physically based (White box)

I. Empirical (black box) models

They are developed, using the measured time series instead of utilizing mathematical expression describing the physical processes in a catchment. Several types of empirical models are observed. One group of empirical models is statistically based using statistical method such as ARIMA (Auto Regressive Integrated Moving Average). Another group of empirical models are based on the unit hydrograph model (or applying principles of unit hydrograph). The third group of empirical models is data-driven using models such as ANN (artificial neural networks).

II. Lumped conceptual (Grey box) models

In lumped conceptual models the parameters and variables represents average values over entire catchment. Therefore, the description of the hydrological cannot be based directly on the equations that are supposed to be valid for individual solid columns. As a result of the equation are semi empirical, but still with a physical basis. The models parameters cannot usually have assessed from field data alone, but have to be obtained through help of calibration. Those models operate with different but mutually interrelated storages representing physical elements in a catchment. The model of operation can be characterized as a book keeping system that is continuously accounting for the moisture content in the storages.

III. Physically based distributed models

In physically based distributed models processes are represented by one or more partial differential equations. And equations and parameters are distributed in space.

2.4 FLOOD FREQUENCY MODELS

In flood frequency analysis, a unique relationship between a flood magnitude and the corresponding recurrence interval T is sought (Roa & Hamed, 2000). The task is to extract information from a flow record to estimate the relationship between Q and T. In order to estimate this natural Q-T relationship from a good quality of continuous hydrometric record of N year's duration, it is necessary to resort to a statistical or stochastic model of the continuous hydrograph which retains information in the hydrograph relevant to the Q - T relationship and discards the rest. Three different models are available for this purpose.

a) Annual Maximum Series Model, AM
b) Partial Duration Series Model, PD
c) Time Series Model, TS

In the annual maximum (AM) flow series, only the peak flow in each year of record is considered. However, the use of an AM series may involve some loss of information. For example, the second or third peak within a year may be greater than the maximum flow in other years, and yet they are ignored. This situation is avoided in the partial duration (PD) or peak over a threshold (POT) model where all peaks above a certain base value are considered. The base is usually selected low enough to include at least one event in each year (Roa and Hamed, 2000).

2.5 DESCRIPTION OF HYDROLOGICAL MODELS

2.5.1 Description of MIKE 11 Hydrodynamic model

MIKE SHE is a derivative of System Hydrologique Européen, SHE and is a deterministic, fully-distributed and physically-based hydrological and water quality modelling system. The preceding studies have shown that the MIKE SHE modelling system was used effectively and widely in many watershed studies, where conventional watershed models could not represent the whole water cycle components (Thompson et al. 2004).

The flexibility of MIKE SHE hydrology component is the integration of various hydrological processes at different timescales. MIKE SHE model comprises the finite difference representation and solution of the theoretical partial differential equations of mass and energy balance, in addition to verified empirical relations.

The model covers the entire hydrological system on a catchment scale. The MIKE SHE modelling system was designed with a modular structure. The water movement (WM) module in MIKE SHE is the basic module of the entire modelling system. The hydrologic simulation consists of subcomponents describing the processes of evapotranspiration, overland and channel flow, saturated flow, unsaturated flow, and channel/surface aquifer exchanges.

Rainfall interception is modelled by using a modified Rutter model, evapotranspiration is modelled using Kristensen and Jensen method based on leaf area index, root depth and potential evapotranspiration for each vegetation type, water movement in unsaturated zones is modelled by the one-dimensional Richards equation.

Three dimensional Boussinesq equation is used for groundwater flow. For channel flow it uses one-dimensional full dynamic wave approximate Saint Venant equations, respectively two-dimensional diffusive wave for overland flow. The original MIKE SHE module for channel flow did not support hydraulic structure representation such as culverts and weirs, which posed a problem for the river flow simulation.
The release of MIKE 11 version 4 is started a new era for the most widely applied dynamic modelling tool for river and channels. MIKE 11 is part of the new generation of DHI software based on MIKE Zero concept.

MIKE 11 is a professional engineering software package for the simulation of flow, water quality and sediment transport in estuaries, rivers, irrigation system, channels and other water bodies. MIKE 11 is a user friendly, fully dynamic, one –dimensional modelling tool for the detailed analysis, design, management and operation of both simple and complex river and channel system.

The Hydrodynamic (HD) model is the nucleus of the MIKE 11 modelling system and forms the basis for most modules including Flood Forecasting, Advection-Dispersion, Water Quality and Non-cohesive sediment transport modules. The MIKE 11 HD module solve the vertically integrated equation for the conservation of continuity and momentum (Saint Venant).

Application related to the MIKE 11 HD module include:

- Flood forecasting and reservoir operation
- Simulation of flood control measures
- Operation of irrigation and surface drainage systems
- Design of channel systems
- Tidal and storm surge studies in river

2.5.2 *Capabilities of a coupled 1D/2D model for flood inundation simulation*

Flood modeling is an important task for decision making in the field of natural risk management. Therefore, river engineers and manage0rs need designed tools, as physically-based models, in order to evaluate flood inundation risk.

The goal of such tools is to simulate probable inundation damage on a given area depending on several flood scenarios with different intensity, duration and return period. Model reliability is assessed by confronting simulation results and real data in a calibration process: starting from a real inundation that occurred, with a given return period, difference between real data and output modeled data is minimized by adjusting some parameters of the model. Starting from these adjusted parameters, the model is then validated by checking that difference is acceptable for other flood events with available real data (Bates and De Roo, 2000). But such model assessment method is not straightforward at all.

2.6 RAINFALL AND SATELLITE–BASED MEASUREMENTS

Precipitation is a crucial link in the hydrologic cycle, and its spatial and temporal variations are enormous. Acknowledge of the amount of regional rainfall is essential to the welfare of society. Rainfall also drives the hydrological cycle, and to improve weather and climate predictions, an accurate global coverage of rainfall records is necessary.

Rainfall can be estimated remotely, either from ground-based weather radars or from satellite. Radars are active devices, emitting radiation at wavelengths ranging between 1 and 10 cm, and receiving the echo from targets such as raindrops. (Arkin, P.A. and P.E. Ardanuy 1989). The maximum range of radars is only about 300 km, so offshore coverage is limited. Also, radars are prohibitively expensive in the Third World. Satellite-based measurements offer global coverage or a good part thereof.

2.6.1 Rainfall Estimation Techniques

Based on different literature review documents there are a lot of the Rainfall Estimation Technics some of the technics are:

- ✓ Microwave Rainfall Estimation Technique
- ✓ CPC Rainfall Estimation Technique
- ✓ ORSTOM Rainfall Estimation Technique
- ✓ TRMM-TMPA

2.6.2 TRMM-TMPA rainfall products

The Tropical Rainfall Measuring Mission (TRMM) is a joint mission between NASA and the National Space Development Agency of Japan (JAXA) that serves to observe and understand how tropical rainfall affects the global climate.

TRMM has five instruments: precipitation radar (PR), TRMM microwave imager (TMI), visible and infrared scanner (VIRS), cloud and earth radiant energy sensor (CERES), lightning imaging sensor (LIS). These instruments can all function individually or in combination with one another, (Huffman *et al.* 2001). The TRMM Multi-Satellite Precipitation Analysis (TMPA) is designed to combine precipitation estimates from various satellite systems and land surface precipitation from gauges. This primary merged microwave infrared product is computed at a 3-hourly temporal and 0.25° x 0.25° latitude–longitude spatial resolution (Huffman *et al.* 2007).

The TMPA is computed as two products for TRMM. One product is an experimental real-time monitoring product that is produced nine hours after real time (TMPA_RT). A second product is

a post-real-time research-quality product that becomes available about ten to fifteen days after the end of each month (research product), (Huffman *et al*. 2001).

The two products can be downloaded at this link: http://gdata1.sci.gsfc.nasa.gov/daac-bin/G3/gui.cgi?instance_id=TRMM_3B42_Daily and http://mirador.gsfc.nasa.gov TMPA depends on input from two different sets of sensors.

First, precipitation related passive microwave data are collected by a variety of low earth orbit (LEO) satellites, including the Microwave Imager (TMI) on TRMM, Special Sensor Microwave Imager (SSM/I) on Defence Meteorological Satellite Program (DMSP) satellites, Advanced Microwave Scanning Radiometer-Earth Observing System (AMSR-E) on *Aqua*, and the Advanced Microwave Sounding Unit-B (AMSU-B) on the National Oceanic and Atmospheric Administration (NOAA) satellite series.

The second major data source for the TMPA is the window-channel (10.7μm) IR data that are collected by the international constellation of geo-synchronous earth orbit (GEO) satellites. This dataset includes grid-box-average Geostationary Operational Environmental Satellite (GOES) Precipitation Index (GPI) estimates computed from LEO–IR data recorded by the NOAA satellite series. These LEO–GPI data are used in the TMPA to fill gaps in the GEO–IR coverage (Huffman *et al.* 2007).

The research TMPA makes use of a third set of data sources: The TRMM Combined Instrument (TCI) estimate, which employs data from both TMI and the TRMM precipitation radar (PR) as a source of calibration resulting in the TRMM Combined Instrument (TCI) 2B31 product (Haddad *et al.* 1997). The GPCP monthly rain gauge analysis developed by the Global Precipitation Climatological Centre (GPCC) (Rudolf 1993), and the Climate Assessment and Monitoring System (CAMS) monthly rain gauge analysis developed by the Climate Prediction Centre (CPC) (Xie and Arkin, 1997).

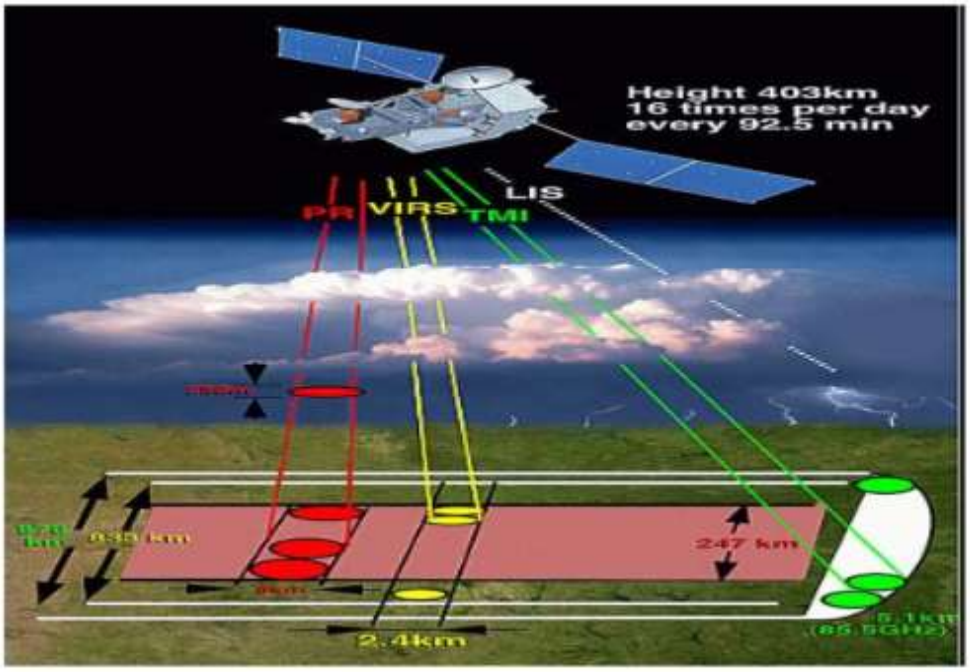

Figure 1:TRMM_3B42RT_Daily v7satellite and instruments(source: **http://mirador.gsfc.nasa.gov**)

2.6.2.1 *Algorithms of TRMM_3B42RT_Daily v7Multi satellite Precipitation Analysis*

The purpose of algorithms TMPA 3B42 and 3B42RT, Figure 2 is to produce TRMM rainfall retrievals merged high quality (HQ)/ infrared (IR) precipitation and root mean square (RMS) precipitation error estimates. The data include retrievals from six different algorithms: VIRS, TMI, PR, and the combination with other satellites (GPI, GPCP and SSMM). Table 1 provides the definition of the TRMM products at each level

*Table 1: The definition of the TRMM products (source: **http://www.maic.jmu.edu/**)*

Level	Definition
0	Unprocessed instrument data, time ordered, qulity checked, no redundancy.
1	Ancillary data and geo referencing data attached to Level 0, and processed to sendor- dependent physical units (e.g. radar reflectivity, brightness, temperature)
2	Meteorological parameters (e.g. rainfall rate) derived from Level 1 data using various algorithms, which will be provided as a 2-or3-dimensional rain map along the TRMM swath.
3	Results of mapping the meteorological parameters (Level 2) on a uniform space and time grid.

The 3B42 is composed of two separate algorithms, which are (i) to produce monthly IR calibration parameters, and (ii) to calibrate the merged-IR precipitation data to produce the daily adjusted merged-IR precipitation and RMS precipitation error estimates (JAXA, 2006).

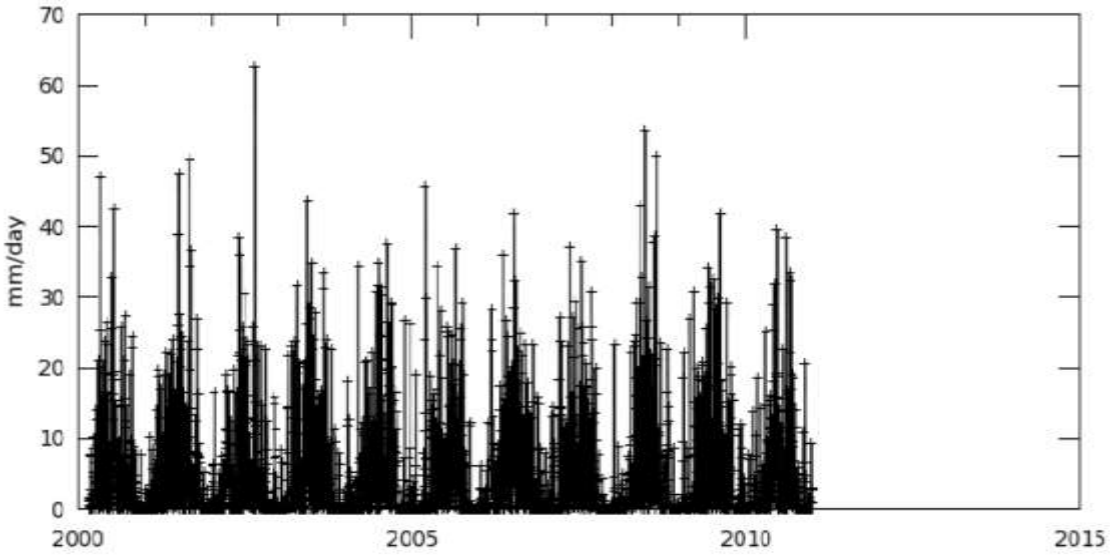

Figure 2: Time series, Area-Average of Near-Real-Time precipitation Rate daily 0.25 deg. [TRMM TRMM_3B42RT_Daily v7]mm/day over 2000-03-01 to 2011-01-01, Reign 36.4307E,7.6025N,36.9141E,7.998N

2.6.3 PERSIANN rainfall products

PERSIANN (Precipitation Estimation from Remotely Sensed Information using Artificial Neural Networks) is G-WADI's flagship decision-support product. The products and tools are developed by the Centre for Hydrometeorology and Remote Sensing (CHRS) of the University of California, Irvine.

PERSIANN is a satellite-based precipitation retrieval algorithm, providing near-real time precipitation products (Hsu et al., 1997; Sorooshian et al., 2000). It uses an adaptive neural network algorithm to combine information from various satellites. This includes high frequency (48 readings a day) geosynchronous satellite based gridded infrared images and low frequency (1–2 readings a day) instantaneous rain derived from the TRMM TMI microwave imager (Hughes et al., 2006; Brown et al., 2006). The adaptive neural network means that the product can be adapted and calibrated flexibly for different precipitation regimes (Asadullah et al., 2008).

The original PERSIANN product has a temporal resolution of 1 hour and a global spatial grid of 0.25° between 60°N and 60°S. Additionally, a Cloud Classification System (PERSIANN-CCS, Hong et al., 2004; Hsu et al., 2013) algorithm is available at spatial and temporal resolutions of 0.04° and 1h, respectively.

The CCS algorithm is optimized for observing extreme precipitation, particularly at very high spatial resolution. Typical applications include flood forecasting, hydrological modelling, drought monitoring, and soil moisture analysis.

A third product, PERSIANN-CDR is a retrospective satellite-based climate data record starting on 1 January 1983. It is aimed at hydrological and climate studies that require long-term consistent data, for instance for trend and risk analysis (Ashouri et al., 2015).

For all PERSIANN products, user-friendly interfaces exist. For example, iRain is a web-based graphical interface to near real-time PERSIANN-CCS data, and an iRain mobile app is available for iOS and Android devices under the name "iRain UCI". RainSphere is a system based on

PERSIANN-CDR that allows the user to visualize and analyse historical and future precipitation at a variety of spatial and temporal scales (Nguyen et al., 2016).

Data for PERSIANN, PERSIANN-CCS and PERSIANN-CDR are all easily downloadable from the CHRS Data Portal.

2.6.4 CMORPH Rainfall Products

The Climate Prediction Centre morphing method (CMORPH) uses motion vectors derived from half-hourly interval geostationary satellite IR imagery to propagate the relatively high quality precipitation estimates derived from passive microwave data. In addition, the shape and intensity of the precipitation features are modified (morphed) during the time between microwave sensor scans by performing a time-weighted linear interpolation.
This process yields spatially and temporally complete microwave-derived precipitation analyses, independent of the infrared temperature field.

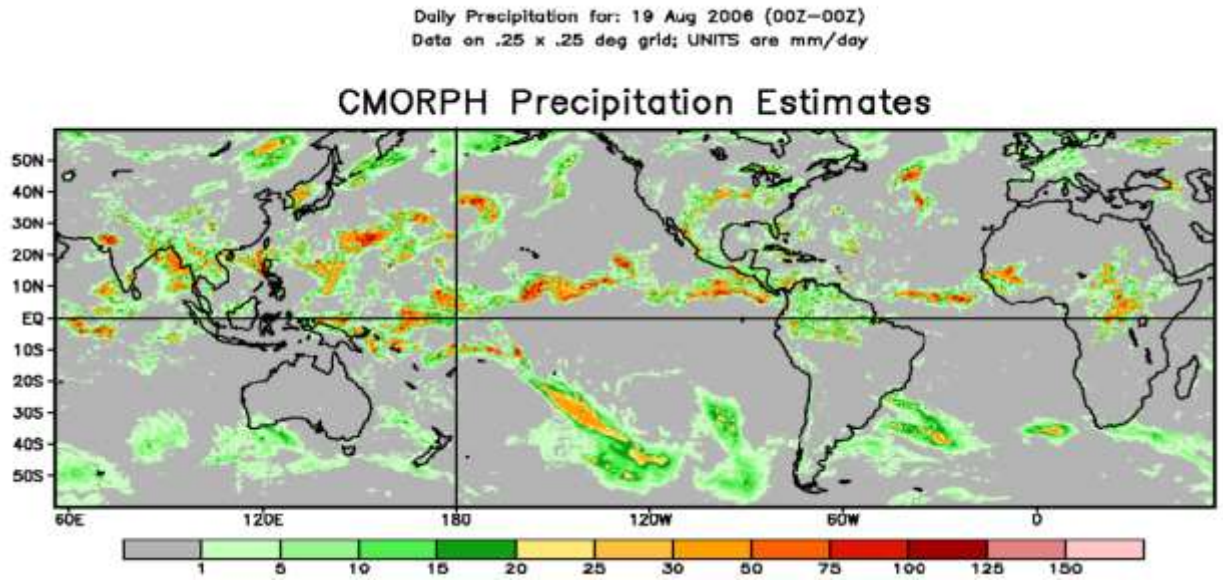

*Figure 3: CMORPH precipitation Estimates (source: **http://mirador.gsfc.nasa.gov**)*

2.7 ADVANTAGE AND DISADVANTAGE OF SATELLITE-BASED RAINFALL ESTIMATION

I. Advantage

- ✓ Relatively time consuming, and easily for large volume of data acquisition and extraction system.
- ✓ Easy to operate and maintain.
- ✓ It is tried and proven, but mainly in tropical zone.

II. *Disadvantage*

- ✓ At night, no visible data are available therefore rainfall estimation are achieved using infrared and, perhaps, microwave data.
- ✓ The techniques for rainfall estimations are based upon assignment of temperature and /or brightness thresholds to rainfall amounts vary in performance with month and seasons.
- ✓ If the satellite sensors fail, there is no possibility of repair until another satellite is launched.

2.8 *PERFORMANCE EVALUATION OF SATELLITE RAINFALL PRODUCT*

2.8.1 Previous Research Works

Several studies have been conducted to evaluate satellite based rainfall estimation for different methods mentioned in the above section. These studies can be classified in terms of two ways.

I. Depending on the purpose of the studies; for example, some to evaluate just the rainfall over the given area based considering the estimated rainfall value.

II. To evaluate how the methods themselves works and their accuracy and reliability in estimating the rainfall.

Xue et al, (2013) evaluated TRMM3B42 satellite rainfall product with different versions (V6 and V7) over the mountainous Wangchu Basin of Bhutan using Coupled Routing and Excess Storage (CREST) hydrologic model. Their results showed that V7 of TRMM3B42 products have significant upgrade from the V6 TRMM3B42 products in precipitation accuracy and can serve as inputs for distributed hydrological modeling in that study area.

Liu et al, (2015) assessed the hydrological potential of TRMM satellite rainfall products for stream flow simulation in Laotian data sparse basins, South East Asia. They undertake the assessment for Nam Khan River basin using physically based distributed hydrologic model, BTOPMC for a period of five years (2000-2004). The authors have used TRMM3B42V7 satellite rainfall estimate before and after bias correction as a model input. They conclude that although larger difference exists in the high stream flow process and the low stream flow process, the daily TRMM based simulations could basically reflect the daily observed stream flow processes and determine the time to peak. They also noted that the performance of the model has increased when bias corrected TRMM satellite rainfall was used.

Liu et al, (2014) conducted an evaluation of three satellite products TRMM3B42, CMORPH and PERSIANN over the Meichuan watershed, Poyang Lake Basin in China. They evaluated satellite products using in situ rainfall data from 52 rain gauge stations for a period of nine years (2001-2005 and 2007-2010); leaving 2006 due to missed values. The evaluation was at different spatial (grid and watershed) and temporal (daily, monthly and annual) resolutions. The authors conclude that at daily temporal resolution, CMORPH had the best performance with highest R^2 value at the watershed scale than others in the study area, whereas at monthly and annual temporal resolutions, TRMM3B42 had the best performance similarly with highest R^2 value at the watershed scale, but PERSIANN had the worst performance among the three products at all temporal and spatial scales. They also pointed out that CMORPH and TRMM3B42 might be used for hydrological applications at daily temporal scale.

Seyyedi, (2014) investigated the hydrologic applicability of a high-resolution satellite precipitation product, particularly TRMM3B42V7 with spatial resolution of 25km x 25km and temporal resolution for 3-hour relative to a global re-analysis product (GLDAS) with spatial resolution of 1degree and 3-hour temporal resolution through comparison with rain-gauge adjusted radar-rainfall estimates in the case of the Susquehanna River Basin, Northeast United States. The investigation was using Hill slope River Routing (HRR) model for a period of ten years (2002-2011). He concluded that the satellite product (TRMM3B42V7) exhibits better error statistics compared to reanalysis product (GLDAS) and for streamflow simulation, the re-

analysis precipitation product shows higher mean relative error compared to the corresponding high resolution satellite product.

Maggioni et al, (2013) investigated uncertainties associated with satellite rainfall products; TRMM3B42V7, TRMM3B42TRV7, CMORPH and PERSIANN-CCS and their subsequent impact on stream flow simulation. The investigation was done on TarPamlico River Basin, South Eastern United States for a period of two years (2004 and 2006). They used NMS Multi sensor Precipitation Estimator (MPE) data sets as a reference to evaluate satellite rainfall products and NWS Hydrology Laboratory Research Distributed Hydrologic Model (HL-RDHM) to simulate stream flow for the area. Their results demonstrated significant dependency of error propagation in the catchment area, i.e. TRMM3B42RT based runoff simulations overestimated the peak runoff in the small basin and underestimated at larger basin, whereas PERSIANN-CCS based simulations did not capture either of the benchmark stream flows at larger scale basins and CMORPH yielded no considerable runoff at any basin scale levels at which Spatial / temporal resolutions.

Stampoulis et al, (2013) analyzed the errors of the CMORPH and PERSIANN satellite rainfall products using rainfall data derived from radar rainfall estimates as a reference over the three different mountainous regions in the Western Mediterranean for a period of 2003, 2005, 2006 and 2007. The satellite rainfall products under consideration were at spatial/temporal resolutions of 0.07^0/ half hourly. They found that both of the satellite rainfall products underestimated the rainfall for all storm cases in all periods, but CMORPH exhibited better performance than PERSIANN.

Vergara et al, (2014) assessed the effect of satellite rainfall products resolution and basin scale on hydrological simulations over U.S. Geological Survey (USGS) station located in Tarboro for a period of eight years (2002-2009). The satellite rainfall product they used for the assessment was TRMM3B42RT and NWS Hydrology Laboratory Research Distributed Hydrologic Model (HL-RDHM) was used by the authors for stream flow simulation. Finally, they pointed out that

resolution degradation introduces a significant amount of error in rainfall fields which intern propagated to the stream flow simulations as a magnified bias.

Yong et al, (2012) assessed evolving periods of TMPA-RT satellite rainfall estimates and their Impacts on hydrologic simulation at daily, monthly and seasonal scales and temporal resolution of 0.25^0 x 0.25^0 over the Laohahe basin in China. They used the VIC-3L hydrologic model for hydrologic simulation for period nine years (2002-2010). They concluded that the performance of TMPA-RT satellite rainfall estimates in terms of precipitation estimation as well as the streamflow simulation has been increased after 3 February 2005 with overestimation during winter months resulted from interference of snow cover in the passive microwave data. They also pointed that after a simple bias correction, the latest TMPA-RT satellite rainfall estimates had showed the best capability in capturing hydrologic response than the previous versions.

Habib et al, (2012) evaluated CMORPH satellite rainfall estimates with spatial resolution of 8 X $8km^2$ and different temporal resolutions (hourly, daily and event scales) using experimental rain gauge networks for a period of 28 months (August 2004 to December 2006) over Isaac-Verot watershed located in south Louisiana, United State. They found that at event temporal scale, although, the underestimation biases were more dominant, CMORPH satellite rainfall product also overestimated the biases whereas at hourly temporal scale CMORPH products have a successful detection skill. They also pointed out that CMORPH satellite rainfall biases underestimation has increased with an increase in the surface rainfall.

Nikolopoulos, (2012) assessed satellite based rainfall estimates for a major flash flood event simulation through triangulated irregular network (TIN) based Real-time Integrated Basin Simulator (tRIBS) physically based distributed hydrologic model over FriuliVenezia Giulia region in northeastern Italy. The rainfall products they considered were TRMM3B42 (0.25^0/1-hr), CMORPH (0.07^0/1-hr) and PERSIANN (0.04^0/1-hr) with their spatial and temporal resolutions. They demonstrated that the evaluated satellite rainfall estimates do not perform satisfactorily on capturing the flood peak in the study area. But they revealed that simulation

hydrographs became meaningful after recalibrating the model with bias adjusted satellite rainfall estimates for each estimate independently.

Gourley et al, (2011) evaluated rainfall estimates from TRMM3B42RT and PERSIANN in comparison to radar rainfall estimates for hydrological simulations using SACramento Soil Moisture Accounting (SAC-SMA) hydrologic model over Ft Cobb basin, Oklahoma. They finally demonstrated that TRMM3B42RT had relatively better performance than PERSIANN for hydrological simulations for the study area, but the authors noticed that the better performance of TRMM3B42RT satellite rainfall estimates for hydrological modeling was only achieved when the model was calibrated at 0.25^0/3-hr resolution. Thus, they pointed out the importance of considering the satellite rainfall estimates resolution during model calibration.

Beighley et al, (2011) predicted streamflow by through the Hill slope River Routing (HRR) hydrologic model with three satellites derived precipitation estimates (TRMM3B42V6, CMORPH, PERSIANN) over the Congo Basin. They found that all three satellite estimates had overestimated over the basin, but among the selected three satellite rainfall estimates TRMM3B42V6 product exhibited the best performance in terms of rainfall data quality as well as simulated streamflow.

Behrangi et al, (2011) investigated the effectiveness by using satellite based rainfall estimates (TRMM3B42V7, TRMM3B42RTV7, CMORPH and PERSIANN) for streamflow simulation at catchment scale over the midsize Illinois River basin. The investigation was at 6-hr and monthly time scale for a period of six years (2003-2008) using SACramento Soil Moisture Accounting (SAC-SMA) hydrologic model for stream flow simulation. They concluded that raw satellite rainfall estimates without bias correction overestimated both precipitation inputs and simulated stream flow, but biasadjustment of satellite rainfall estimates has significantly increased the ability of capturing streamflow patterns and magnitude.

Shen, (2010) examined the performance of high resolution satellite rainfall products (TRMM3B42, TRMM3B42RT, CMORPH and PERSIANN) at hourly temporal and 0.250 spatial resolutions for a period of three years (2005-2007) over China. They showed that all of the satellite rainfall estimates were capable of capturing the overall spatial distribution and temporal variation of rainfall, but relatively CMORPH satellite rainfall estimates performed best in capturing spatial as well as temporal variations of the rainfall in the area.

2.8.2 Previous Studies in Ethiopia

The historical background of satellite weather forecasting technic in Ethiopia is Half-hourly digital data from European Meteorological Satellite METEOSAT has been received at the Ethiopian Meteorological Service's site since 1990. Apart from weather forecasting the digital data is used for estimating ten-day total rainfall by applying TMSAT methodology developed at the University of Reading, UK (Milford and Dugdale, 1989).

Estimates are being validated using data collected from rain gauge network. Results found are in good agreement with the observed data. However, the network density of conventional stations does not adequately reflect the various climatic zones of the country in fact, the rain economically viable. Therefore, this problem can be alleviated through the application of satellite data. The fact that satellite derived data is continuing in space and could be obtained regularly has made it very useful for early warning purposes. From 1990 there are several scholars are done different researches based on satellite based weather forecasting, Rainfall estimation, stream simulation and other based on let us see some previous studies in Ethiopia:

Alemseged, (2012) study focuses on the evaluation of the NOAA–NCEP Climate Prediction Center (CPC) morphing technique (CMORPH) satellite-based rainfall product at fine space–time resolutions (1 h and 8 km). The evaluation was conducted during a 28-month period from 2004 to 2006 using a high-quality experimental rain gauge network in southern Louisiana, United States. The dense arrangement of rain gauges allowed for multiple gauge. The results suggest

that the CMORPH product has high detection skills: the probability of successful detection is 80% for surface rain rates 2 mm and probability of false detection ,3%.

Alemseged et al, (2012) Climatology-Focused Evaluation of CMORPH and TMPA Satellite Rainfall Products over the Nile Basin. The journal focused on operational satellite rainfall products being available for long periods, it is now possible to examine whether these products can reproduce climatologically known rainfall characteristics over large river basins that suffer from poor surface monitoring resources. Such assessment is a prerequisite for any further hydrologic applications that rely on these products.

Ambaw, (2016) tested the effectiveness of CMORPH satellite rainfall estimates at high spatial and temporal resolutions (1-hr temporal and 8 km x 8 km spatial resolution) for runoff simulation over the Upper Gilgel Abbay catchment. He used Representative Elementary Watershed (REW) model for runoff simulation for a period of five years (2006-2010). The author has indicated that although CMORPH based simulations were able to capture the shape of the measured flow hydrograph, in situ based simulations had better reproduce the measured stream flow hydrograph than CMORPH based simulations.

Habib et al, (2014) examined effects of bias correction of CMORPH satellite rainfall estimates on runoff simulation through HBV hydrologic model in the Gilgel Abbay catchment. They tested three different bias correction schemes (space and time invariant, time variant and spatially invariant and space and time variant) on CMORPH satellite rainfall estimates. The authors conclude that space and time variant bias correction scheme performs better than others and the capability of HBV hydrological model in capturing the measured hydrograph patterns and volume had increased when bias corrected CMORPH satellite rainfall estimates were used as a model input.

Ashenafi and Hailu, (2014) evaluated the performance of SWAT model for stream flow simulation using rainfall input data from CMORPH satellite rainfall estimates (with 0.25^0 x 0.25^0 spatial and 3-hr temporal resolutions) and in situ based rainfall data for a period of six years

(2003-2008) for the Gilgel Abbay catchment. They concluded that the SWAT model yields good results for CMORPH satellite rainfall estimates based simulations than in situ rainfall data based simulations. They pointed out that the better performance of the model with satellite rainfall estimates was associated with the inadequacy of point rainfall measurements.

Haile et al, (2013) evaluated CMORPH satellite rainfall estimate with high resolution (1hr temporal and 8km x 8km spatial resolutions) in Gilgel Abbay watershed. They evaluated the satellite rainfall estimate for three months using experimental in situ rainfall data networks. The authors indicated that the accuracy of the CMORPH satellite rainfall estimate was dependent on the basin area and the satellite rainfall estimate was poorly correlated with in situ rainfall data observations. They also pointed that the CMORPH satellite rainfall estimate had underestimated the seasonal rainfall depth in the area.

Haile et al, (2012) performed an evaluation the climate prediction center (CPC) morphing technique (CMORPH) rainfall product on hourly time steps over the source of Blue Nile River Gilgel Abbay, Ethiopia, and showed the applicability of satellite based precipitation estimation in an area with few rain gauges.

Bitew and Gebremichael, (2011) assessed the use of satellite rainfall estimates (CMORPH, TRMM3B42RT, TRMM3B42 and PERSIANN) for stream flow simulation in Koga and Gilgel Abay watersheds. They used a SWAT hydrologic model to simulate daily stream flow for both of the selected watersheds for a period of five years (2003-2007). The authors concluded that the use of satellite rainfall estimates for SWAT based hydrological modeling has been significantly depending on the product type, thus SWAT hydrologic model was best when TRMM3B42RT and CMORPH satellite rainfall estimates were used as a model input than TRMM3B42 and PERSIANN for stream flow simulation in the area.

3. MATERIALS AND METHODOLOGY

3.1 GENERAL

In watershed management hydrology is indispensable tool. Adequate basic data are essential to any science and hydrology is no exception. In fact, complexity of hydrologic phenomena makes it difficult to apply rigorous deductive reasoning. But it is necessary to interpret observed data and form this analysis to establish the systematic pattern that governs these events.

Hydrologic analysis is one of the important components in developing rainfall-runoff model and determining cause of flood. Accuracy of the model depends on the precision taken on hydrologic analysis. However, each hydrologic problem is unique in that it deals with a distinct set of physical condition with in specific river basin. Hence quantitative conclusions of one analysis are not directly transferable to another problem. But the general solution for most problems can be developed from application of few relatively basic concepts.

3.2 DESCRIPTION OF THE STUDY AREA

3.2.1 Omo-Gibe River Basin

3.2.1.1 Location and Coverage

The Omo-Gibe river basin is a surface drainage basin in southern Ethiopia, extending between latitude of 4°27' to 9°21'North and longitude of 35° 00'to 48° 25' East. The distance from north to south is about 544 Km, with maximum east-west width of 251 Km, and an average width of 91 Km. This gives an area of about 78,937 Sq.Km with 25% falling in Oromiya region and the balance in SNNPR. About 51% of the basin falls in low lands. This basin is locked by other Ethiopian basins except that it is bounded by Lake Turkana in south; it is bounded by Baro-Akobo to the west, Rift valley lakes to the east, Blue-Nile to the north and northeast and A wash basin also bounds with small area in the northeast (See figure 4).

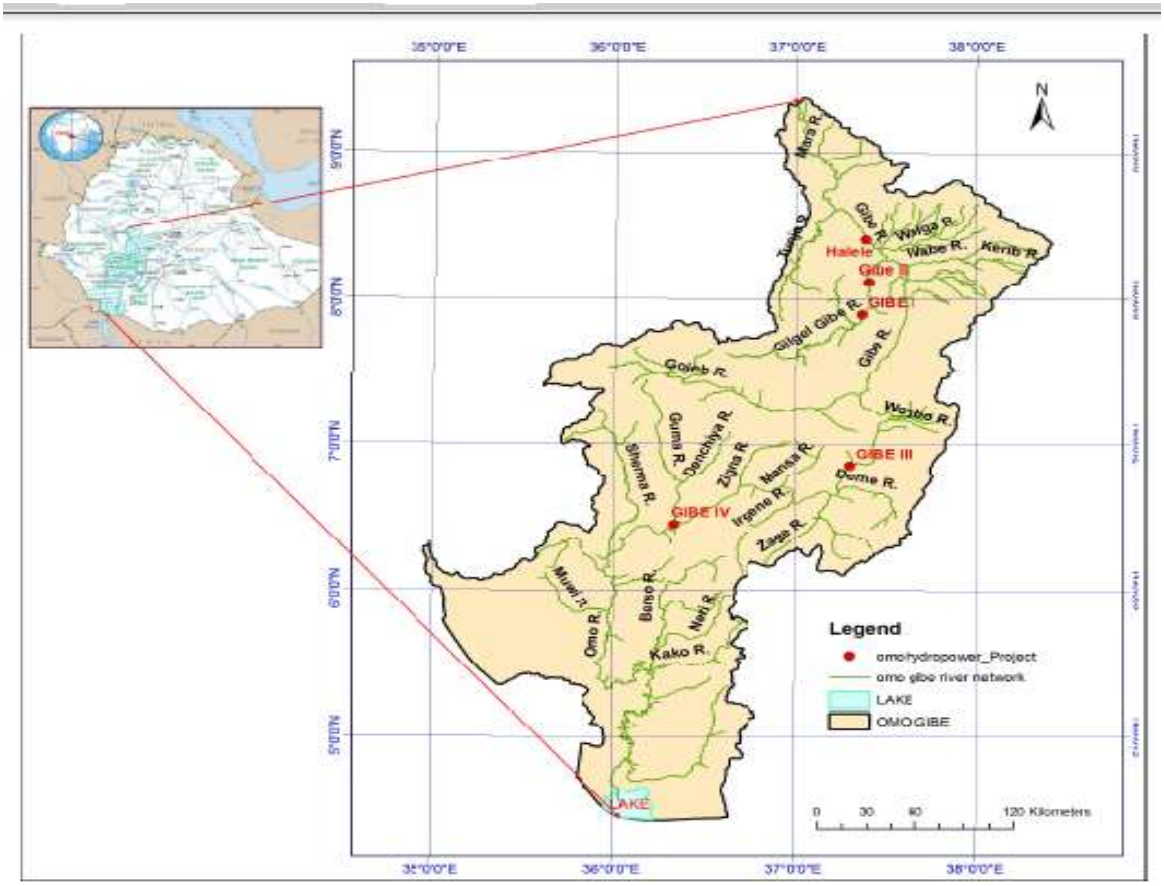

Figure 4: Map of Ethiopia, the Omo Gibe River Basin showing the main and tributaries of river network system of the watershed. (source: OGRBIDMPS, Volume VI)

The basin divides sharply and almost exactly into highlands in the northern half and lowlands in the southern half. This division reflected in all other aspect of the basin. The northern highland is deeply dissected and drained by the Gibe and Gojeb river system merging to form the Omo in deeply entrenched gorge (Richard and Associates, 1996). Steep slope with dissected hills characterized the highlands while the lowlands are characterized by relatively gentle and undulating slopes. The highlands area has an elevation as high as 4200 masl on mount Guge while the lowland areas fall in altitude of up to 500 masl. Around the northern and central part of the basin and for greater part of the eastern and western altitude is at minimum elevation of 2000m, frequently exceeding 2400m, and for the Wabe river catchment reaches 3500. Within a river distance of 50Km and much less around the north and north-east segment of the catchment

the streams, tributaries and main stem river to the elevation of the highland plateau typically between 1650m at Bako, in the north and 1350m at Jinka in the south-east.

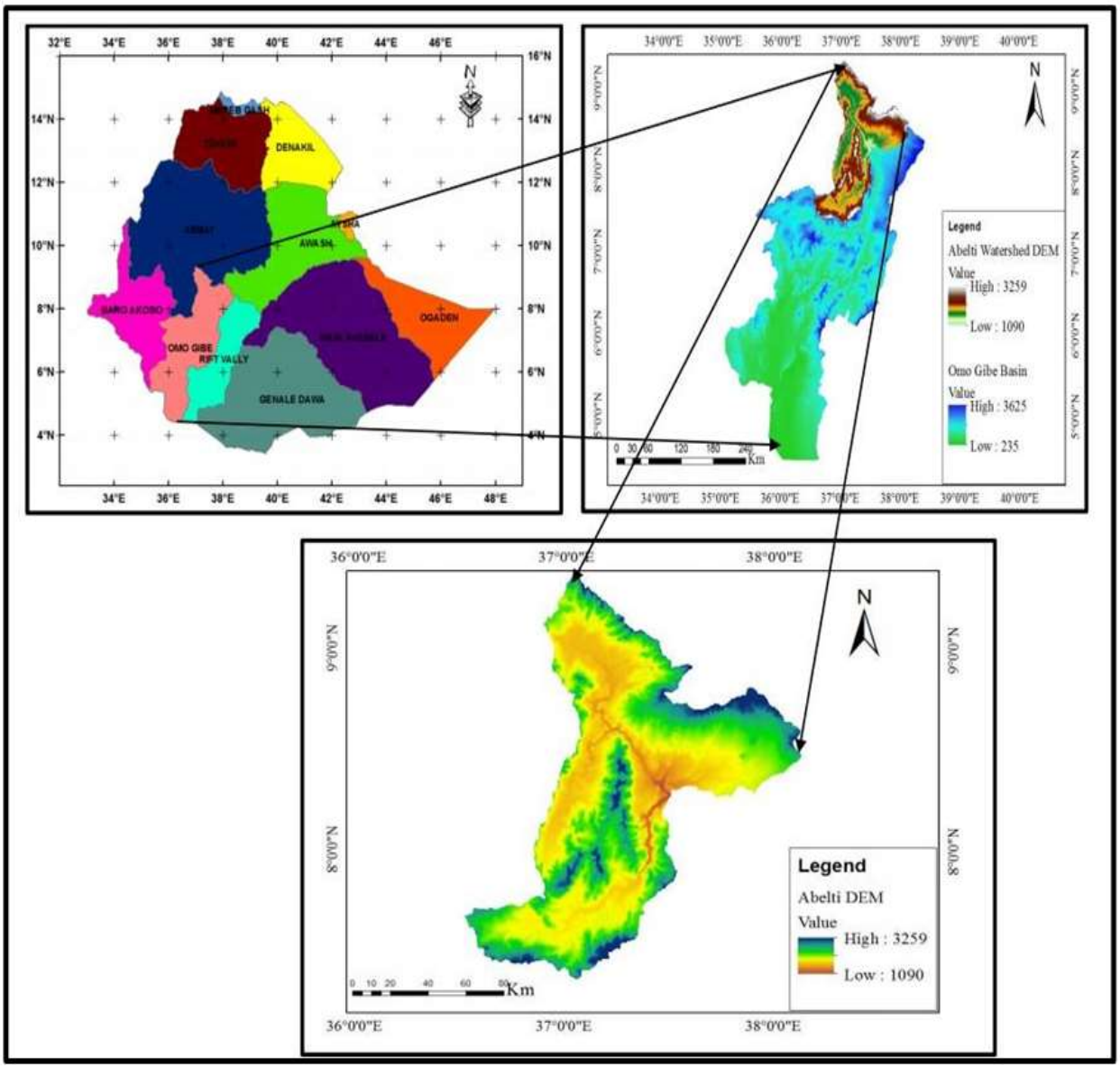

Figure 5: Location of the study Area

3.2.1.2 Climate

The climate of Omo-Gibe River valley varies from a hot arid climate in the southern most parts of the flood plain to a tropical humid one in the highlands that include the extreme north near Bako, the areas surrounding Jimma and around the head waters of the Gojeb River. Intermediate between these extremes and for greater part of the Basin the climate is tropical sub humid.

As climate is associated with altitude the highlands have cool climate with moderate temperature and sufficient rainfall while lowlands have harsh climate of high temperature and low to moderate rainfall. Annual rainfall varies from 400 mm in extreme south lowlands to 1900 mm in the highlands with the average being 1140 mm. the mean annual temperature in the basin varies from less than 17°c in the west highlands to over 29°c in the south lowlands. Based on the altitude and temperature, the basin can be classified into four agro-ecological zones, namely, Wurch, Dega, Weina Dega and Kolla (NMSA).

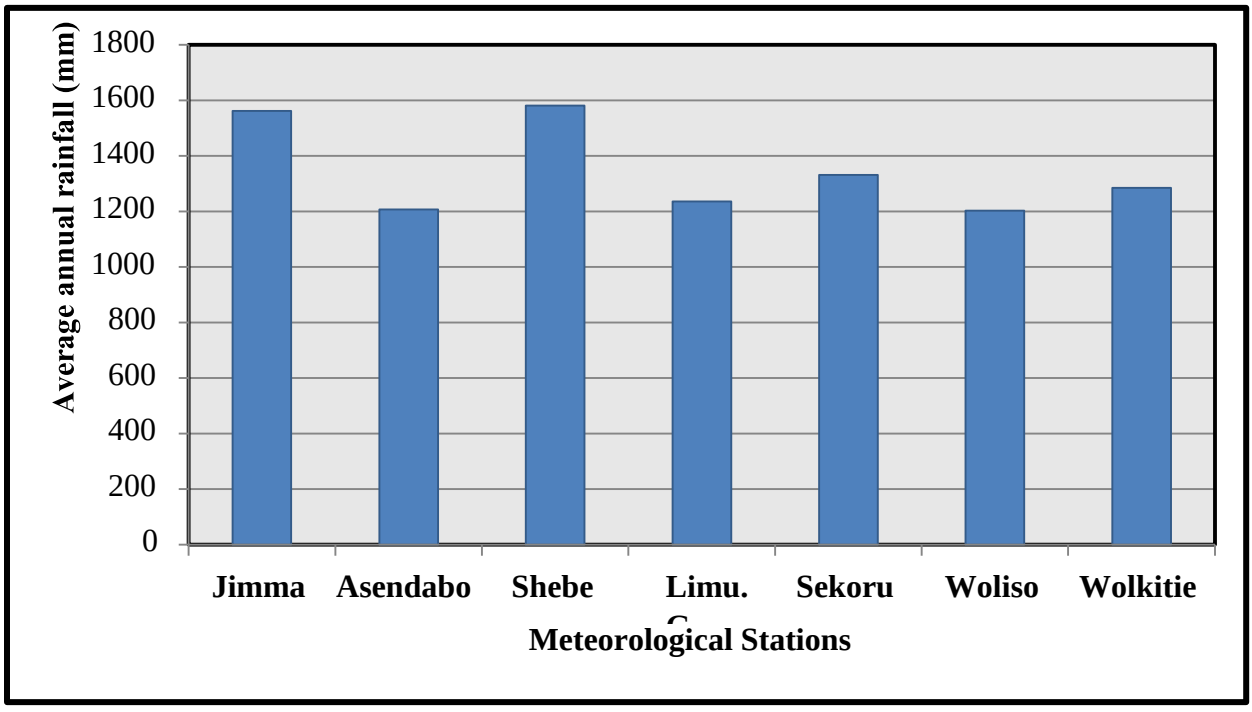

Figure 6: Average Annual Rainfall Distribution in the study area (2000-2012)

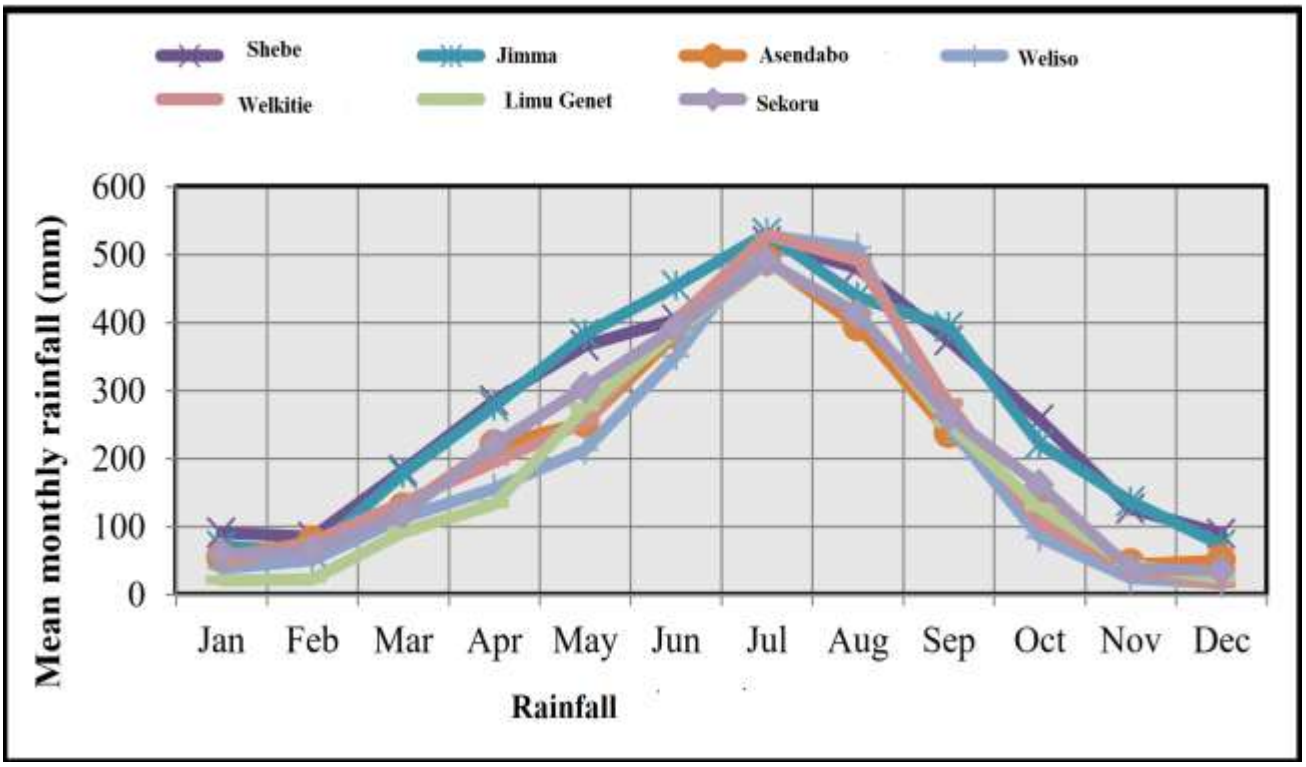

Figure 7: Mean monthly Rainfall Distribution in the study area (2000-2012)

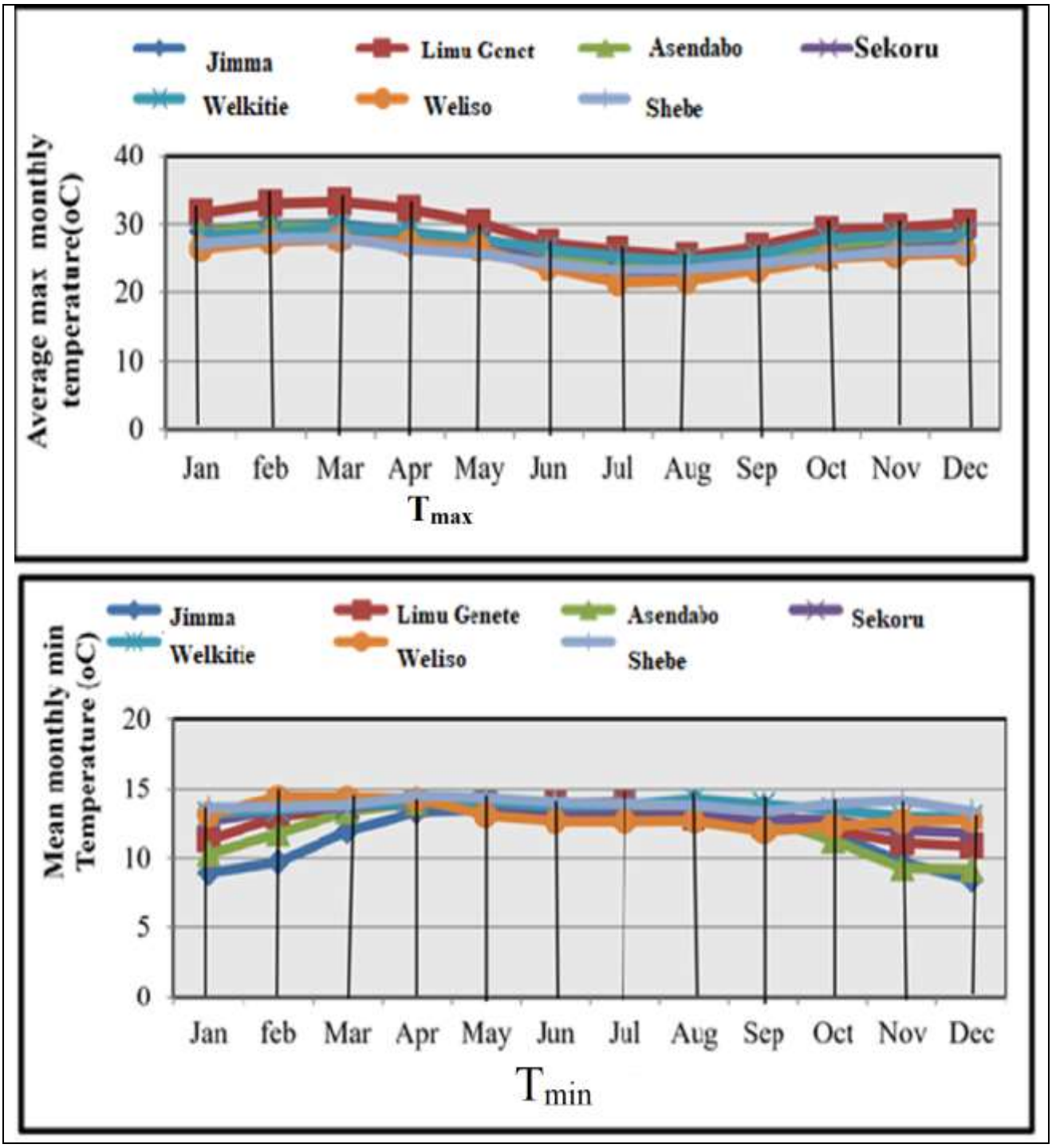
Jimma
Limu Genet
Asendabo
Sekoru
Welkitie
Weliso
Shebe
Average max monthly temperature(oC)
40
30
20
10
0
Jan feb Mar Apr May Jun Jul Aug Sep Oct Nov Dec
Tmax
Jimma
Limu Genete
Asendabo
Sekoru
Welkitie
Weliso
Shebe
Mean monthly min Temperature (oC)
20
15
10
5
0
Jan feb Mar Apr May Jun Jul Aug Sep Oct Nov Dec
Tmin

3.2.1.3 Land use

The land cover type of the basin consists of cultivated lands including fallow (28.6%), forest lands (13.5%), wood lands (28.8%), grass lands (15.7%) and bush and shrubs (13.4%) some of the two-third of the forest area can be classified as contiguous forest of significant importance both for watershed protection, soil conservation and timber. With regards to land use the high land areas are used primarily for cultivation sometimes mixed with grassing (agro-pastoral) or tree (agro-silvicultural). Silviculture land use consider with the contagious forest areas and pastoral land use with grass land areas. In the other case more than 67.06% of the watershed land cover was agricultural land. The land use of study area categorized mainly as agricultural 67.06%, Forest 6.14%, Urban 10.82%, range grasses (2.11%), Coffee (6.05%) water 0.52 % and Corn 0.34% respectively. Land use/Land cover map of the study area is shown in Figure 9 below.

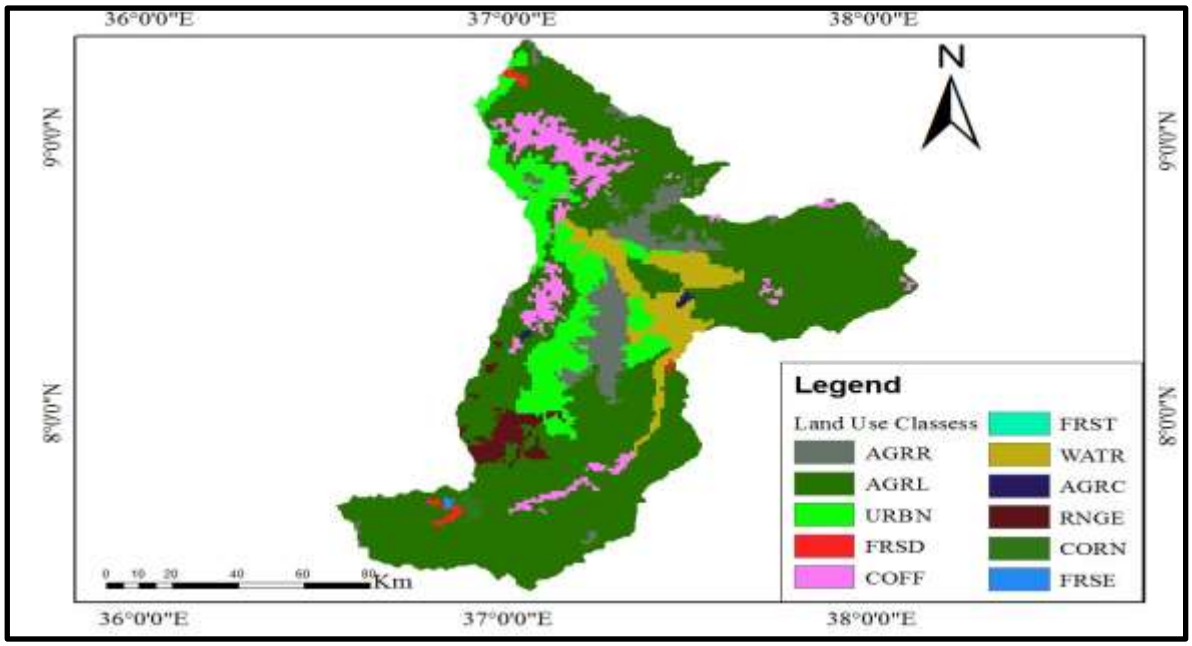

Figure 8: Land Cover Map of the Study Area

3.2.1.4 Hydrology

Great Gibe near Abelti is the gauging station of this river which is the biggest contributor river flow of the watershed above the dam. For this reason, the Ethiopian Minister of Water Resources installed the gauging station downstream of the main route river near Abelti.

This flow data was obtained from MoWIE. Based on the data from 2000 - 2012 records the watershed has an average annual flow of 211.8m^3/sec. The monthly average discharge at the Abelti gauging station is shown below in Figure 10

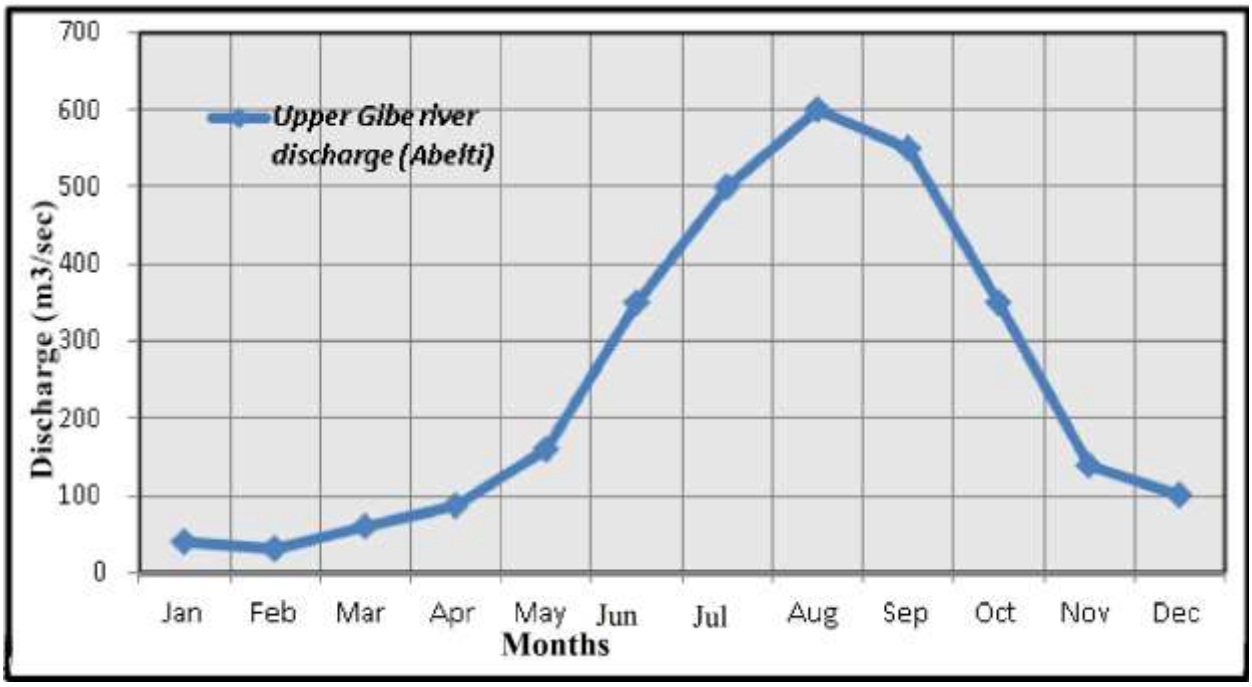

Figure 9: Monthly average Discharge at the Abelti gauging station

3.3 GENERAL METHODOLOGY

The study required different materials and models to arrive at the stated objectives as shown in figure 11 below.

For this study, meteorological, hydrological, and river cross section data were required. Data such as rainfall, temperature and other climate parameters for estimations collected from the National Meteorological Agency (NMA) of Ethiopia and Satellite. Stream flow obtained from Ministry of Water, Irrigation and Electricity and River cross section data from Ethiopia water Construction and supervisor Dam Design Team.

Regionally Downscaled Climate change data also provided from IWMI. The data derived from HadGEM2-ES Global climate model outputs that are dynamically downscaled by the CORDEX-

Africa program (http://wcrp-cordex.ipsl.jussieufr) using RCA4 regional model for the Representative Concentration Pathway scenario - RCP 4.5 projection scenario.

The development of the flood hazard map under present and future climate scenarios in the study area is based on a two-dimensional flood modelling MIKE FLOOD modelling it couples a 1D channel flow model (MIKE 11) with a 2D overland flow model (MIKE 21) applied on Upper Gibe catchment. Outputs of the hydrological model used as input for MIKE FLOOD. This method of flood modelling has the capability to estimate flood depths, velocities, extents. The developed flood hazard maps would be vital for planning any structural and non-structural measures that need to adopt to mitigate climate change induced flooding effects.

Arc GIS 10.1 and QGIS used to analyze spatial data including preparing base maps, land use land cover map and other maps that serve as inputs to the other models used in this study.

In this study, two basic hydrological and Hydraulic modelling systems that were developed to meet the objectives of the study.

The overall conceptual flow chart of the research methodology is presented as the following flow chart.

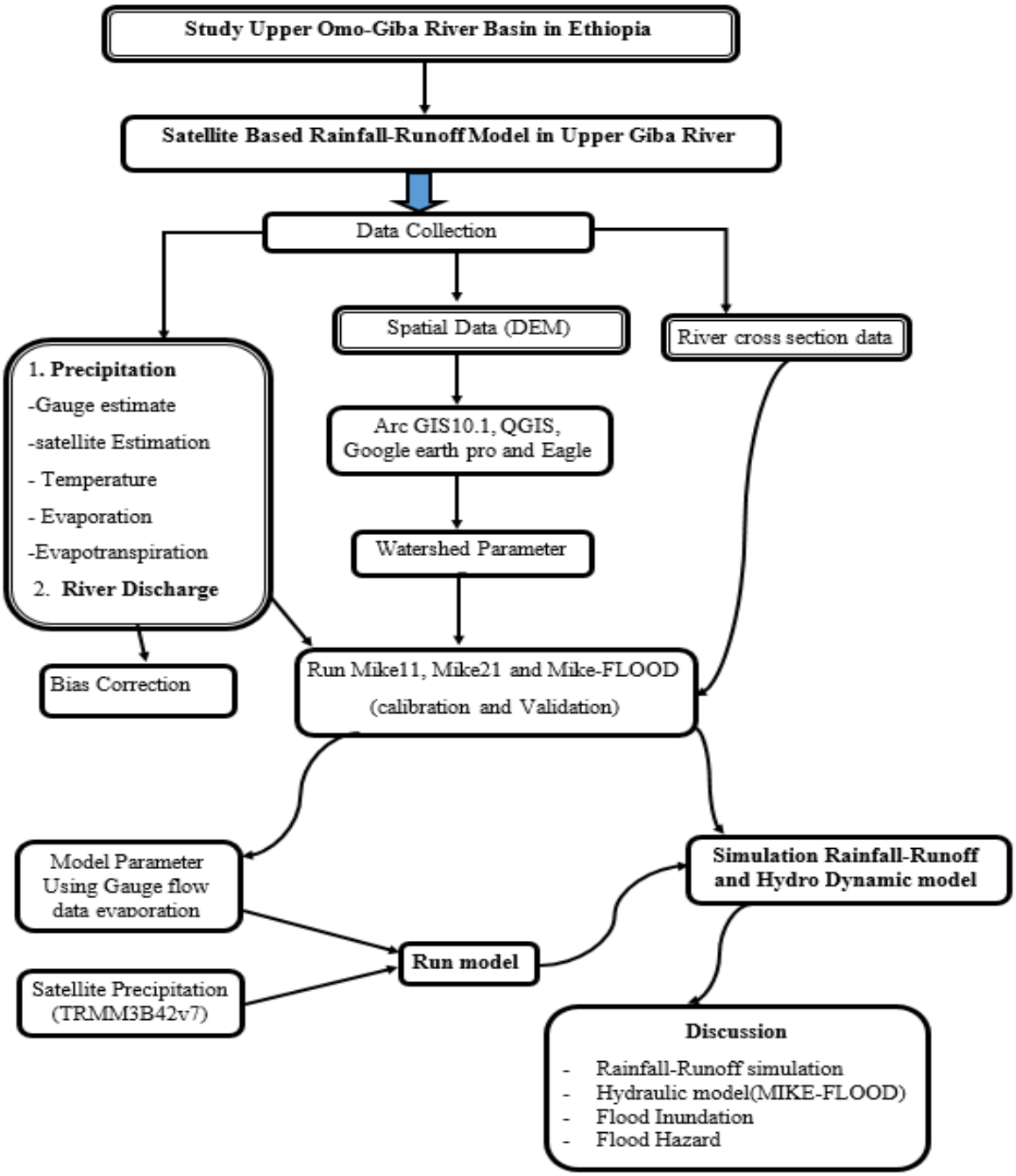

Figure 10: Schematic Diagram of Methodology of the stud

3.4 *DATA COLLECTION AND ANALYSIS*

In order to have reliability in this research work, having relevant information or data is mandatory. These data are Meteorological data (rainfall, temperature, relative humidity, wind speed and sunshine hour), hydrological data (stream flow), satellite precipitation product data (TRMM TMPA 3B42v7, CMORPH and PERSIANN) and other data which is catchment physio-graphical data are required. With these, MIKE-11, MIKE-21 and MIKE-FLOOD model are requiring. Meteorological and Hydrological input data in daily time step including discharge, rainfall, temperature, and evaporation. All data arranged as per the requirement of the model in selected stations and the record length of these stations is 13 years.

3.4.1 Meteorological Variables

MIKE 11, MIKE21 and MIKE-FLOOD models need climate data for hydrological simulation. In the study area meteorological stations of different classes are found and collected from the Ethiopian National Meteorological Services Agency (NMSA). Based on the classification of the Agency there are principal, also termed as class one station, where precipitation, air temperature, wind speed, relative humidity and sunshine duration measurements are taken every three hours. Another set of stations are class three stations (ordinary stations), where precipitation and air temperature measurements are taken daily. In addition, Class four stations only serve for precipitation measurements at daily base. Based on this classification Jimma and Wolkite are principal stations whereas, Asendabo, Bako, Shebe, Woliso, Limugenet and sekoru are Class three stations. Measurements time series covers a period of 2000 – 2012. The meteorological variables collected for this study, meteorological station names and their locations are shown below

Table 2: Metrological data availability on selected site (source: NMSA)

S.No	Station Name	Station ID	Latitude (degree)	Longitude (degree)	Elevation (m)	RF	Temp (Max,Min)	Relative Humidity	Sun hr	Wind speed
1	Asendabo	RR01	7.77	37.53	1764	✓	✓	X	X	X
2	Jimma	RR02	7.4	36.5	1725	✓	✓	✓	✓	✓
3	Limugene	RR03	8.05	6.573	1690	✓	✓	X	X	X
4	Sekoru	RR04	7.34	37.5	2100	✓	✓	X	X	X
5	Shebe	RR05	7.55	37.25	1813	✓	✓	X	X	X
6	Wolkite	RR06	8.27	37.75	1550	✓	✓	✓	✓	✓
7	Woliso	RR07	8.33	37.59	1960	✓	✓	X	X	X
8	Hosanna	RR08	7.5	36.52	1650	✓	✓	X	X	X

Note: - **'✓' represent data available 'X' represent data not available**

3.4.2 River Discharge Data

River discharge data of the basin was collected from the Ministry of Water, Irrigation and Electricity (MoWIE), Hydrology department for a period of 13 years (2000- 2012). The River discharge data is then used for time series value for calibration and validation of the model. For discharge analysis daily discharge data in the basin are gauged at 47 stations and we have available flow data at 29 stations. For this particular thesis work we use flow gauging stations namely Abelti (Great Gibe) and Walkite (Wabe). The collected rainfall data were analyzed to determine different hydrological relations essential for rainfall-runoff modeling. The list of all flow gauging stations of Omo-Gibe River basin are tabulated and mapped below with their specific location.

Table 3: Flow Gauging Stations (OGRBIDMPS, Volume VI)

River	Site	Ref	UTM	Area (km2)	Remarks
Great Ghibe	Abelti	91001	307230 910432	15746	Calibrated
Aku	Maji	91002			Abandoned
Rebu	Welkite	91003	366029 923114	480	Calibrated
Wabe	Welkite	91004	367809 904680	1866	Calibrated
Megecha	Gubre	91005	367809 904680	286	Calibrated
Gotam	Imdibir	91006	380684 899116	65	Calibrated
Gogeb	Imdibir	91007	378801 895435	109	Calibrated
Gilgel Ghibe	Asendabo	91008	299648 857010	2966	Calibrated
Gibe Jun.	Nono	91009	415638 950628	3654	Not Operated
Walga	Welkite	91010	345831 921338	1792	
Gojeb	Shebe	91011	211147 820587		
Gojeb	Shebe	91012	211147 820587	3494	Calibrated
Ghibe Limu	Limu	91013	303249 838563		Abandoned
Gibe	Limu Genet	91014	239771 991915	2394	Calibrated
Rebu	Weliso	91015	389941 943316		Abandoned
Kebala	Dimtu	91016	307049 868039		Abandoned
Seka	Seka	91017	251750 840646	294	Calibrated
Wedessa	Tole	91018	310965 925162		
Bidru Awa	Sekoru	91019	323620 875345	41	Calibrated
Ghibe	Bako	91020	285693 1008237	288	Calibrated
Amara	Bako	91021	294836 1004502	68	Calibrated
Werabessa	Tole	91022	347713 934232		
Kito	Jima	91023	261004 851661	85	
Awaitu	Jima	91024	260995 849817	72	
Woshi	Dimbira	91025		240	Calibrated
Kulit	Tedele	91026	353212 932370	350	
Darghe	Tedele	91027	340372 934258	266	
Gibe	Beda Buna	91028			
Upper Darghie	Darghie	91029			
Bulbul	Serbo	91030		532	Calibrated
Omo	Bele	92001	326899 762909		Simulated
Gecha	Bonga	92002	192644 805944	175	Calibrated
Sheta	Bonga	92003	194486 805933	191	Calibrated
Guma	Anderacah	92004	196238 791167	231	Calibrated
Dincha	Anderacha	92005	199956 796678	443	Calibrated
Sawula	Alasawla	92006	247328 685794		
Donba	Borka	92007	313805 703976	200	
Mazie	Morka	92008	300922 711392	937	Calibrated
Soke	Araka	92009	358286 790456	103	
Ajancho	Araka	92010	358271 784928	306	

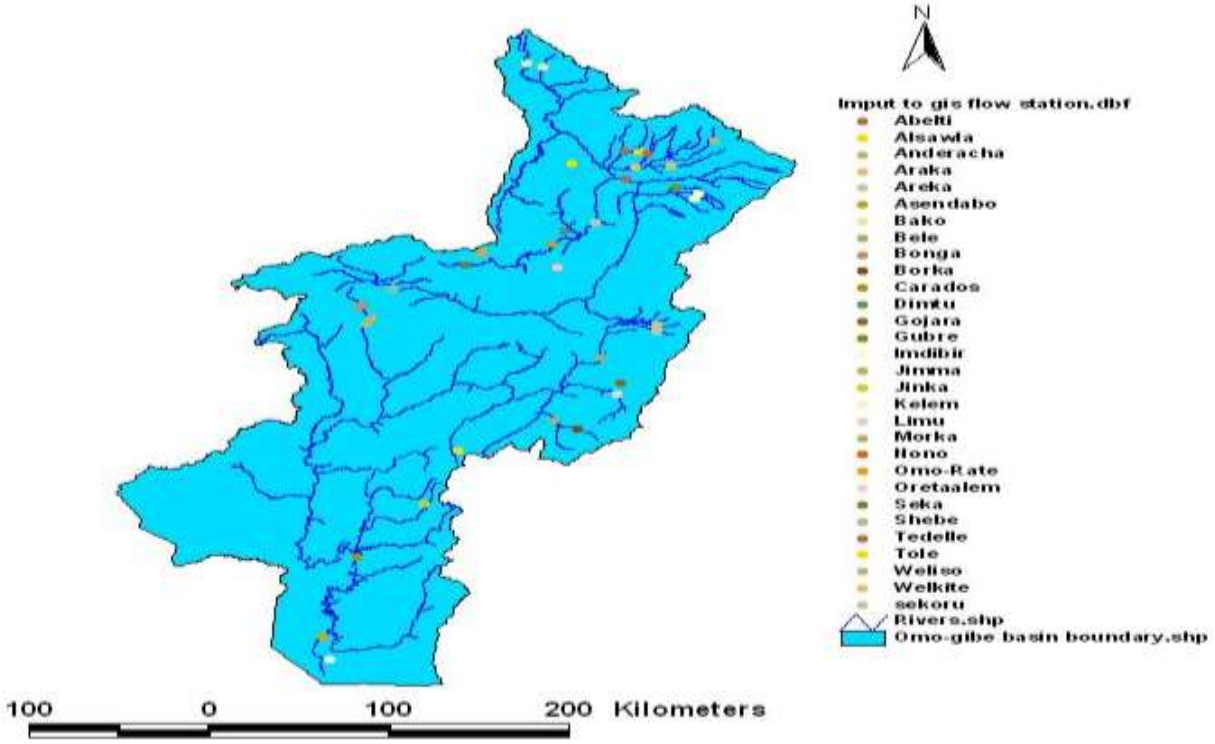

Figure 11: *Stream flow gauging stations*

3.4.3 Digital Elevation Model

A Digital Elevation Model (DEM) gives the elevation, slope and defines the location of streams network in a basin. The DEM used in this study was obtained from Ministry of Water, Irrigation and Electricity (MoWIE), GIS and Remote sensing department with a spatial resolution of 1 Arc – second (30 x 30 m). The DEM was then used into MIKE ZERO model for watershed delineation, Mesh generation and completing river network.

3.4.4 Land Use/Land Cover Data

The land use/land cover map gives the spatial extent and classification of various land use/land cover classes in the study area. The land use/land cover map of the study area was obtained from Ministry of Water, Irrigation and Electricity (MoWIE), GIS and Remote sensing department. It is used for analysis factor that the flood occurrence in the area.

3.4.5 Satellite Rainfall Products (SRPs)

Satellite based rainfall product (estimation) is decisive in a stream flow simulation which is a major concern of hydrological modeling. In particular, in developing countries where stream

gauging stations and meteorological stations are poor, hydrological modeling using satellite products is unique. Many researches carry on a satellite derived as a gift to overcome the problem of gauging data scarcity.

3.4.6 CMORPH Satellite Products

The CMORPH rainfall product is available since December 1998 at various spatial and temporal resolutions (e.g., 8 x 8km^2, 0.25^0 x 0.25^0; 30min, 3 hourly and daily) for regions that are situated between 60^0N-S. Version 0.x CMORPH products can be freely accessed.

In this study CMORPH version_0.x product with spatial and temporal resolution 0.25^0 x 0.25^0, daily.

Rainfall data from January 2000 to December 2012 were extracted. Fortunately, in situ rainfall measurements are at daily scale (from UTC 00 to UTC 24). Thus, the daily aggregated CMORPH products were used in this study. It is to be noted that CMORPH has also released an additional bias corrected precipitation product (CMORPH V_1.0), which uses gauge observations for bias correction. The reason why V_1.0 was selected for this study is to assess both of the selected satellite rainfall estimates similarly, since TRMM3B42v7 have no bias corrected version.

3.4.6.1 **TMPA_3B42RT_Daily v7** *Rainfall Product*

Tropical Rainfall Measuring Mission (TRMM) Multi-satellite Precipitation Analysis (Huffman, 2007) uses MW data to calibrate the IR-derived estimates and creates estimates that contain MW-derived rainfall estimates when and where MW data are available and the calibrated IR estimates where MW data are not available. The TMPA rainfall products are available in two versions: a near-real-time version (TMPA 3B42RT, or 3B42RT for short) and a gauge-adjusted post-real-time research version (TMPA 3B42, or 3B42 for short). The 3B42 products are released 10–15 days after the end of each month.

The precipitation estimates from several microwave instruments are calibrated against the merged radar and radiometer precipitation products from TRMM, and then merged to produce a near-global 3-hour, daily and monthly precipitation but we use daily precipitation product. The

pixels with no microwave instrument observations are filled with measurements from IR instruments on board, geostationary satellites that are calibrated using Passive Microwave (PMW) measurements. The TRMM 3B42v7 is the real-time version of the product that does not have a gauge correction.

A new version (TRMM3B42v7) rainfall product is available at various spatial and temporal resolutions and 0.25^0 x 0.25^0 – daily current version (V_7) TRMM3B42v7 rainfall estimates from January 2000 to December 2012 were obtained with total time step is 4758.

3.4.6.2 PERSIANN Rainfall Products

Both raw PERSIANN product and bias-corrected PERSIANN product can be obtained from GPCP. The bias-corrected PERSIANN precipitation maintains total monthly precipitation estimates to be consistent with GPCP (global precipitation climatology project) product. In this study, the raw PERSIANN data at the spatial resolution of 0.25°x0.25° and temporal resolution of daily were downloaded from the global precipitation climatology.

Generally, in this study mainly focus on evaluating the performances of three commonly used satellite precipitation products (TRMM3B42v7, CMORPH, and PERSIANN) rain gauge data at consistent temporal and spatial scales and it provided insight for hydrologist in the Great Gibe watershed on the level of estimation error in each satellite rainfall product, implications for stream flow forecast in this watershed and simulating the flood event on the lower part of the River using 1D and 2D MIKE model Tools. The three satellite rainfall products were evaluated in this study are Tropical Rainfall Measuring Mission (TRMM, TMPA3B42v7), The Climate Prediction Center's morphing (CMORPH) and Precipitation Estimation from Remotely Sensed Information using Artificial Neural Networks (PERSIANN) product.

3.5 SOFTWARE'S USED FOR EXTRACTION OF SATELLITE RAINFALL PRODUCTS

Net-CDF is a set of software libraries and machine-independent data formats that support the creation, access, and sharing of array-oriented scientific data. It is also a community standard for sharing scientific data. The Uni-data Program Centre supports and maintains Net-CDF programming interfaces for C, Java, and FORTRAN. Programming interfaces are also available for Python, IDL, MATLAB, R, C++, Ruby, and Perl. Data in Net-CDF format is: - Self-Describing, portable, scalable, append able, sharable and achievable (Rew, 1990).

Panoply is a cross-platform application which plots geo-gridded arrays from Net-CDF, HDF and GRIB datasets. With the help of Panoply, we can slice and plot geo-referenced latitude longitude, latitude-vertical, longitude-vertical, time-latitude or time-vertical arrays from larger multidimensional variables, plot longitude-latitude data on a global or regional map and overlay continent outlines or masks on longitude -latitude map plots. Panoply Net-CDF, HDF and GRIB data viewer software was freely accessed using the following URL1 and used for online visualization of satellite rainfall products downloaded in Net-CDF data format for further analysis.

3.6 DATASETS FOR HYDRODYNAMIC MODELING

In order to operate MIKE 11, MIKE 21 and MIKE FLOOD, an important set of input data is required. In flood extent predictions, the quality of the input will account for the overall quality of the model.

Recent techniques allow the use of high resolution DEM, airborne and synthetic aperture radar (SAR) imagery to improve quality and validation of flood extent models. Topography is constantly under modification due to erosion, transport and deposition of sediments. Quality of the bathymetry and topography is the most important factors of the overall quality of the model. Therefore, more recent data collection was required for this study.

3.6.1 Methodology for Model Set up

The methodology used to generate the flood hazard map is to assign the various flood hazard the ground truth surveys and the flood history to the various villages with the study area. The Ground truth survey carried out to identify the villages in the study area and the agricultural productive areas within the villages. The ArcGIS software is used for the Digitizing the map, GIS study and Geo referencing respectively. The model used for the analyses consists of two parts, a one-dimensional network model and a two-dimensional ground elevation model. These configured separately before they coupled.

3.6.1.1 River cross section and Flood plain data

River cross section data represent the geometric boundary of the stream. Cross sections are required at representative locations throughout the stream and at locations where changes occur in discharge, slope, shape, roughness; at locations where levees begin and end; and at hydraulic structures (bridges, culverts, and weirs).

The cross sections provided for river reach at an average interval of 1km. A raw data entered by setting insert branch. The MIKE 11 model's River Network file is the common link to the various MIKE 11 files. The raw data then automatically processed into a form used in the hydrodynamic calculations; that is, the hydraulic parameters, cross-sectional area, hydraulic radius and storage width calculated for different water levels between minimum.

Cross-sections were the main input to the 1D-Hydraulic Model used for the analysis of flood maps of the study Area. The raw data was from Ethiopia water Construction and supervisor Dam Design Team. The cross section data measured from Bank Top Left, Bank Bottom Left, River Centre Line, Bank Bottom Right and Bank Top Right five character points starts from Gojeb to Great Gibe.

Forty-three cross sections derived in Upper Gibe River. The parameters required to define the cross sections are spatial location of the extreme end of the cross section (left and right) and the elevations of the cross section is to be defined along the chainage from left to right end. These parts of cross sections not used for simulation. Only used Left high flow channel (Left levee

bank), Low flow channel (Lowest point) & Right high flow channel (Right levee bank) for simulation. (See Appendix-E).

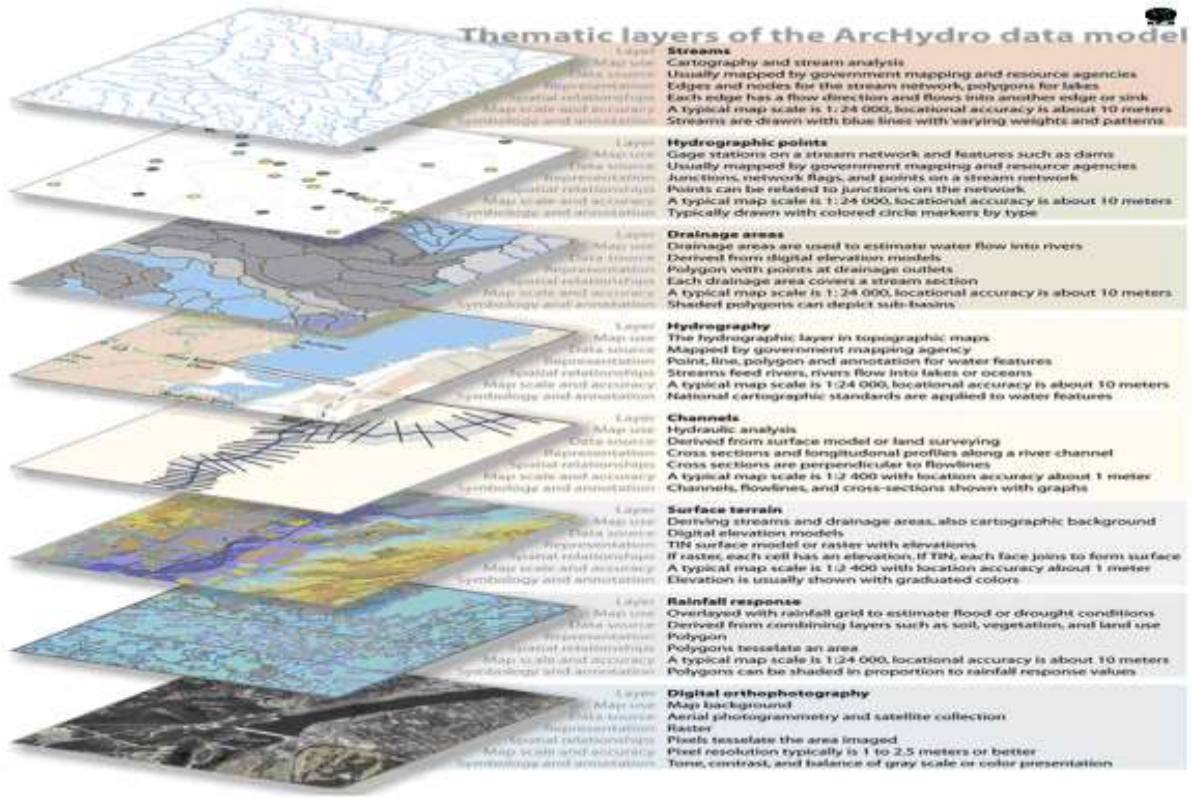

Figure 12: Thematic Layer of Arc hydro data model **(***source: Gennadiy Donchyts UCEWP, Kiev***)**

3.6.1.2 MIKE-11 Hydrodynamic Model

MIKE 11 is a hydrological model created by the Danish Hydraulic Institute (DHI) in 1987. The model consists of a network of cross sections that linked by a one-dimensional channel. MIKE11 is software developed by DHI to simulate 1D flow problems. The software enables the user to simulate unsteady flow in river networks as well as looped networks using an implicit finite difference scheme. Sub-critical as well as supercritical flow conditions are calculated. The one-dimensional model based on the cross-sectional averaged Saint-Venant equations, describing the development of the water level and the discharge or the mean flow velocity. It is best simulation model to simulate the river / stream / channel conditions. These river / stream / channels described in cross section along the chainage from upstream to downstream with boundary condition in the form of water level database in the observed time step in the field.

The MIKE 11 is an implicit finite difference model for one dimensional unsteady flow computation and applied to looped networks and quasi-two dimensional flow simulation on floodplains. MIKE 11 is capable of using kinematic, diffusive or fully dynamic, vertically integrated mass and momentum equations the "Saint Venant" equations. The solution of the continuity and momentum equations based on an implicit finite difference scheme.

This scheme is structured to be independent of the wave description specified (i.e. Kinematic, Diffusive or dynamic). When using a fully dynamic wave description, MIKE 11 HD solves the equations of conservation of continuity and momentum (MIKE Zero, 2016).

Saint-Venant Equations

Solving the problem of an arbitrary flow of water through three-dimensional canals is computationally impractical. Fortunately, the geometry of pipes and canals allows for a set of approximations, which naturally fit the problem space. The approximations rely on the following assumptions:

- Water is incompressible and homogeneous, i.e., it has negligible variations in density
- The bottom slope of pipes and canals is small, so that the cosine of the angle it makes with the horizontal taken as one.
- The Wavelengths are large compared to the water depth. This ensures that the flow everywhere regarded as having a direction parallel to the bottom, i.e. vertical accelerations neglected and a hydrostatic pressure variation along the vertical assumed.
- The flow is sub-critical (a super-critical flow modelled in MIKE 11; however, more conditions that are restrictive are applied).

With these assumptions, two simplified equations derived from the Navier-Stokes equations, which usually called the Saint-Venant equations, or Shallow Water equations:

Continuity equation:

$$\frac{\partial Q}{\partial x} + \frac{\partial A}{\partial t} = q \quad \text{.....[3.3]}$$

Momentum equation:

$$\frac{\partial Q}{\partial t} + \frac{\partial\left(\alpha \frac{Q^2}{A}\right)}{\partial x} + gA\frac{\partial h}{\partial x} + \frac{gQ|Q|}{C^2 AR} = 0 \quad \text{.....[3.4]}$$

Where,

Q – Discharge, (m^3/s)

A – Flow area, (m^2)

q – Lateral inflow, (m^2/s)

h – Stage above datum, (m)

C – Chezy resistance coefficient, ($m^{1/2}/s$)

R – Hydraulic or resistance radius, (m)

α – momentum distribution coefficient

The four terms in the momentum equation are local acceleration, convective acceleration, pressure, and friction (Source: www.dhigroup.com). MIKE 11 solves the Saint-Venant equations by means of a finite difference scheme.

The momentum equation expresses conservation of momentum; the first two terms on the left side of the momentum equation represent the inertia forces (local and convective acceleration), the third term represents pressure forces due to gravity, and the last term represent resistance/friction. The right-hand side represents an external momentum forcing.

A systematic MIKE 11 model generation executed from the MIKE Zero for the whole Upper-Gibe watershed channel network as reputed below:

Model Input

The five basic input parameters to specify for the MIKE-11 HD setup are the river network layout, cross sections, boundaries conditions, hydrodynamic parameters, Rainfall-Runoff parameters(RR) and simulation parameters.

A. Generation of time series data at gauge station

The layout of MIKE-11 river network was prepared by providing Map projection and the location of working area in detail. The daily hydrological gauge data obtained from the MWIE, rainfall taken from TRMM3B42_7. The data for gauge stations starting from 1st January, 2000 to

31st December, 2012. The daily inflow discharge data at Gibe River gauging stations (hydrograph) using MIKE ZERO and make a. dfs0 file extension.

- **Flood frequency mapping**

The most important factor determining flood hazard is flood frequency. The objective of flood frequency analysis was to relate the magnitude of floods to their frequency of occurrence using probability distribution. In order to commence this objective, the calculation of the statistical parameters of the proposed distribution made by the method of moments from the given data. In this study, the occurrence of flood in August 2006 the annual maximum runoffs for three different periods (base line, 2010's and 2020's) calculated for different return period floods.

The probability analysis is to provide reliable answers it must start with a data series that is relevant, adequate and accurate. Flood frequency analysis performed to develop relationships between flood magnitude and flood recurrence interval. The same achieved by performing a statistical analysis on time series of peak flows. Extracting peak flow data from a discharge series the annual maximum and peak over threshold methods in this paper used annual maximum method.

- **Flood Frequency Models**

In this study, for the selection of best distribution Easy Fit software used to analyze flood frequency in the catchment. Easy Fit is automatically fits selected distributions, performs goodness of fit tests, and displays graphs of fitted distribution. Sequential steps used to estimate the floods of given recurrence intervals involved selecting the highest peak flood in a hydrological year. The highest peaks in each hydrological year arranged in descending order of magnitudes and ranks then assigned. The return period of each of the ordered value and the probability of each event being equal to or exceed were computed using the Weibull's method. Four frequency distributions including the Generalized Extreme Value distributions (GEV), the Gumbel's or Extreme Value type 1 distribution (EV1), the Log-normal distribution and the Log-Pearson type III distribution (LP3) were compared for flood estimation.

The result compared with the frequency analysis results considering different techniques. The methods applied in this paper selected based on their efficiency and simplicity. However, the

primary criterion is their correlation with the simulated flow data of the Gibe River. They are selected using software called best fit for selection of methods. According to the output, the following four popular methods selected.

B. Time Series comparator (tsc.) Parameters

It is used to compare the performance satellite data with respect to the in situ data.

C. River Boundary conditions

MIKE-11 requires discharge at all upstream open boundaries and the water level or Discharge–Water Level relationship at the downstream open boundaries. The two open boundaries in this study provided with the inflow at upstream boundary condition and a constant water level at downstream boundary condition. A boundary defines the interaction between a model and its external surroundings. Two boundary conditions defined for the river reach in question. For the upstream boundary conditions, it consisted time-series of daily river flows at river gauging station. This obtained from flood frequency analysis for different return period with and without climate change. The downstream boundary condition consisted of a time series of water level for the Gojeb-River for the corresponding period as for the river flow.

The choice of the boundary conditions depends upon the availability of the data; but, in this case, estimated values taken based on the available measured hydrographs and the river water level.

D. Hydrodynamic (HD) Parameters

The final data required to run a simulation is the HD parameters. In this study, the riverbed resistance value and the initial conditions of discharge and water level/depth specified. The calibrated Manning's value of discharge and water depth of specified. The Manning's (n) resistance formula adopted and a resistance number (n) of 0.033 specified as an overall resistance for the whole stretch of the river under study.

E. Rainfall Runoff Model(NAM)

The NAM model is a deterministic, lumped and conceptual Rainfall-Runoff model. It considers river basin as one unit and based on considerations of the physical processes, these are highly relevant for this specific river basin under study and the simulation of the desired long- term flow. Furthermore, it is also as complete and efficient modelling program that allows flexibility

for further research. MIKE 11 NAM is a software package developed by Danish Hydraulic Institute (DHI), Denmark. This is a one-dimensional modelling tool developed since 1972, particularly for water resource planning. The MIKE11 NAM software is specifically meant for simulation of irrigation channels, rivers and other water bodies.

The hydrological model simulates at the catchment scale, the process of rainfall runoff. Within the same modelling framework; single catchment or a large river basin with numerous catchments and network of rivers can be treated as single unit. Four dissimilar and interconnected storages simulate the NAM model, these includes surface storage, ground water storage, root zone storage and snow storage. NAM model can therefore be prepared for the numbers of parameters of model, but considering the surface zone storage, root zone storage and ground water storage, model automatically accounts only 9 parameters as default.

The MIKE 11 NAM model was setup for upper Omo Gibe river basin to carry out R-R modelling. Catchment area of river basin in the confluence is 1732 km^2 Daily data of rainfall, runoff and evapotranspiration for the period of 13 years from 2000 to 2012 was used for modelling. Daily time series dfs file of rainfall, runoff evapotranspiration is created using MIKE ZERO. Then the model was calibrated and validated.

F. Simulation Parameters

Before running the model simulation, control parameters such as simulation period, simulation time step, data to be stored and storage time specified.

3.6.1.3 MIKE-21 Hydrodynamic Model

MIKE-21 HD is the basic computational 2D hydrodynamic model that simulates the water level variations and flows. The water levels and flows are resolved on a rectangular grid covering the area of interest. MIKE-21 solves the full, time-dependent, non-linear equations of continuity and conservation of momentum. The two dimensional model is based on the depth averaged Saint-Venant equations, describing the evolution of the water level and two velocity components (DHI 2016). The two velocity components permit a detailed description of the flow velocity on

complex floodplains. The two-dimensional model simulates the water depth and the velocities on a two-dimensional grid.

3.6.2 Model Calibration

Model was calibrated using the daily rainfall data of 13 years i.e. from January 2000 to December 2005. In the process of calibration, model parameters are modified to reduce the error between the simulated stream flow and some portion of the observed flow record and also the MIKE FLOOD model for the catchment was calibrated August, 2006 flood event which is the largest flood event recorded while both gauging stations have been operational. The infiltration and roughness coefficients for the MIKE 21 grid, and roughness coefficient for the MIKE 11 channels/drains were the main calibration parameters for this study.

3.6.3 Model Validation

It tests the ability of model of estimated runoff. In the process of validation, the model parameters were kept as the parameters obtained during model calibration and runoff was simulated for the remaining period of 7 years i.e. from January 2006 to December 2012.

For rainfall runoff modelling of Upper Omo Gibe river basin using MIKE11 Nam different data required i.e. rainfall, discharge and metrological data for the calculation of potential evapotranspiration and DEM (digital elevation model) for catchment delineation.

3.7 DATA ANALYSIS

3.7.1 Estimating Missing Precipitation

Failure of any rain gauge or absence of observer from a station causes short break in the record of rainfall at the station. The gaps estimated first before we use the rainfall data for any analysis. The surrounding stations located within the basin help to fill the missing data on the assumption of hydro meteorological similarity of the group of stations.

In this study Arithmetic mean method and Normal ratio method are used. Arithmetic mean method used when the normal annual rainfall of the missing station is within 10% of the normal annual rainfall of the surrounding stations. This is the case for the stations near the study area.

The general formula for computing missing precipitation by this method is:

$$P_x = \frac{1}{n}(P_1 + P_2 + ... + P_n) \quad \text{[3.1]}$$

Where P_1, P_2. . . Pn are the precipitations of index stations and

P_x is that of the missing station,

n is the number of index stations.

In Normal Ratio Method is used when the normal annual precipitation of the index stations differs by more than 10% of the missing station. This is the case for the stations near the study area. The general formula for computing missing precipitation by this method is:

$$P_x = \frac{N_x}{n}\left(\frac{P_1}{N_1} + \frac{P_2}{N_2} + ... + \frac{P_n}{N_n}\right) \quad \text{[3.2]}$$

Where P_1, P_2. . . P_n are the rainfall data of index stations,

N_1, N_2. . . N_n the normal annual rainfall of index stations,

P_x and N_x the corresponding values for the missing station x in question and

n is the number of stations surrounding the station x.

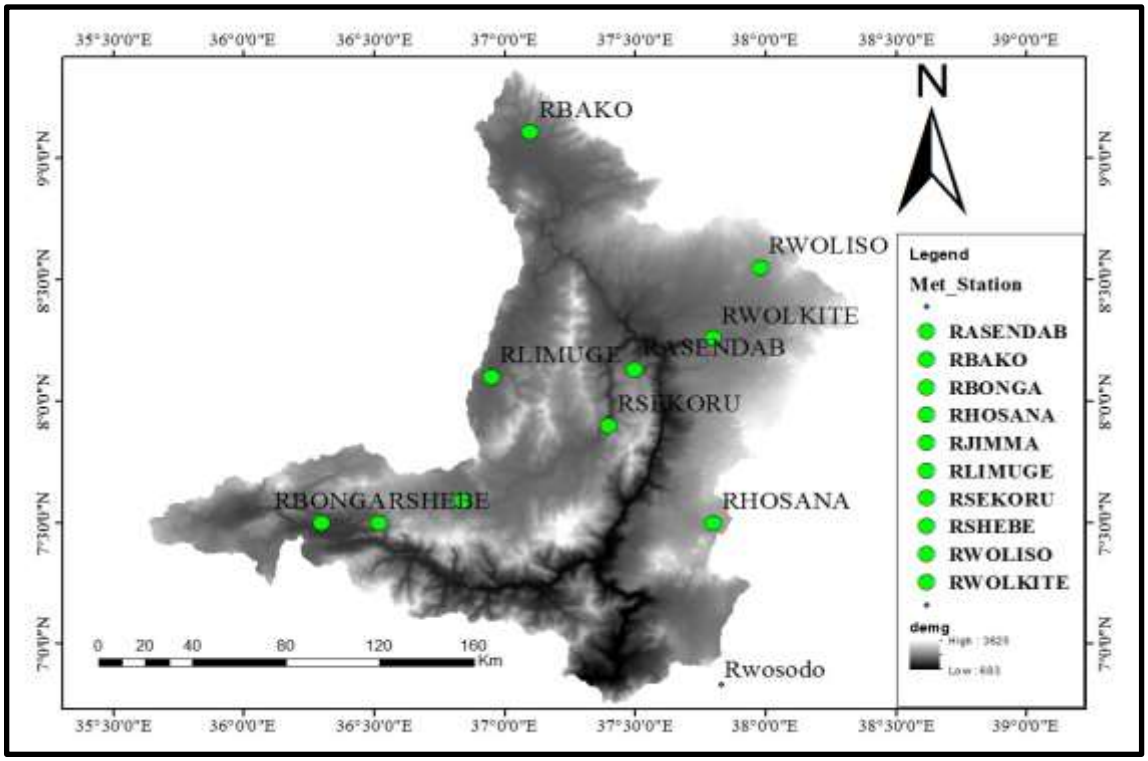

Figure 13: Distribution of Meteorological stations in the upper Omo Gibe

Table 4: Method used Estimating Missing Precipitation different gauge

SN	Stations	% missing	Method
1	Asendabo	2.0	Arithmetic Mean
2	Shebea	2.81	Arithmetic Mean
3	Jimma	10.13	Arithmetic Mean
4	Sekoru	18.56	Normal Ratio
5	Limu Genet	10.31	Arithmetic Mean
6	Welkita	13.23	Normal Ratio
7	Woliso	20.5	Normal Ratio
8	Hosaina	25.2	Normal Ratio

3.7.2 Transposing flow data to Abelti station

There are situations when the flow data of tributary at a certain station is available and the flow data at a confluence of the main river is required. To solve the problem, the area of tributary catchments up to the gauging station and the corresponding residual catchments at the downstream up to the confluence point may be calculated. And a flow relationship for daily records may be synthesized using an equation developed at the confluence site with an area ratio of the upstream and the downstream catchments. The area ratio method is adopted with the assumption that the gauged upstream and the residual downstream catchments are considered to be hydrological homogeneous.

Table 5: Summary of Area Ratio Calculation

Tributary river	Gauging station	Catch. Area at gauging station (Km^2)	Catch. Area at the confluence (Km^2)	Area of residual catch. =(4)-(3)	Area ratio
(1)	(2)	(3)	(4)	(5)	(6)
Great Ghibe	Abelti	15804	15804	0	1.00
Wabe	Welkite	1866	1943	77	1.041265
Megecha	Gubre	1096	1221	125	1.114051

3.7.3 Consistency Test

Estimating missing precipitation is one problem that hydrologists need to address. Rainfall data reported from a station may not be always consistent over the period of observation of rainfall record. A second problem occurs when the catchment rainfall at rain gages is inconsistent over a period and adjustment of the measured data is necessary to provide a consistent record. A consistent record is one where the characteristics of the record have not changed with time.

Inconsistency may result from Change (unreported shifting of the rain gauge) in gauge location, significant construction work in the area might have changed the surroundings, Change in observational procedure incorporated from a certain period and A heavy forest fire, earthquake or landslide might have taken place in that area.

Such changes at any station are likely to affect the consistency of data from a station. It is difficult to set out direct analysis to detect possible errors. However, through checking consistency of individual stations, the data qualities with regard to possible temporal variations or errors been investigated by double Mass curve.

Double Mass Curve Analysis used to adjust inconsistent data. In this method, the accumulated annual rainfall of a particular station compared with the concurrent accumulated values of mean rainfall of groups of 5 to 8 surrounding base stations. The procedure consists of comparing the accumulated annual (or seasonal, monthly, weekly, daily, or hourly) precipitation at the station in question with the accumulated annual (or seasonal, monthly, weekly, daily, or hourly) precipitation for a group of surrounding stations. (Wijngaard, 2003).

If the station affected by the trend, a break in the slope of the curve would indicate that conditions have changed at that location and needs to adjusted for the consistency of the record.

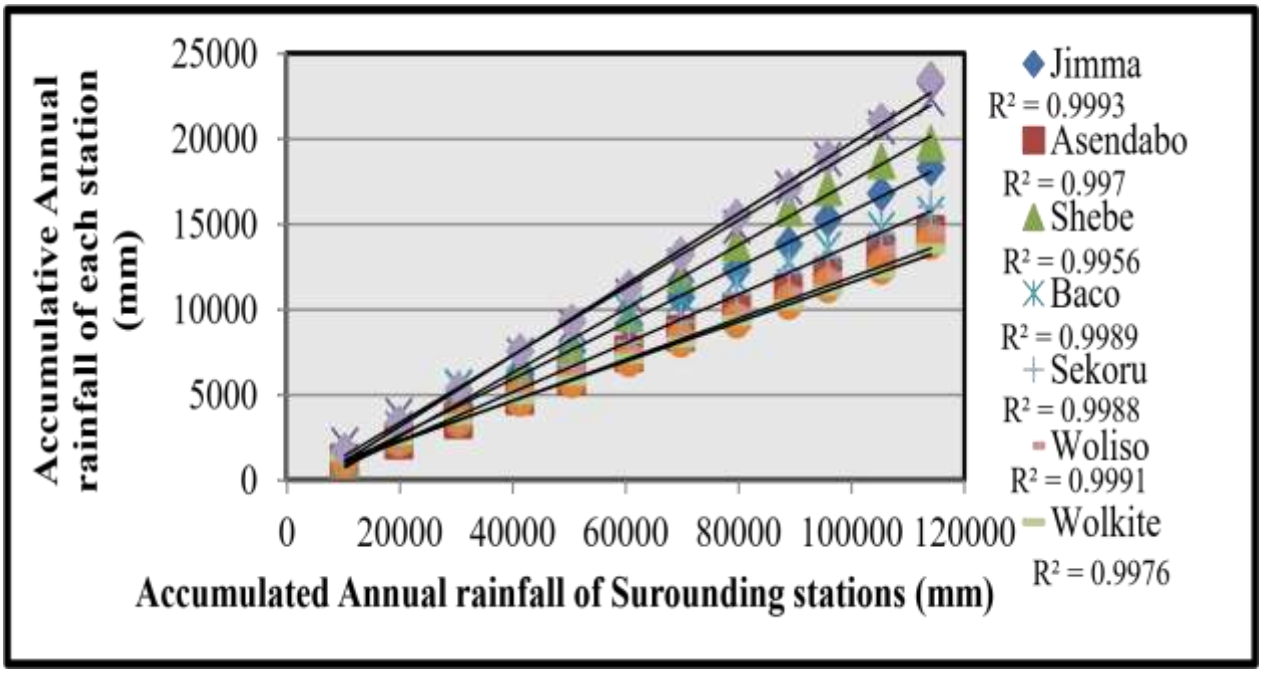

Figure 14: Double Mass Curves for the selected Meteorological Stations

3.7.4 Checking Homogeneity of Meteorological Stations

Homogeneity analysis is used to identify a change in the statistical properties of the time series data which is caused by either natural or man-made factors. These include alterations to land use and relocation of the observation station. The homogeneity test of time serious may be classified into two groups as absolute method and relative method. In the first method, the test applies to each station separately. In the second method, the neighboring (reference) stations are also used in testing (Wijngaard, 2003).

According to Peterson (1998), the recommended method to apply homogeneity has been tested with respect to neighboring stations that is supposedly homogeneous.

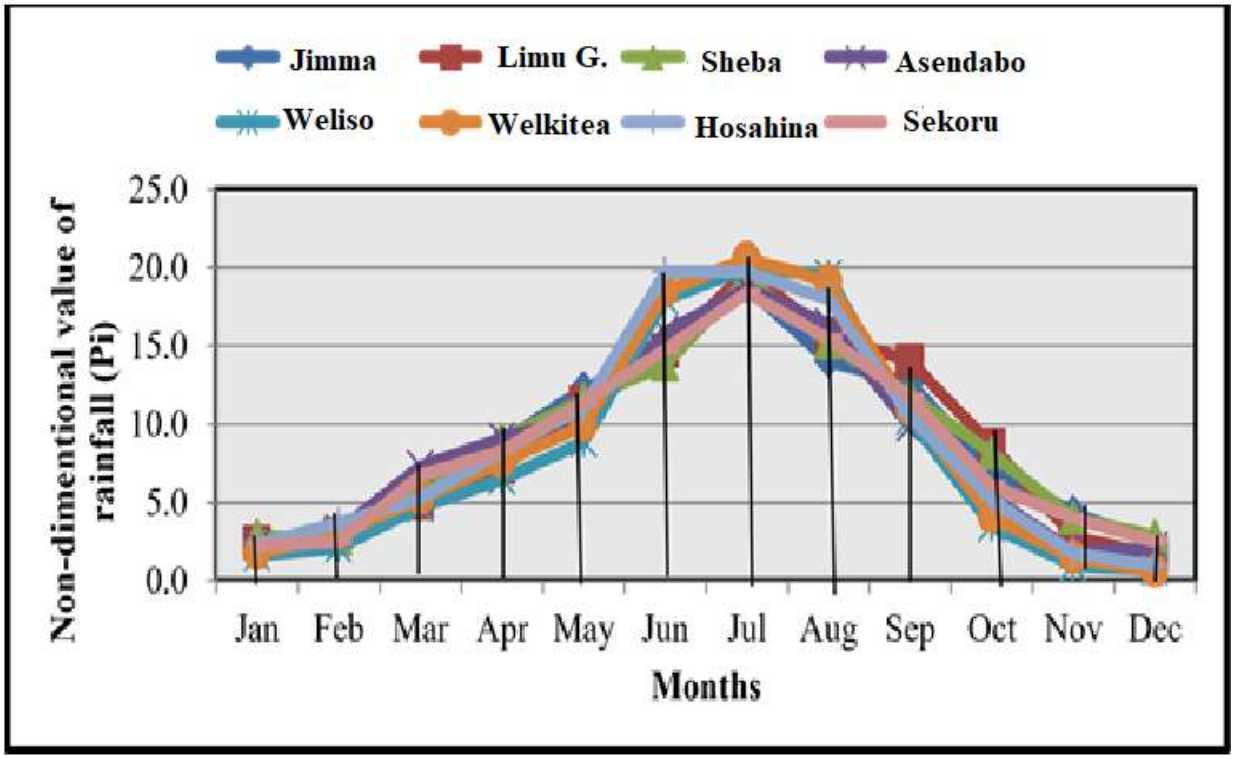

Figure 15: Computation of the Area rainfall with each selected site

3.7.5 Hydrological data analysis

Performances of any water resource project depend on the correct prediction of future hydrologic events. Information on the past observed records helps to derive statistical parameters based on which on the future occurrences are predicted. To arrive to the desired objective observed records called historical data which are the outcome of complex natural hydrologic phenomena

should be available. Therefore, it is necessary to make ready these historical data for further analysis. For our study, we have used three hydrological data analysis. These are estimating missing flow data, transposing flows to Abelti and generation of flow data for Abelti catchment.

3.7.6 Estimating missing flow data

Stream flow is that part of precipitation which appears in a stream as a surface runoff and represents the total response a basin undergoing sequent interactions between its various processes and storages. Then it is important to have a complete daily series of flow data of selected flow gauging station. In developing countries like Ethiopia it is difficult to obtain sufficiently complete metrological and hydrological data easily. Some of the available data are not complete and are therefore missed.

There are three flow gauging stations selected for our target to develop the rainfall-runoff model of upper Omo-Gibe catchments. These flow data of selected three stations are also missed and this missing data ranges from 9.44% at Walkite to 42.458% at Abelti. Even though data of the gauging station available in our hands were long term flow data and we need only a 13 year daily data there were partially missed in the year between 2004.2007 and 2008 G.C.

Table 6: Summary of missed stream flow data

Station	Missed data in number	Missed data in %
Abelti	1551	42.46
Gubre	830	22.72
Walkite	345	9.44

These missed data are tried to be filled by correlating two gauging stations assuming that they are hydro-metrological homogeneous.

A mathematical relation between two flow gauging stations needs to be developed so that the event can be predicted from the knowledge of the others. Thus a future sequence ca be synthesized preserving the characteristics of historical data. This can be achieved by regressing one set of data on the other set of data, one being dependent and the other independent in way the

regression coefficients describes them. In our case, the base station for which a long term data is available is taken as independent variable(X) and the station for which missing flow data is to be computed is taken as dependent variable(Y).

There are two methods available to fit a curve between the given sets of data, the graphical and the analytical method. In graphical method X and Y coordinates are drawn to scale on rectangular system and all points are marked on it. The resulting plot is called scatter diagram. A curve is traced by eye approximation such that it passes through the mean. The limitation of such procedure is that it may be subjected to large errors, if the best fit curve passing through them is not drawn. In analytical method we may fit a curve passing through the scatter points of the scatter diagram in such a way that the sum of the squares of departures of observed points from the fitted function is minimal. We can approach both methods by RAINBOW software using computer with a high precision.

1.linear---------- Y=a+bx
2.exponential ---------- $Y=be^{aX}$
3.logarithmic---------- Y=b+aln(X)
4.polynomial ---------- Y=a1 +a2X+a3X2 +……+…. +an+1Xn
5.power or parabolic ---------- Y=b Xa

Out of the above equations, a linear regression which is represented by a straight line(Y=a+bX) is simpler and can also be done manually. Where a and b are regression coefficients. The coefficients can be computed from the relation

$$a=\frac{\sum y_i \sum x_i^2 - \sum x_i \sum x_i \sum y_i}{N\sum x_i^2 - \left(\sum x_i\right)^2} = \frac{\sum y_i - b\sum x_i}{N} \quad \text{..... 3.1}$$

$$b = \frac{N\sum x_i y_i - \sum x_i \sum y_i}{N\sum x_i^2 - \left(\sum x_i\right)^2} \quad \text{..... 3.2}$$

And the relation between the two sates of variables is represented by the coefficient

$$r = \frac{\sum x_i y_i - \left(\sum x_i \sum y_i\right)/N}{\sqrt{\sum x_i^2 - \left(\sum x_i\right)^2/N}\sqrt{\sum y_i^2 - \left(\sum y_i\right)^2/N}} \quad \ldots\ldots\ldots\ldots\ldots\ldots 3.3$$

In which r lies between 0 to +1 as it is positively correlated. A value of 0.839 to 1.00 indicates good correlation.

3.7.6.1 RAINBOW Homogeneity Hydrological Test

Rainbow software used to check the homogeneity of data. Frequency analysis of rainfall data and flow data and their potential use in agro meteorological decision-making processes requires that the data be of long series; they should be homogeneous and independent. The restrictions of homogeneity assure that the observations are from the same population. In RAINBOW, the test for homogeneity based on the cumulative deviation from the mean. The following figures 17 shows the homogeneity test of data's.

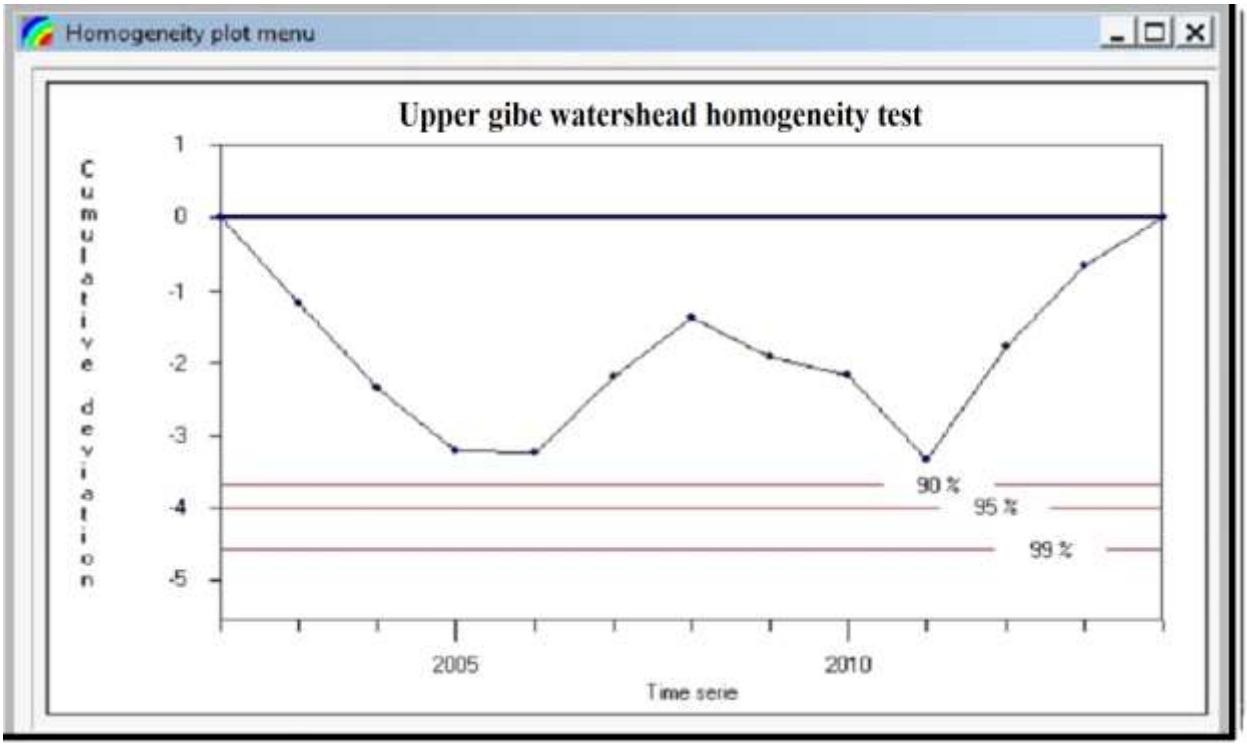

Figure 16: Rescaled Cumulative deviations for the total annual flow at Upper Gibe

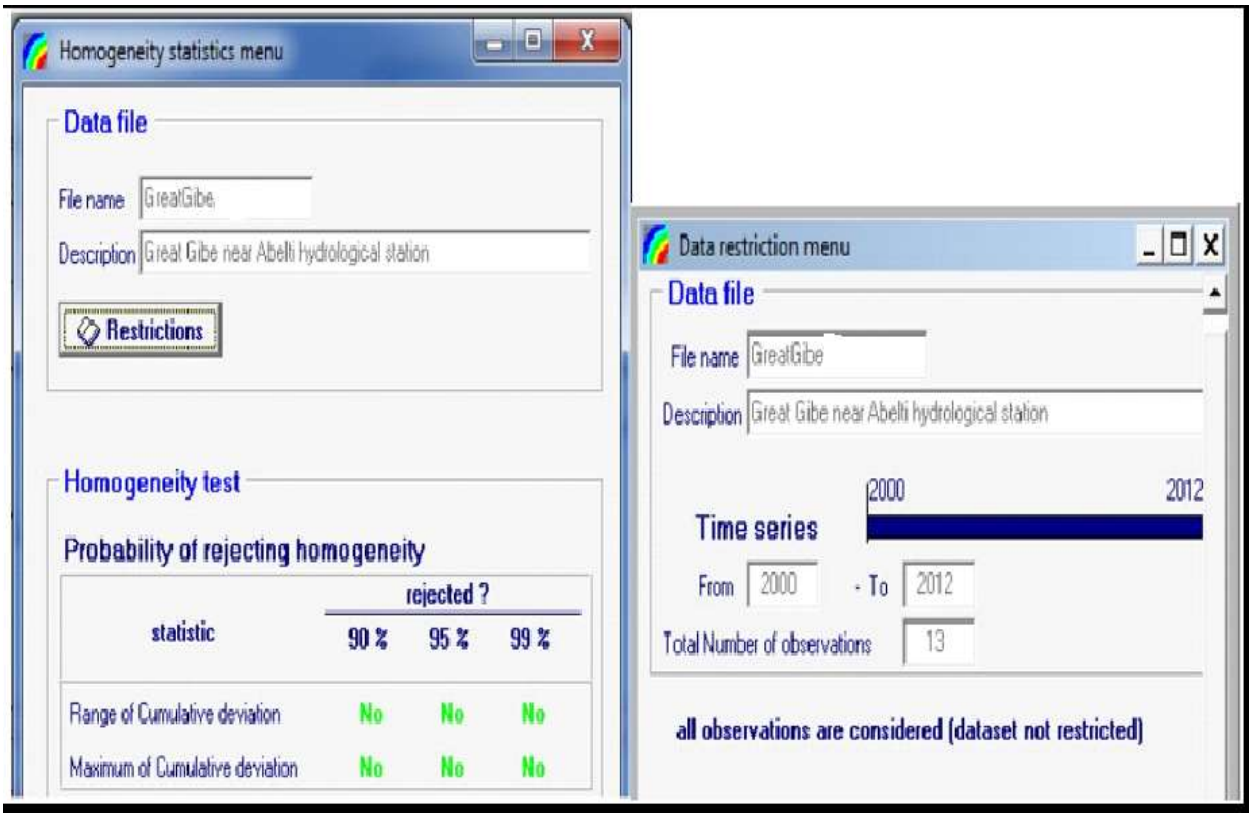

Figure 17: Probability of rejecting homogeneity of annual flow at Upper Gibe station

3.7.7 Processing Satellite Rainfall Products

3.7.7.1 Extraction of Satellite Rainfall Estimates

The satellite rainfall products used in this study were obtained on a Network Common Data Form (Net-CDF) gridded format from January 1st 2000 to December 31st 2012. These 4748 files (note that there are four more days because 2004, 2008 and 2012 are Leap Years) for each of the satellite product types were downloaded by the Convert to Net-CDF 'service of from the website and some of the satellite data in CSV format.

It creates a URL List which was saved to a specific location on the local computer as myfile.nc (Net-CDF file extension). Then, in order to extract the rainfall data for the study area and to export the data in to excel for each pixel, Panoply Net-CDF, HDF and GRIB data viewer version 4.5.1 were used.

Statistical indices like mean Absolut value, Root mean square Error, standard deviation, Max. value, NSEI value, R^2 and Average value were used for evaluating the performance of the selected satellite rainfall estimates against gauge measurements. This helps to get an overall impression of the performance of the selected satellite rainfall estimates in the study period and area.

Panoply Net-CDF converter was used to extract and export the rainfall data in to excel for the study area and period for satellite rainfall estimates. Finally, with the use of this software ‘s and computer programs, twelve years daily satellite based rainfall estimates were extracted in suitable format for further analysis.

Time and Space variant bias correction scheme (Habib, 2014) was applied to examine the effect of bias correction on satellite rainfall products ‘performance for hydrological modeling after using them without bias correction by using R-studio.

3.7.7.2 Model Sensitivity Analysis

Sensitivity analysis is essential in deciding how model is sensitive to some of the parameters. Sensitivity analysis is helpful for a range of uses; this includes evaluating the robustness of the results of a model or system. In the analysis of sensitivity of the MIKE 11 NAM model, all nine parameters were selected and the value of each parameter is changed by 20% on both side of the value obtained from the calibration. Sensitivity of each parameter is depends on the accuracy determiners of the model. Sensitivity analysis is done based up on the statistical performance indices i.e. coefficient of determination, Nash Sutcliff Efficiency Index, root mean square error and sum of square error. Results of various parameters value are plotted against R2, EI, RSME, and SSE for sensitivity analysis. In Appendix E Part we can conclude that the model parameters CQOF, CK12 were found most sensitive, Lmax and TOF were found moderate sensitive and CKIF is low sensitive parameter for modelling. (See Appendix F)

4. RESULTS AND DISCUSSION

In this chapter the findings of this study are presented for each of the objectives proposed in the introduction section. The results are discussed with reference to other scientific works and also compared with findings from previous efforts in the study theme.

4.1 COMPARISONS OF GAUGED AND SATELLITE ESTIMATES RAINFALLS

The eventual objective is to be able to use a combination of historical gauge and satellite derived rainfall data as inputs to hydrological models. In that regard, perhaps the best approach for assessing the satellite rainfall data would be to calibrate the model using historical gauge data and then apply the model using the satellite data.

However, simpler and quicker preliminary analyses have been undertaken and are based on pair-wise comparisons of the gauge data with the satellite data (and in some cases comparisons between gauges in close proximity and between the sources of satellite data).

All of the comparisons are based on monthly rain- fall totals, as the data are intended for use with monthly time-step hydrological models. The comparisons are based on visual interpretations of the time series of monthly rain- falls, as well as simple statistics (R^2 and slope) of the best fit linear regression line between the time series pairs. No further statistical measures of fit have been used during this phase of the study, although it is recognized that additional measures may be useful prior to the use of the data within a hydrological model. As aforementioned the rainfall data used in this study was the data obtained from gauged measurements, and three satellite based rainfall estimation products; CMORPH, PERSIANN and TRMM 3B42RT v7 for a length of 13 years from 2000 to 2012. To assess the reliability of satellite rainfall estimates, analysis was aimed at comparing in situ measurements to pixel values for those pixels which overlap ground based stations.

Comparison aimed at daily estimates for which descriptive statistics are calculated like mean Absolut error, standard deviation, Maximum Values, Root mean square Error, Nash and Suticliffe efficiency index (NSEI), coefficient of determination (R^2) and Mean values. The

period of analysis is 13 years (4748 days) but only those days with rainfall estimates, larger than 0 for satellite rainfall estimates as well as in situ measurements were selected.

Based on daily mean values, weliso station indicated almost same value between gauged and PERSIANN when compared to other stations which is 4.027 mm/day. PERSIANN also underestimates in Wolkite, Hosahina, Asendabo, Limugenet, Shebe, Woliso and sekoru (1.830 mm/day, 1.13 mm/day, 1.251 mm/day, 3.614 mm/day, 2.249mm/day, 4.027 mm/day and 3.5 mm/day) respectively. Limu Genet (4.024 mm/day) station indicated a wider difference between gauged and CMORPH when compared to other stations and Hosahina, Jimma, Asendabo and Sekoru stations almost have the same value (3.461 mm/day, 4.112mm/day, 3.623mm/day and 3.510mm/day) respectively. CMORPH also underestimates in weliso (1.525mm/day). In the case of TRMM3B42V7 the difference is much smaller than PERSIANN and CMORPH satellite products almost all stations., Asendabo, Jimma, Limugenet, Shebe, Sekoru, Hoshina and wolkite have the same mean value (>3mm/day) while the other stations like Weliso under estimate (1.525mm/day). The results of the analysis are shown below in Table 7

Table 7: Comparisons of gauged and Satellite Estimates Mean rainfalls

Station Name	Station ID	Gauged (mm/day)	TRMM3B42V7 (mm/day)	CMORPH (mm/day)	PERSIANN (mm/day)
Asendabo	RR01	3.08	3.781	3.623	1.251
Jimma	RR02	4.246	4.474	4.112	2.098
Limugenet	RR03	5.651	5.180	4.024	3.614
Sekoru	RR04	3.572	5.152	3.510	1.598
Shebe	RR05	3.324	3.861	4.608	2.249
Welkite	RR06	3.102	4.08	3.950	1.830
Weliso	RR07	4.040	1.525	1.525	1.130
Hosanna	RR08	3.120	3.95	3.460	4.027

Generally, it is noted that the difference between in situ and satellite rainfall estimates showed elevation dependent trends, PERSIANN showed relatively higher difference in high elevation

areas whereas TRMM3B42V7 and CMORPH showed relatively higher difference in low elevation areas. This result is consistent with findings of (Hirpa, 2010) conducted in, Awash River basin, Ethiopia.

Mean values for all ground based stations are higher than satellite rainfall estimates and thus indicate that, both of the selected satellite rainfall estimates underestimate rainfall compared to in situ measurements across the Great Gibe watershed. This result is consistent with recent findings of Bitew and Gebremichael, 2010a and 2010b, Haile, 2013 and Hirpa, 2010 conducted in Ethiopia.

Based on standard deviation values, the following stations Asendabo, Jimma, Limugenet, Sekoru, Shebe, Welkite, Hosahina and Weliso indicated relatively a higher value (> 7 mm/day) for TRMM3B42V7 and on station Asendabo, Jimma, Hosahina, Weliso and Welkite PERSIANN and CMORPH are relatively the same values (>4mm/day) and Shebe, Sekoru and Limugenet relatively higher difference in standard deviation than the above stations. According to statistics of standard deviation, which is a measure of the spread of the rainfall estimates from the mean, both of the satellite rainfall estimates underestimated rainfall than the gauge and follow the pattern of the mean.

The coefficient of variation the degree of variation from satellite rainfall estimates and gauge data can be computed the ratio of standard deviation to mean, Root mean square Error, R^2 and NSEI. As shown in Table 8 less variation is indicated in satellite rainfall estimates than gauge rainfall, which indicated the less temporal variability of satellite rainfall estimates than gauge rainfall estimates.

Table 8: Summary of Bias correction on daily statistics in situ and Satellite rainfall products estimates

Station	Rainfall Estimation.	Root mean square Error	Max. Values	Std. Deva.	R2
ASENDABO					
	• In situ	10.05	87.20	7.34	0.0068
	• TRMM3B42_7	10.05	73.74	7.46	0.0061
	• CMORPH	7.59	32.97	4.24	0.0511
	• PERSIANN	8.87	33.06	4.78	0.0011
JIMMA					
	• In situ	11.38	74.60	8.08	0.0023
	• TRMM3B42_7	11.37	90.61	8.36	0.0020
	• CMORPH	8.25	34.81	4.63	0.0670
	• PERSIANN	8.46	55.57	5.86	0.0110
SHEBE					
	• In situ	10.45	90.30	7.11	0.0058
	• TRMM3B42_7	10.36	69.70	6.71	0.0064
	• CMORPH	7.86	31.42	4.62	0.0470
	• PERSIANN	8.05	46.01	5.86	0.0065
SEKORU					
	• In situ	11.54	80.10	6.88	0.0061
	• TRMM3B42_7	11.51	84.98	9.67	0.0062
	• CMORPH	7.0594	45.34	4.21	0.0725
	• PERSIANN	7.3461	39.75	5.15	0.0122
LIMU GENET					
	• In situ	30.98	218.0	11.93	0.0003
	• TRMM3B42_7	15.11	84.98	9.67	0.0016
	• CMORPH	11.8317	36.03	4.86	0.0689
	• PERSIANN	29.28	46.94	6.51	0.0001

HOSAHINA					
	• In situ	10.593	77.01	6.96	0.0
	• TRMM3B42_7	10.592	96.27	7.96	0.001
	• CMORPH	7.1436	45.34	4.21	0.072
	• PERSIANN	7.776	29.82	4.72	0.0002
WELISO					
	• In situ	11.37	340	7.78	0.001
	• TRMM3B42_7	11.48	96.27	7.96	0.001
	• CMORPH	9.061	31.10	4.13	0.002
	• PERSIANN	7.449	33.37	4.91	0.001
WELKITEA					
	• In situ	10.09	67.30	6.91	0.0094
	• TRMM3B42_7	10.1304	84.54	8.04	0.0094
	• CMORPH	7.488	36.29	4.73	0.0514
	• PERSIANN	7.1159	28.49	4.83	0.0115

The average rainfall magnitudes, which were derived from satellite rainfall products from CMORPH, TRMM-3B42V7 and PERSIANN, and rain gauge stations, were estimated for the comparison. Therefore, the comparison in the study is based on the average values of rainfall data from the abovementioned sources.

As the objective of the comparison is to select the most reliable satellite rainfall products for stream flow simulation, the mean monthly and mean annual rainfall were used. Figure 19 clearly shows that the inter-annual variation of rainfall is observed to perform better for those the inputs are based on rain gauges, CMORPH and TRMM3B42v7 satellite rainfall products for the year 2001 – 2011. Yet, CMORPH and TRMM3B42v7 satellite rainfall products have slightly overestimation during the year (2012).

The new version satellite product, TRMM-3B42V7, shows good performances in capturing inter-annual variation of rainfall compared to all other products mentioned above. For the majority of the months, CMOPRH and TRMM-3B42V7 satellite rainfall products showed similar

performance with some overestimation, while PERSIANN consistently gave higher underestimation.

a. Asendabo (Gauged Vs TRMM3B42_7)

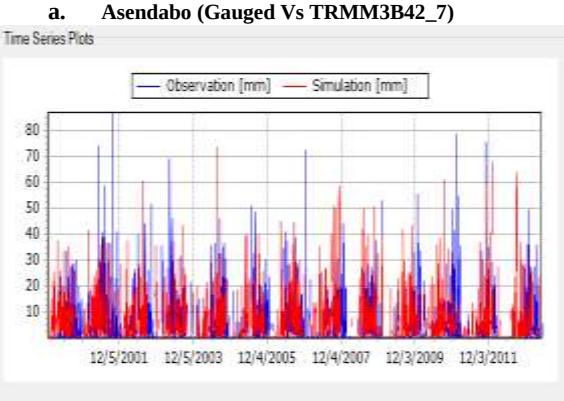

a) Time series plot

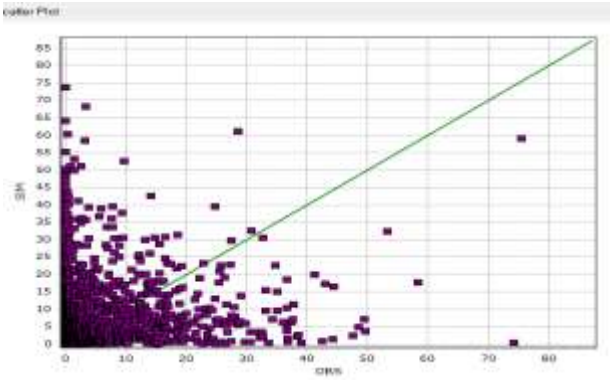

b) Scatter plot

b. Asendabo (Gauged Vs CMORPH)

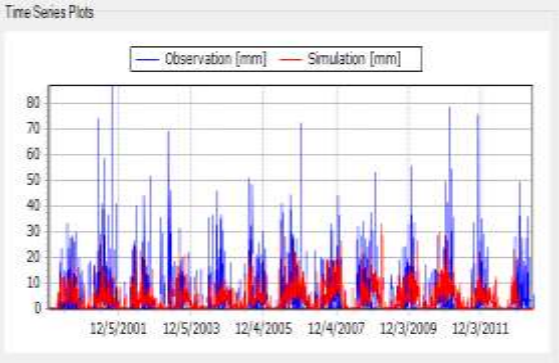

a) Time series plot

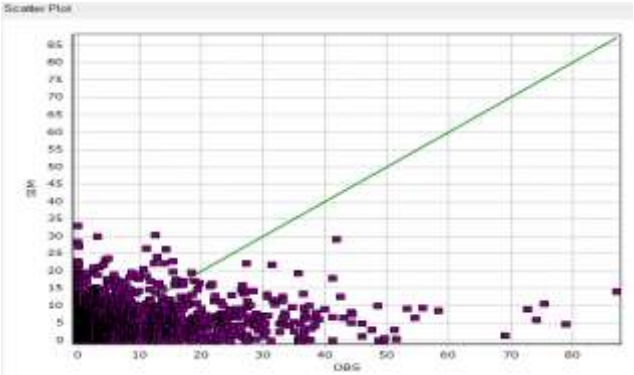

b) Scatter plot

c. Asendabo (Gauged Vs PERSIANN)

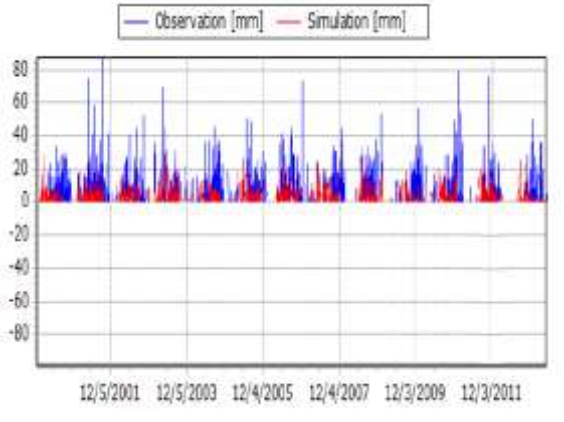

a) Time series plot

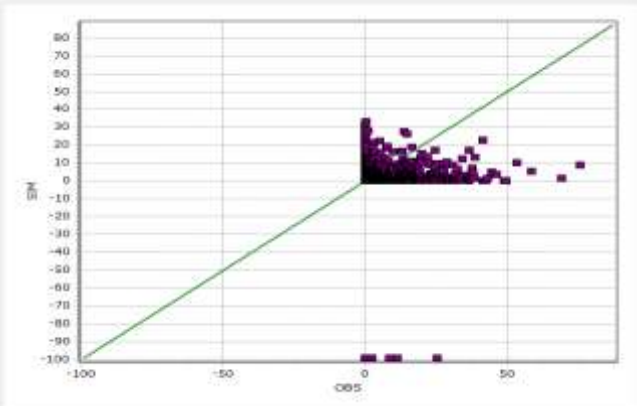

b) Scatter plot

Figure 18: Annual Rainfall comparison simulated and observed flow at daily time scale based on rainfall input data typical example Asendabo station (a) in situ v_s TRMM (b) in situ v_s CMORPH (c) in situ v_s PERSIANN

The annual rainfalls of TRMM-3B42v7 satellite products found to be similar to the rain gauge measurement value. These show that there is no significant difference between rain-gauged measurements and satellite product such as, TRMM3B42_7. and CMORPH Have less relative performance than TRMM3B42_7. In the contrary, PERSIANN exhibited high underestimation of the mean values when compared with rain gage estimate (refer the graph below).

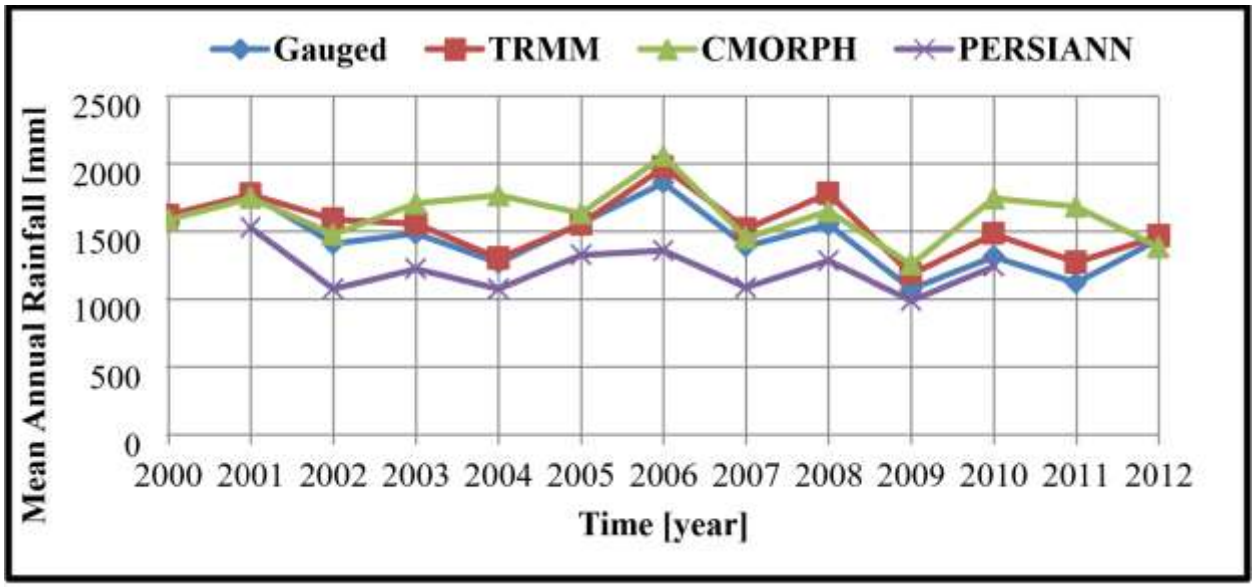

Figure 19: Mean annual rainfall of observed and SRPs (2000 – 2012).

The annual rainfalls of TRMM-3B42v7 and CMORPH satellite products found to be similar to the value of 1607.7 mm. On the other hand, the mean rainfall of the rain gauge measurement was estimated to be 1595.8 mm. These results show that there is no significant difference between rain-gauged measurements and satellite products such as, TRMM-3B42v7 and CMORPH. In the contrary, PERSIANN exhibited high underestimation, 1104.5 mm, of the mean values when compared with rain gage estimate.

4.2 RAINFALL- RUNOFF SIMULATIONS USING MIKE11 NAM FOR UPPER GIBE CONFLUENCE

The application of MIKE 11 model for rainfall runoff estimation can be divided into two (2) stages. The first stage is the calibration process to determine an optimum values of the model parameters. The second stage is the streamflow simulation using the estimated model parameter during the calibration process. The inputs used to develop these models are 13years (2000-2012) daily available satellite based precipitation and stream flow data's. The 13 years daily available data are divided into two, to be used for calibration and verification separately. The greater part of these data is used for validation and it accounts 60% of the total available data.

The rainfall data is a daily areal rainfall over the catchment and the stream flow data are obtained by transposing the stream flow data available at Abelti/Great Gibe (including Jimma, Limugenet, Sekoru and Asendabo) and Walkite (Wabe River) gauging stations to the Gibe confluence. Since the distance between these confluence points and the Abelti Stream Flow Gauging Station (Great Gibe) are very small the transposed data are simply added to the flow data available at Abelti to form the total outflows from Abelti catchment.

In the calibration procedure, several model parameters have to be adjusted using trial and error to obtain optimum values. These optimum values are considered as the representative coefficient to determine the runoff within the catchment area. (See Appendix G)

Runoff Simulation at Daily Timescale We first present the results of rainfall-runoff simulation at daily timescale. Figure 21 presents the Hydrographs Model Plot discharge at daily time scale for selected site in upper Gibe River basin.

Discharge Vs Time Hydrograph at Asendabo(RR01)

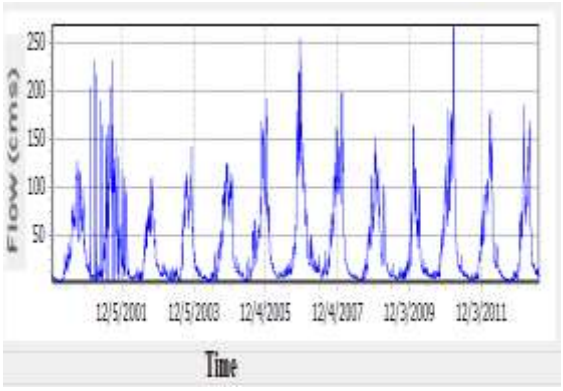

(a)

Discharge Vs Time Hydrograph at Jimma (RR02)

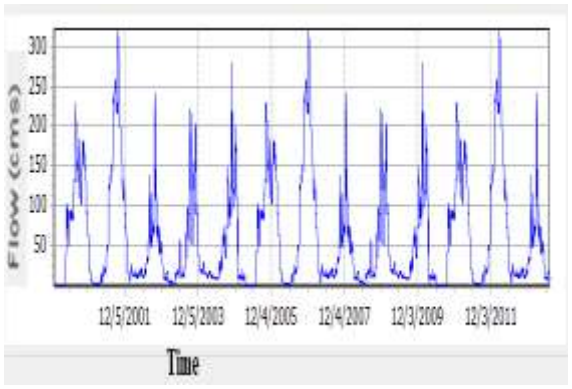

(b)

Discharge Vs Time Hydrograph at Limugenet (RR03)

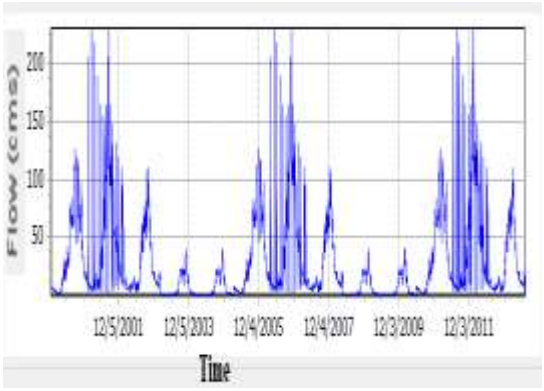

(c)

Discharge Vs Time Hydrograph at Sekoru (RR04)

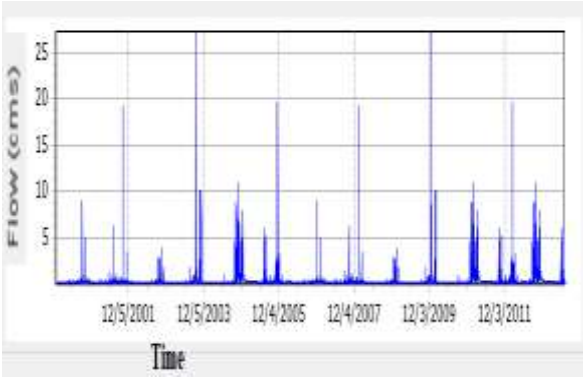

(d)

Discharge Vs Time Hydrograph at Shebe (RR05)

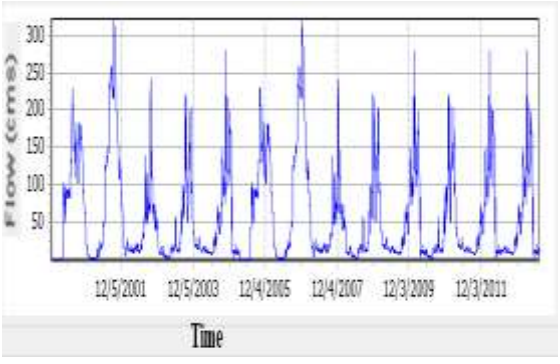

(e)

Discharge Vs Time Hydrograph at Welkite (RR06)

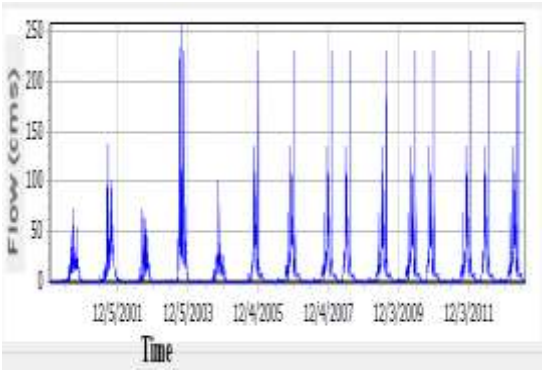

(f)

Figure 20: Hydrographs model Plot discharge at daily time scale for selected site.

4.2.1 Model calibration and validation

- MODEL CALIBRATION

Some parameters were highly sensitive to changes as shown in Table 9 The calibration had been carried out using records of daily rainfall and runoff from January 2000 to December 2005. Figure 22 represents the results of simulated and observed flow in the MIKE11 model calibration. Obviously, it can be seen that the MIKE 11 model cannot easily incorporate the peak discharges in the model optimization. The factors that contribute to the calibration inaccuracy are problems in data acquisitions, the nature of rainfall pattern and flood problem. The on-site data acquisition problems are the accessibility for regular maintenance and disturbance due to different factor like animal and human interruption. The nature of rainfall pattern is spatial resulting in an uneven rainfall distribution within the catchment area. This factor directly affects the rainfall-runoff model calibration. The different flood phenomena and human interruption like incorrect reading surrounding the gauging site significant problem in data acquisition system and reduce the accessibility for observation and maintenance. The problem of missing data was handled by the application of adjustment. The adjustment procedure employs the interpolation and method of proportion in the rainfall-runoff relationship.

Table 9: NAM calibrated parameter values and their range

Parameter	Unite	Description	Model parameter value	Parameter range	Change	Effect
U_{max}	mm	Maximum water content in surface storage	10.721	5.76-20	Increase	Peak runoff decreased Runoff volume reduced
L_{max}	mm	Maximum water content in root zone storage	256.268	100-300	Increase	Peak runoff decreased Runoff volume reduced
C_{QOF}		Overland flow runoff coefficient	0.910	0.1-1	Increase	Peak runoff decreased Runoff volume increased
C_{KIF}	hrs	Time constant for routing interflow	942.388	200-1000	Increase	-
C_{KIK2}	hrs	Time constant for routing overland flow	20.601	10-50	Increase	Peak runoff decreased The triangular shape expand horizontally
T_{OF}	-	Root zone threshold value for overland flow	0.925	0-0.99	Increase	Peak runoff decrease Runoff volume also decrease
T_{IF}	-	Root zone threshold value for inter flow	0.058	0-0.99	Increase	-
T_G	-	Root zone threshold value for GW recharge	0.762	0-0.99	Increase	-
C_{KBF}	hrs	Time constant for routing base flow Lower base flow	3436.632	500-10000	Moderate	Moderate Base flow

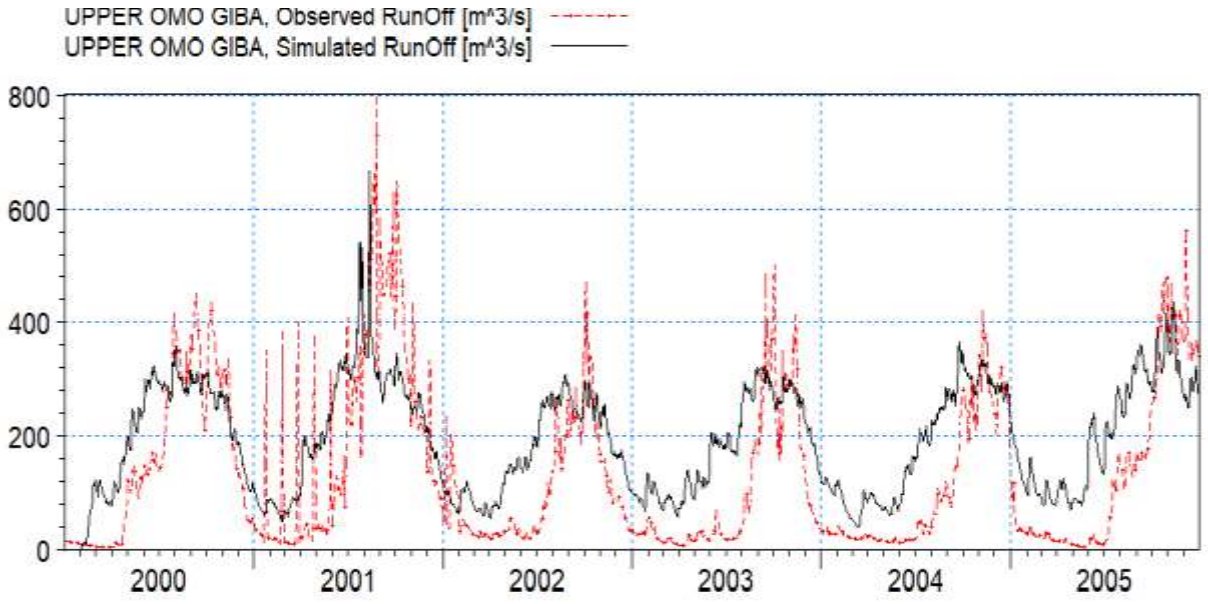

Figure 21: Comparison between observed and simulated runoff hydrograph during calibration period (x axis time period in year, y axis discharge in cumec)

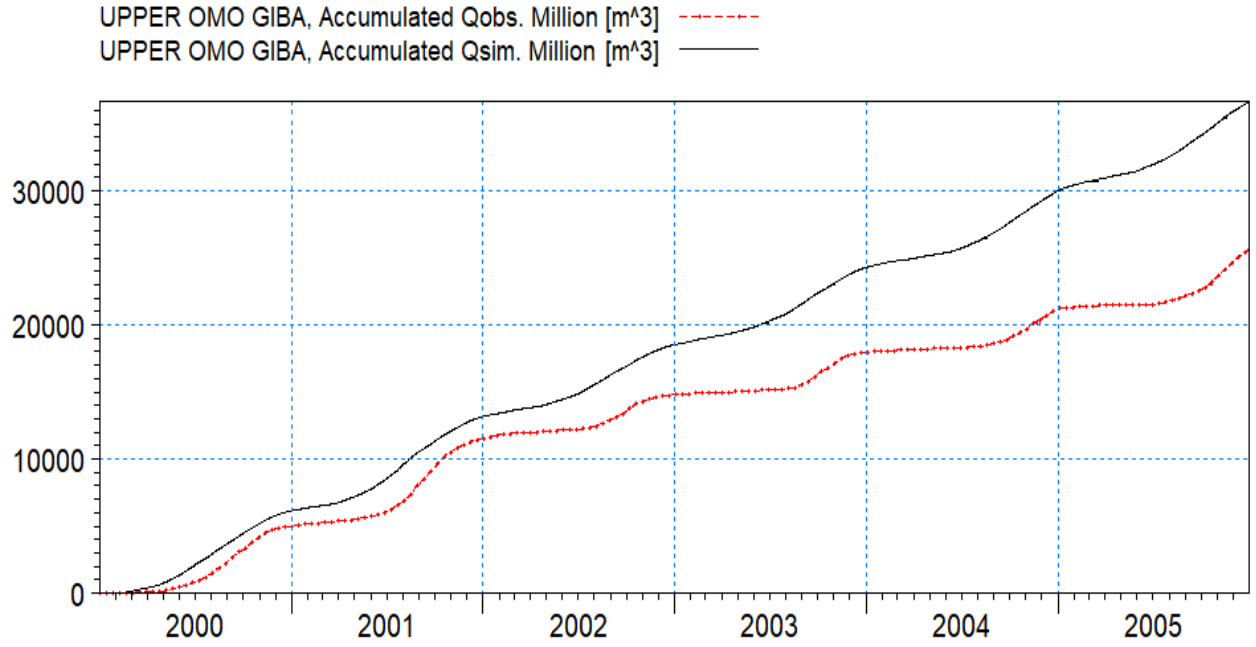

Figure 22: Double mass curve during calibration period (x axis time period in year, y axis discharge in cumec)

Table 10: Model calibration results

Period	Q-obs	Q-sim	%diff	Rainfall	PotEvap	ActEvap	CapFlux	Recharge	Pumping	Irrig.	OF	IF	BF
2000/ 3/ 1 - 2001/ 3/ 1	735.6	690.8	6.1	1290.8	0.0	0.0	0.0	823.5	0.0	0.0	76.3	87.1	527.3
2001/ 3/ 1 - 2002/ 3/ 1	949.6	1355.0	-42.7	1466.3	0.0	0.0	0.0	1223.7	0.0	0.0	134.9	99.2	1120.9
2002/ 3/ 1 - 2003/ 3/ 1	488.2	1238.5	-153.7	1195.0	0.0	0.0	0.0	986.4	0.0	0.0	111.9	98.5	1028.0
2003/ 3/ 1 - 2004/ 3/ 1	594.4	1264.0	-112.6	1249.1	0.0	0.0	0.0	1035.1	0.0	0.0	115.9	99.6	1048.6
2004/ 3/ 1 - 2005/ 3/ 1	688.5	1252.7	-82.0	1257.0	0.0	0.0	0.0	1043.3	0.0	0.0	116.8	99.0	1036.9
2005/ 3/ 1 - 2005/12/31	712.9	1148.6	-61.1	1288.5	0.0	0.0	0.0	1083.1	0.0	0.0	121.2	84.3	943.2
2000/ 3/ 1 - 2005/12/31	4169.2	6949.5	-66.7	7746.7	0.1	0.1	0.0	6195.0	0.0	0.0	677.0	567.6	5704.9

Coefficient of determination: R2 = 0.509

The model output simulation results performance is analyzed based up on the coefficient of determination and Nash-Sutcliffe coefficient, during the calibration it is found to be 0.509 and 0.64 respectively and the total water balance error during calibration is 14.75%. (See Appendix H). Figure shown above illustrates the comparison of observed and simulated discharge during calibration period. Peak and low flows between observed and simulated hydrograph were found matching well. The simulated peak flow occurs in the year 2001 and 2003 with approximate values are 1355.5 m3 /s and 1264.0 m3 /s respectively.

- MODEL VALIDATION

Model output simulation results performance are analyzed based up on the coefficient of determination and Nash Sutcliffe coefficient, during calibration it is found to be 0.645 and 0.675 respectively and during validation the total water balance error during validation is 17.5%. Figure 24 illustrate the comparison between observed and simulated runoff hydrograph during calibration period. Auto-calibration was done during calibration, NAM model parameters were obtained and then the simulated discharge was compared with observed discharge

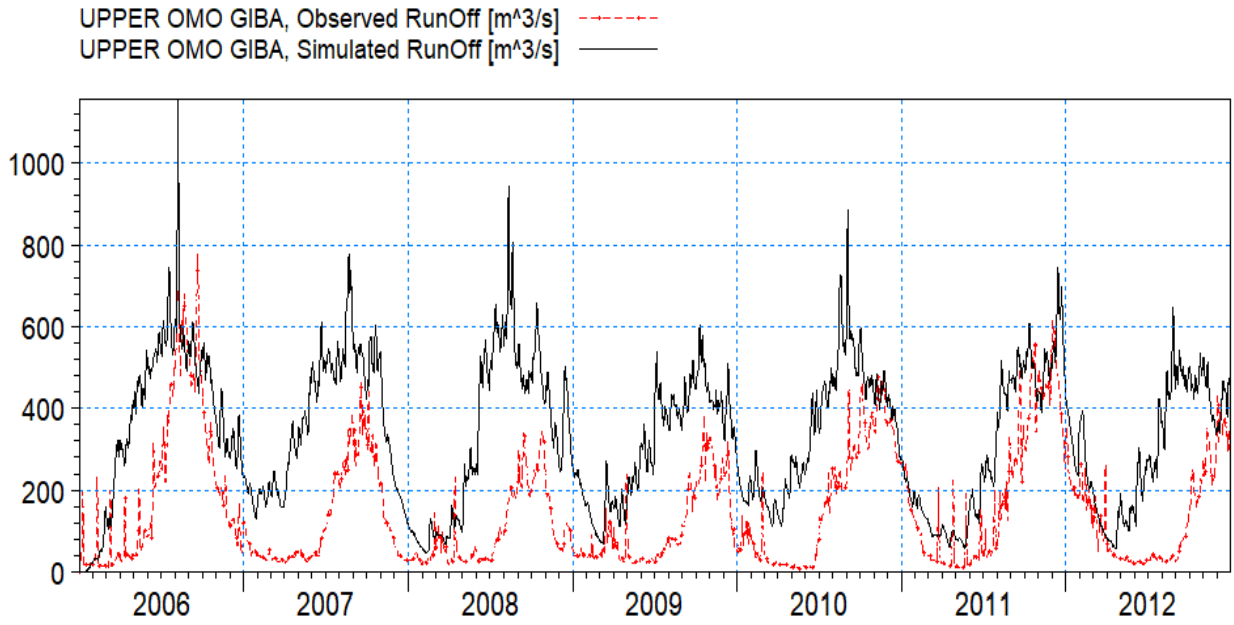

Figure 23: Comparison between observed and simulated runoff hydrograph for validation period (x axis time period, y axis discharge in cumec)

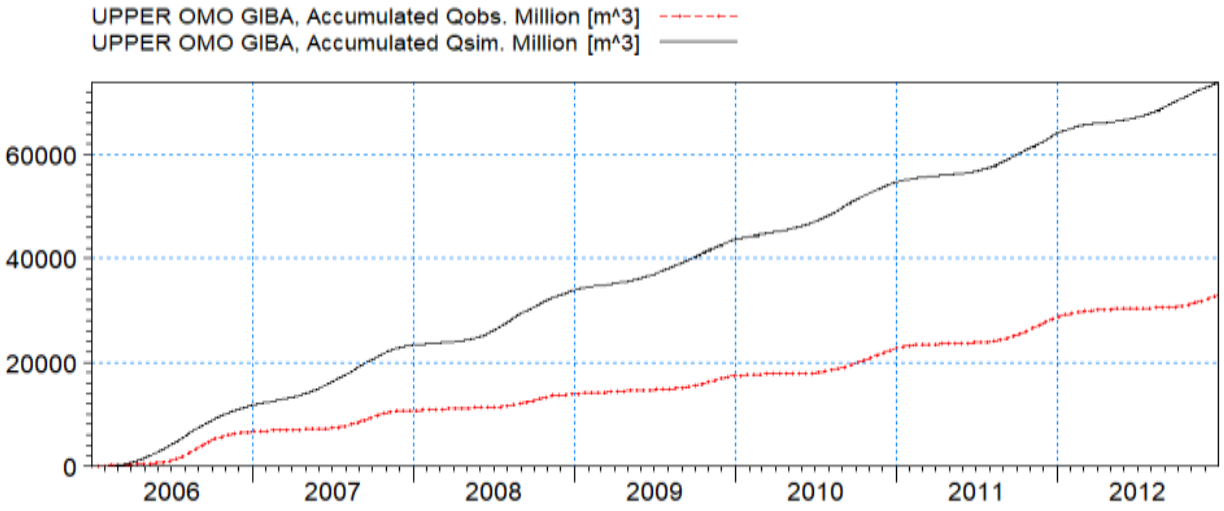

Figure 24: Comparison between observed and simulated runoff hydrograph for validation period (x axis time period in year, y axis discharge in cumec)

Table 11: Model validation results

Period	Q-obs	Q-sim	%diff	Rainfall	PotEvap	ActEvap	CapFlux	Recharge	Pumping	Irrig.	OF	IF	BF
2006/ 1/ 1 - 2007/ 1/ 1	2005.5	6977.4	-247.9	7525.4	0.0	0.0	0.0	1665.7	0.0	0.0	5483.4	90.3	1403.7
2007/ 1/ 1 - 2008/ 1/ 1	1231.6	6544.2	-431.4	6460.8	0.1	0.1	0.0	1145.5	0.0	0.0	5218.6	106.1	1219.5
2008/ 1/ 1 - 2009/ 1/ 1	980.4	6313.6	-544.0	6395.2	0.0	0.0	0.0	1132.4	0.0	0.0	5158.5	104.1	1051.1
2009/ 1/ 1 - 2010/ 1/ 1	1020.6	5634.5	-452.0	5630.4	0.0	0.0	0.0	994.0	0.0	0.0	4527.3	106.6	1000.5
2010/ 1/ 1 - 2011/ 1/ 1	1622.1	6356.9	-291.9	6378.1	0.0	0.0	0.0	1128.8	0.0	0.0	5132.0	106.8	1118.1
2011/ 1/ 1 - 2012/ 1/ 1	1826.1	5702.2	-212.3	5783.4	0.0	0.0	0.0	1021.8	0.0	0.0	4661.1	106.9	934.2
2012/ 1/ 1 - 2012/12/31	1261.8	5540.6	-339.1	5517.6	0.0	0.0	0.0	974.9	0.0	0.0	4413.2	101.4	1026.0
2006/ 1/ 1 - 2012/12/31	9948.2	43069.3	-332.9	43690.8	0.3	0.3	0.0	8063.1	0.0	0.0	34594.0	722.1	7753.2

Coefficient of determination: R2 =0.645

Q=Discharge, RF=Rainfall, PET=Potential Evapotranspiration, AET=Actual Evapotranspiration, GWR=Ground Water Recharge, BF=Base Flow, OF=Overland Flow, IF=Inter Flow)

The simulated minimum and maximum runoff for 13 years' period (2000-2012) show that the maximum annual runoff varies between 1466.3 mm to 7525.4 mm. The runoff at the confluence site was simulated with the help of NAM model. The simulated runoff was maximum for the month of August (6977.4 m^3/s) and minimum for the month of April (5540.6 m^3/s).

4.3 HYDRODYNAMIC MODEL RESULT

4.3.1 Flood Hazard Mapping for Baseline Period (2010's and 2020's)

The results of the flood hazard analysis discussed below. Flood modeling and mapping requires reliable inputs that are often difficult to obtain. Maps showing inundation depth and extent for several return periods (1, 2, 5, 10, 25, 50, and 100 years) represent flood hazard.

To simulate flood hazard, we used the MIKE FLOOD Hydrology Suite, which is a model combining a hydrological model and a 1-D/2-D hydraulics model.

Flood hazard mapping and identified flood hazard areas along streams and lakes using design flood levels established as part of flood hazard studies. This is majorly important to prepare for the decision makers to take the decision about the planning for the mitigation measures to reduce the impact of the flood the surrounding areas. For this analysis, the study addresses constructing flood mapping, most of the analysis focuses on the 25, 50 and100-year return period flood. Maps

of the inundation area for events with different return periods are one of the most common categories of map used to illustrate flood hazard.

I. Results from MIKE 11

A one-dimensional flood model is start to estimate flood-mapping characteristics for different return periods. For this study, the one-dimensional hydrodynamic model MIKE 11 results discussed in this sub topic based on the methodology described in the chapter 3. The MIKE 11 simulations based within the river. The floodwater at the cross section obtained for the simulation time step for the flood event. The results of MIKE 11 simulations used in MIKE VIEW. MIKE View displays longitudinal profile animations of both stage height and discharge resulting from a MIKE 11 unsteady simulation but in our instance the MIKE View no full version in the internet license. It also can display stage height at any given cross-section, as well as provide rating curves at a specified location along the river network.

A. Calibration and Validation of MIKE-11

The only parameter used in MIKE-11 for the calibration and validation was Manning's roughness coefficient(n) in the hydrodynamic parameters for MIKE-11. During the process of calibration, the local and global values of Manning's n adjusted to bridge the gap between the observed and simulated water levels as well as discharges at the gauging stations. By changing the roughness coefficient and fixing the roughness coefficient at 0.00km chainage of river as constant, the setup simulated and the results compared with the observed values. The final value of the global roughness coefficient found to be 0.033333.

The performance of the model evaluated using two goodness-of-fit criteria, that is, the Nash–Sutcliffe coefficient (modelling efficiency), ENS, and the index of agreement, d. reasonably good values of ENS and R^2 obtained for the calibration at gauging station. The calibration period 2000-2005 and validate the calibrated model, the data for the period of the years 2006 and 2012 were used.

B. Model responses

Model responses checked simultaneously as the calibration. The aim was to estimate optimum parameters for the model. The parameter was subjected to a change in values while. Observed and simulated water levels at were then compared. The efficiency of the model assessed by looking the root mean square error and the R^2 Nash and Sutcliffe efficiency parameter.

Table 12: Model responses with the average observed and simulated

Manning's n	Calibration		Validation	
	ENS	R^2	ENS	R^2
0.027	0.580	0.501	0.610	0.630
0.033	0.640	0.509	0.675	0.645
0.041	0.801	0.810	0.751	0.850

II. Results from MIKE 21

The simulation for MIKE 21 was generated the model requirement was fulfilled by generating bathymetry-topography grid shown in Figure 26. The DEM, ASCII raster converted to dfs2 then define the boundaries cells (1st/last rows/columns). For defining the Flood and Dry parameters minimum water depth allowed at a point before it is taken out of calculation for drying depth are given, and also the water depth at which the point will be re-entered into the calculation for flooding depth.

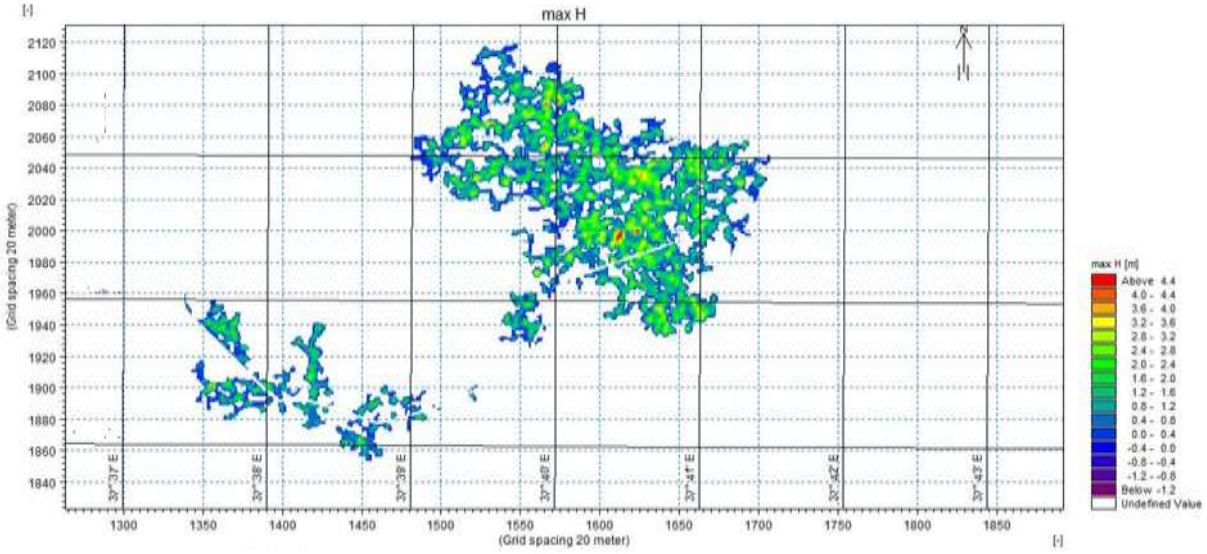

Figure 25: Maximum flood depth and extent flood plain

III. Simulation of flood hazard map using MIKE FLOOD

The single flood event of year 100 in the upper part of Gibe confluence flood plain simulated using MIKE FLOOD, which integrated the calibrated and validated 1D MIKE-11 hydrodynamic model with 2D hydrodynamic model MIKE-21 for the flood plain.

The flood inundation results of the simulated MIKE FLOOD model generated at a time step of one-hour interval in two-dimensional grids. The model generates different flooding scenarios (inundation depth, Velocity & magnitude) for return period of 100 years on the study area.

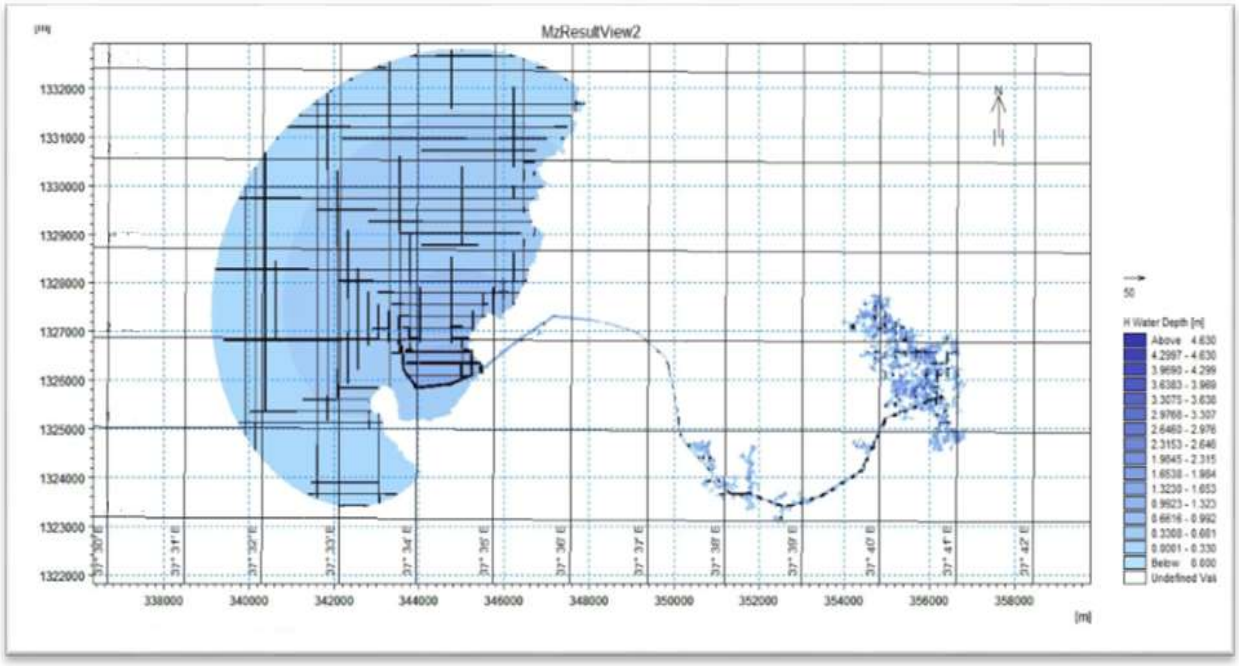

Figure 26: 100 years flood map and depth for the study area (Mike-View visualization)

A. Simulated Flood Extent, Level, Depth and Velocity

Figure 27 shows the maximum flow depths and extent for simulation period which simulation started on 12/2/2020 at 10:00:00 pm and simulation ended on 13/2/2020 10:00:00 AM. Maps of flood extent, level, depth and velocity developed using 100 years return periods flow. The figure below shows the static max flood area calculate in baseline simulation for the 100-year return period flood. This period flood has the inundation area of 1732.5 km^2 while the simulated flood extent has flood depths is between 0.00010 m and 1.653 m.

The graph result indicates no significant of the flooding occur in the outlet part of the river it indicated that the lower part of the basin is never much more affected by flood in the next 100 years' where the flow behavior is mainly dominated by the constant inflow from the Gibe river.

Analysis for maximum flood velocity from MIKE 21 outputs called Current speed. The simulated velocity of the Upper Omo Gibe River in the confluence ranges between 0 m/s and 3.2m/s to the flood plain**.**

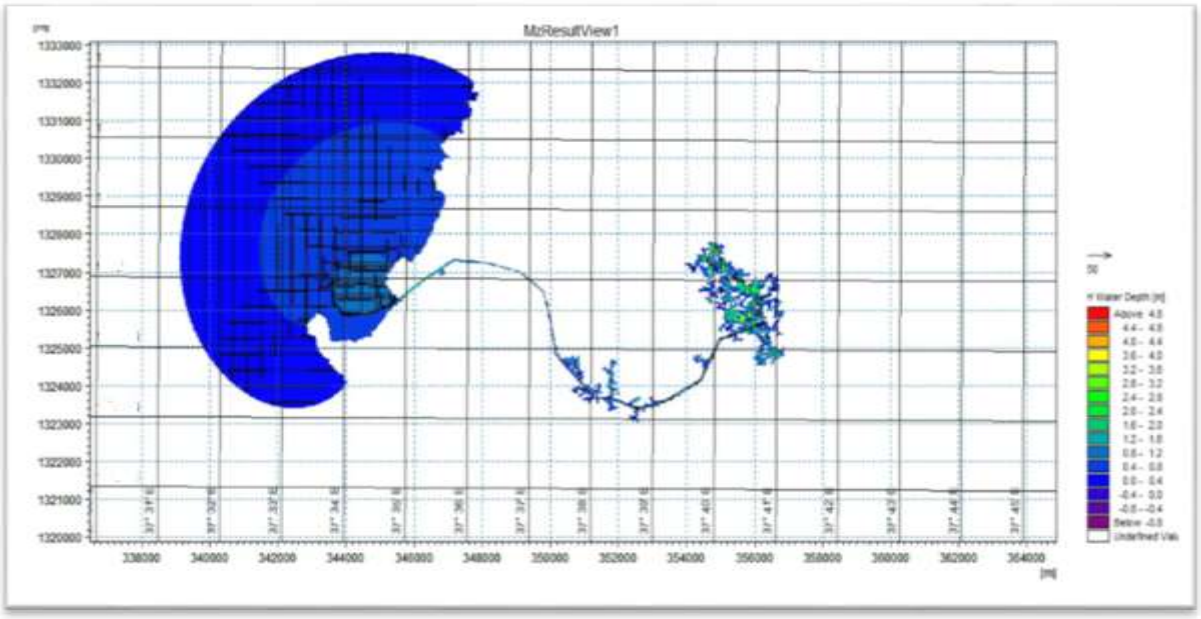

Figure 27: 100 year Max depth

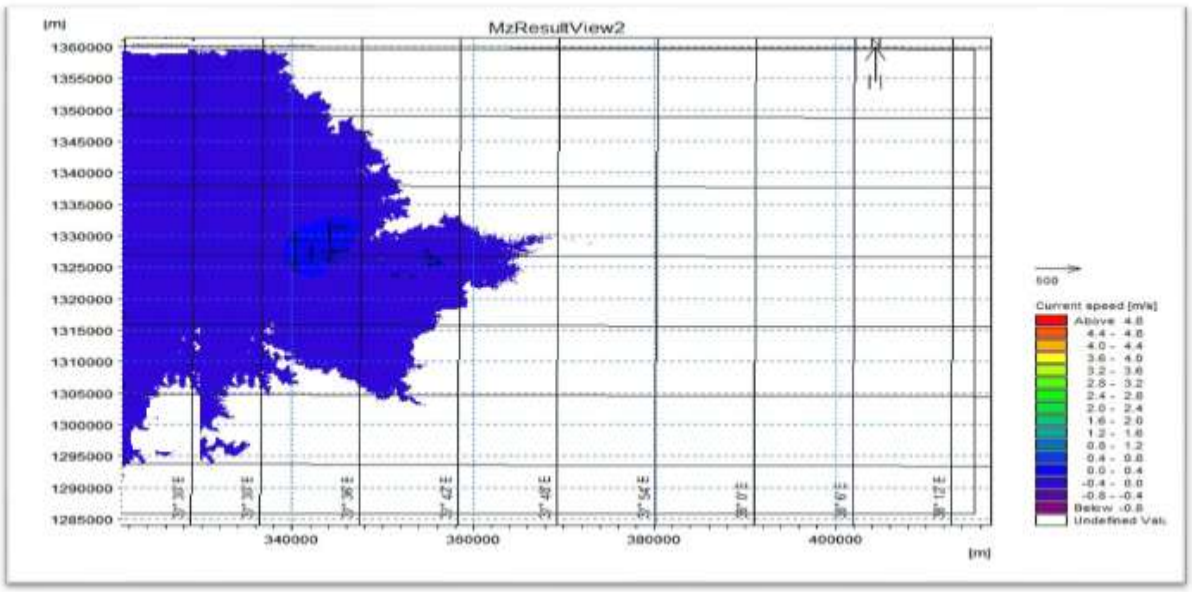

Figure 28: 100 year's Current speed

B. Simulated flood extent, level, depth and velocity Future Flood Inundation Area

The simulation carried out for the present and future scenarios of extreme rainfall events. Future flood inundation areas simulated for 2040's and 2080's with respect to RCP 4.5 scenarios.

Figure 30 shows the maximum flow depths consider to climate change (discharge and rainfall) 100 year return period. The simulation started on 12/2/2020 at 11:37:18 AM and simulation ended on 13/2/2020 at 6:13:47 PM. The maximum flood depth, flood extent, level and velocity developed using 100 years return periods flood. The figure shows the static max flood area calculate in baseline simulation for the 100-year return period flood. This period flood has the inundation area of 1574 km^2 for 2040's (around welkite catchment) and 1732 Km^2 for 2080's (around Abelti catchment) while the simulated flood extent has flood depths is between 1.2m and 1.6m for two scenarios, respectively.

The simulation result indicates no significant flooding effect occur in the lower part of the Great Gibe (Omorate) where as the flow behavior is mainly dominated by the constant inflow from the upper part of the river by the effect of the Dam. Analysis for maximum flood velocity from MIKE 21 outputs called Current speed. The simulated velocity of the Gibe River ranges between 0 m/s and 3.2 m/s to the flood plain**.**

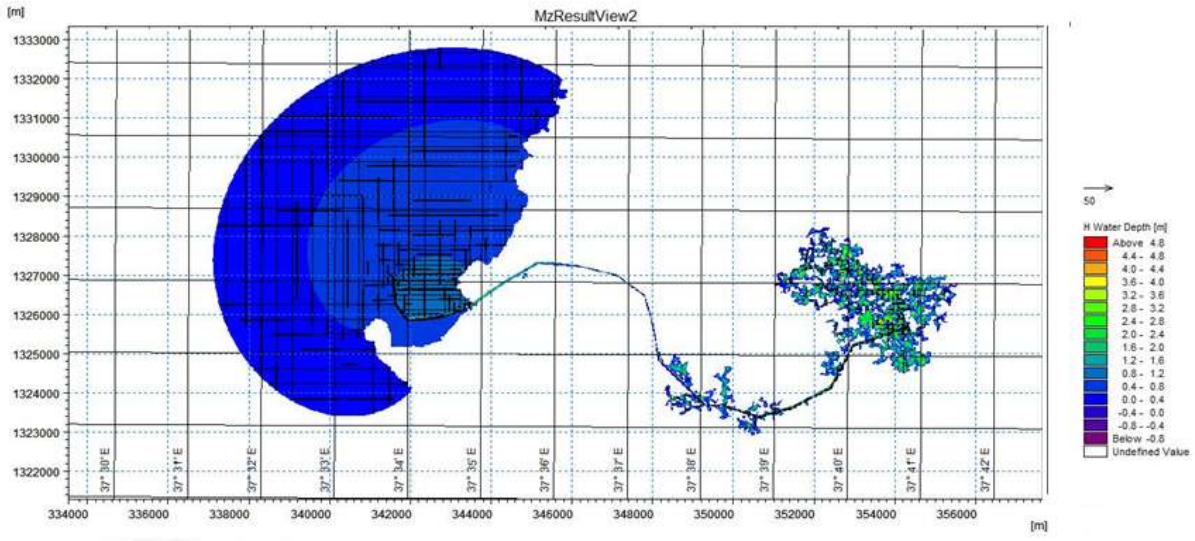

Figure 29: 100-year flood inundation

C. Hazard Index in the lower omo floodplain

Flood hazard mapping is to determine Areas with a probability of a flooding event for a defined return period. From MIKE FLOOD results shows the degree of flood hazard such as flood inundation area, flood velocity and inundated depths.

Tu and Tingsanchali (2010) which described as the degree of flood hazard based on inundation depth was very high extream danger with deep water and four the hazard index.

4.4 THE POSITIVE IMPACT OF THE DAM FOR FLOOD CONTROL

The Ethiopian government has staked its political future on achieving highly ambitious economic growth targets and shifting the country to an urbanizing industrial economy (GRBIDMPS, Volume VI). One of its major endeavors, Gibe III, wich is the highest dam in Africa. Together with already built Gibe I Dam and Gibe II power station (which draws its water from the Gibe I reservoir) and the yet to be built Gibe IV and V, it is expected to transform the Omo Valley into an agro-industrial powerhouse.

The construction of the Gibe dam series will substantially limit the annual floods from the Omo River, whether or not there is any irrigated agriculture. This will lead to a more constant flow in

the river of relatively sediment-free water, which in turn will lead to the loss of the ecologically productive floodplain used by wild species, fish, domestic stock and agriculture alike. Proponents of the dam initially claimed that ending the floods would be beneficial to all concerned (a common fallacy about river basin productivity).

The Gibe III dam is important to contribute the flood effect on the lower part and also regulate the seasonal flow of the Omo River it is show that there is no significant flood in the next 100 years. However, as critics of the dam point out, flow regulation and water abduction for commercial agriculture could compromise the livelihoods of downstream rural communities and thus feed into existing grievances against the Ethiopian state, or exacerbate communal conflicts across the Kenyan-Ethiopian border (Adusei, 2012; Vidal, 2015; HRW, 2014a, Johannes et al., 2015).

5 CONCLUSIONS AND RECOMMENDATIONS

5.1 CONCLUSIONS

- In this study the performance of MIKE11 NAM hydrologic models to simulate the Rainfall Runoff event in the Area using daily temporal and 0.250 x 0.250 spatial resolution satellite rainfall products has been evaluated for upper Omo Gibe Basin located in Ethiopia for reproducing the stream flow measurement at the outlet of the catchment (Great Gibe). Hydrological data obtained from the hydrological and meteorological data obtained from eight stations inside the basin area were used as ground reference to evaluate the performance of the satellite rainfall estimates as well as the models. Simulation of the stream flow of the great Gibe catchment using Mike Zero (MIKE11) models for the period of 13 years (2000-2012) was done using input data from satellite rainfall estimates (TRMM3B42v7 CMORPH and PERSIANN) and gauged rainfall measurements independently. Additionally, simulation with bias corrected satellite rainfall estimates was also done to investigate the effect of bias correction on the performance of the model for reproducing the observed stream flow hydrograph.
- During our observation it is noted that the difference between in situ and satellite rainfall estimates showed elevation dependent trends, PERSIANN showed relatively higher difference in high elevation areas whereas TRMM3B42V7 and CMORPH showed relatively higher difference in low elevation areas.
- In the process several intermediary steps were performed. Homogeneity and consistency of meteorological stations and stream flow homogeneity test was analyzed. Extraction of satellite rainfall estimates (TRMM3B42v7, CMORPH and PERSIANN) for the study area and study period using MATLAB R2013a and Panoply Net-CDF, HDF and GRIB data viewer has been done. Model inputs including hydro-meteorological data and spatial data (DEM, Land use/Land cover and River cross section) were prepared accordingly. Watershed delineation, areal rainfall computation and preparation of weather generator data were performed. Statistical techniques of mean, standard deviation, determination of NS Efficiency Index and Coefficient of determination were used to evaluate the performance

of satellite rainfall estimates. Objective functions EI, The Root Mean Square Error (RMSE), R^2 and water balance, were applied to assess how well the stream flows were reproduced in simulations were used to investigate the model outputs and parameters uncertainty. The sensitive analysis, calibration, validation and uncertainty analysis was performed using Mike11, Mike 21 and Mike Flood.

- During study our objective was to develop Rainfall Runoff Model in upper part of the river basin to simulate the extreme flood event in Omorate by using MIKE11 NAM model it is a realistic hydrological modelling. Model was found appropriate for simulation of discharge in upper part of the river basin. The coefficient of determination and Nash-Sutcliffe coefficient, during the calibration and is found to be 0.509 and 0.64 respectively, during validation it is 0.645 and0.675 respectively. The total water balance error during calibration and validation is 14.75% and 17.5% respectively it is good match of results which indicates that the NAM model is suitable for the catchment to analyses the rainfall runoff estimation. During sensitivity analysis model was found sensitive to the parameter like Lmax, CQOF, CKIF, CK12, and TOF, out of which CQOF and CK12 was found highly sensitive modelling and also the Catchment Area have great impact for the simulation result which means the catchment Area is increase the value of Nash-Sutcliffe coefficient and coefficient of determination also vary based on the simulation parameter.
- The 1D hydrodynamic MIKE 11 model has been implemented for the lower part of the Omo Gibe river. The network file, cross section file, boundary conditions file, and model parameter file has been created for this river and the components of MIKE 11 river hydrodynamic model were implemented efficiently for River.
- In the present study, the MIKE FLOOD Hydrodynamic model was set up and evaluated for flood hazard mapping in Omo-Gibe River Basin, Ethiopia. MIKE FLOOD was coupled with a 1D MIKE 11 and a 2D MIKE 21. Flood hazard mapping is a very complex approach that needs accurate data sources, continous hydrological and time series data and digital maps. Flood hazard maps show areas that are flood prone by

delineating, either the extent of historical flood or the areas inundated by hypothetical floods of particular occurrence frequencies.

- The result MIKE FLOOD showed that large area with a high depth and velocity in the lower part of the basin inundate in the future. Therefore MIKE FLOOD is a powerful tool to map floodplain of any extent provided that there are suffient data to be fed.
- Flooding around Omo-Gibe River causes a considerable damage to life and property. Large coverage of the area with cultivated land makes the problem hard. Past flood forecasting of the area lacks the use of modern software. This study presents a systematic approach in the preparation of flood map and simulation with the application Unsteady flow models MIKE11,MIKE21 and MIKE FLOOD.
- To suggest the likely cause of the flooding occurred in 2006 at Omorate, the daily and seasonal rainfalls of the long term record (2000-2012) is compared to that of the year 2006. The comparison was carried out for eight representative rainfall gauging stations throughout the Omo-Gibe basin in three different aspects; these are the sum of the June, July & August, the sum of July and August and the maximum daily rainfall of 1st-20th August. But in all the three aspects the analyses indicate that the rainfall pattern in the flooding year does not differ from the past 13 year's record and the resolute of the rainfall in the year 2001 and 2006 are almost the same, So the 21st August 2006 flooding problem resulting in serious damage on life (human being and animals) and property may be caused due to change in land use pattern and human activities (constructing large dam structures) in the basin rather than local inundation or saying "it is caused by extreme rainfall event''.
- The simulation result indicates in the next 100 years no significant flooding occur in the Area and also in the lower part of the Basin which means no more catastrophic disaster will be happening where as the flow behavior is mainly dominated by the inflow from the upper part of the river. Analysis for maximum flood velocity from MIKE 21 outputs called Current speed, but the responsible body will have great roll for protecting the land use and land cover change it may have negative impact for the next 100 years.

5.2 RECOMMENDATIONS

- Satellite rainfall estimates specially TRMM3B42v7 satellite rainfall estimates at daily temporal and 0.25^0 x 0.25^0 spatial resolution has reasonably represented rainfall amount and distribution after bias correction. Thus, using this satellite rainfall estimates after removing biases and at finer temporal and spatial resolutions may lead to get advantage for hydrological modeling.
- Science more than 30% of the data used for the development of the model is filled as a missing data and it have effect on the quality of the model output which leads to incorrect decision for the purpose it used and may also lead to improper winding up, to use the selected model for practical purpose further study should be carried out with sufficient and good quality data based on this the satellite precipitation products can be used to represent gauge rainfall estimated with major and minor improvements, and CMORPH satellite rainfall estimates better than PERSIANN satellite rainfall estimates.
- Flow data: There was no gauged flow data at the confluence of the river specially at the middle and downstream of the river, flow data of long time duration is also necessary for the calibration and validation of hydrologic model. Unavailability of hourly meteorological data should be addressed.
- Based on the above result this type of model is highly advantages for rainfall simulation, water resources management, soil conservation and flood forecasting techniques rather than other model.
- As conclude in the above the flood problem is caused by land use land cover change, so the responsible body have play great roll for protecting the cachmnt in the case of constructing large dam and othe construction.
- Protecting the catchment by mobilizing the community thereby constructing dykes that limits the flux of river water entering to the flood plain.
- Here in Ethiopia most Flood hazard mapping reaserch commonly used 1D flood model while simulating their data, but some have used 2D free available model softwares with a limited access.

- This is due to financial constraint they have to purchase the full licence. Unlike others, MIKE by DHI have given me online student license for a year so that I can access the full MIKE ZERO(MIKE 11, MIKE 21 and MIKE FLOOD) application for free. This helped me to carry both 1D and 2D integrated simullations to obtain a good results.

REFERENCES

Alsdorf, D. E., E. Rodriguez, and D. P. Lettenmaier, 2007: Measuring surface water from space. Rev. Geophys., 45, RG2002,

American Civil Engineering Society (ASCE), A. S. (1996). Hydrology Hand Book . New York: 784pp. McGraw-Hill,Inc.

Arkin, P.A. and P.E. Ardanuy 1989. Estimating climatic-scale precipitation from space: a review. J. Climate, **2**, 1229-38

Beven, K. (2000). Rainfall-Runoff Modeling . Washigten DC: The primer johnwilly and sons,360pp.

Birkett, C. M., 1998: Contribution of the TOPEX NASA radar altimeter to the global monitoring of large rivers and wetlands. Water Resource.

DHI (2007a). MIKE-21, Short introduction and tutorial, Danish Hydraulic Institute.

DHI (2007b). MIKE-21, User guide, Danish Hydraulic Institute.

Dinku T, Ceccato P, Grover-Kopec E, Lemma M, Connor SJ, Ropelewski CF, (2010a).

Dinku, T., P. Ceccato, and S. J. Connor (2011), Challenges of satellite rainfall estimation over mountainous and arid parts of east Africa, Int. J. Remote Sens., 32(21), 5965– 5979, doi:10.1080/01431161.2010.499381.

Dinku, T., S. Chidzambwa, P. Ceccato, S. J. Connor, and C. F. Ropelewski (2008), Validation of high-resolution satellite rainfall products over complex terrain, Int. J. Remote Sens., 29(14), 4097–4110, doi:10.1080/01431160701772526.

Ehret, U., Zehe, E., Wulfmeyer, V., Warrach-Sagi, K. and Liebert, J., 2012. HESS Opinions" Should we apply bias correction to global and regional climate model data?". Hydrology and Earth System Sciences, 16(9), p.3391.

FLOOD, M., 2011. 1D-2D Modeling, User Manual. DHI Water & Environment.

Gebremichael, M., & Hossain, F. (2010). Satellite rainfall applications for surface hydrology. Dordrecht: Springer.

Hong, Y., K.-L. Hsu, S. Sorooshian, and X. GAO, 2004: Precipitation estimation from remotely sensed information using an artificial neural network cloud classification system. J. Appl. Meteor., 43, 1834–1853, doi:10.1175/JAM2173.1.

Huffman, G. J., R. F. Adler, D. T. Bolvin, E. J. Nelkin, 2010: The TRMM Multi-Satellite Precipitation Analysis (TMPA). Chapter 1 in Satellite Rainfall Applications for Surface Hydrology, F. Hossain and M. Gebremichael, Eds. Springer Verlag, ISBN: 978-90-481-2914-0, 3-22.

Huffman, G. J., R. F. Adler, D. T. Bolvin, G. Gu, E. J. Nelkin, K. P. Bowman, Y. Hong, E. F. Stocker, D. B. Wolff, 2007: The TRMM multi-satellite precipitation analysis: Quasi-global, multi-year, combined-sensor precipitation estimates at fine scale. J. Hydrometeor., 8(1), 38-55.

Huffman, G.J., 1997: Estimates of Root-Mean-Square Random Error for Finite Samples of Estimated Precipitation, J. Appl. Meteor., 1191-1201.

Huffman, G.J., R.F. Adler, B. Rudolph, U. Schneider, and P. Keehn, 1995: Global Precipitation Estimates Based on a Technique for Combining Satellite-Based Estimates, Rain Gauge Analysis, and NWP Model Precipitation Information, Journal of Climatology., 8, 1284-1295.

Huffman, G.J.; R.F. Adler, Morrissey, M.; Bolvin, D.T.; Curtis, S.; Joyce, R.; McGavock, B.; Susskind, J. Global precipitation at one-degree daily resolution from multi-satellite observations.

Intergovernmental Panel on Climate Change, 2014. Climate Change 2014–Impacts, Adaptation and Vulnerability: Regional Aspects. Cambridge University Press.

IPCC, 2000: Special Report on Emissions Scenarios: A Special Report of Working Group III of the Intergovernmental Panel on Climate Change. Cambridge, UK: Cambridge University Press. 570 pp.

IPCC, 2007: Climate Change 2007: Synthesis Report. Contribution of Working Groups I, II and III to the Fourth Assessment Report of the Intergovernmental Panel on Climate Change [Core Writing Team, Pachauri, R.K and Reisinger, A. (eds.)]. IPCC, Geneva, Switzerland, 104 pp. Journal of Hydrometeorology 2001, 2, 36-50. Jj

Joyce, R. J., and P. Xie, 2011: Kalman filter–based CMORPH. J. Hydrometer

Kemal, M. (2007). Developing of Flood Warning and Forcasting System for Omo Gibe River Basin.

Khan, S. I., and Coauthors, 2012: Microwave satellite data for hydrologic modeling in ungauged basins. IEEE Geosci. Remote Sens. Lett., 9, 663–667, doi:10.1109/ LGRS.2011.2177807.

Leander, R. and Buishand, T.A., 2007. Resampling of regional climate model output for the simulation of extreme river flows. Journal of Hydrology, 332(3), pp.487-496.

Merz, B., Thieken, A.H. and Gocht, M., 2007. Flood risk mapping at the local scale: concepts and challenges. In Flood, risk management in Europe (pp. 231-251). Springer Netherlands.

Moriasi D. N., Arnold J. G., Van Liew M. W., Bingner R. L., Harmel R. D., and Veith T. L. 2007, Model evaluation guidelines for systematic quantification of accuracy in watershed simulations. Transactions of the ASABE, Vol. 50, No. 3, pp. 885–900.

NAPA, 2007. Climate Change National Adaptation Programme of Action (NAPA) of Ethiopia.

Neitsch, S.L., Arnold, J.G., Kiniry, J.R., Williams, J.R. and King, K.W., 2005. Soil and water assessment tool theoretical documentation. Grassland.Soil and Water Research Laboratory, Temple, TX.

Nijssen, B., and D. P. Lettenmaier, 2004: Effect of precipitation sampling error on simulated hydrological fluxes and states: Anticipating the Global Precipitation Measurement satellites.

Omo-Gibe River Basin Integrated Development Master Plan Study (volume VI and XI)

Omo-Gibe River Basin Integrated Development Master Plan Study Volume vI and XI (2006). n.d

Penning-Rowsell, E. ed., 1994. Floods across Europe: hazard assessment, modelling and management (pp. 135-66). London: Middlesex University Press.

Perera, B.U.J., 2009. Ungauged catchment hydrology: the case of Lake Tana (Doctoral dissertation, MSc thesis ITC, Enschede, The Netherlands, p 61).

Prudhomme, C., Wilby, R.L., Crooks, S., Kay, A.L. and Reynard, N.S., 2010. Scenario-neutral approach to Climate change impact studies: application to flood risk. Journal of Hydrology, 390(3), pp.198-209.

Refsgaard, J.C., 1997. Parameterisation, calibration and validation of distributed hydrological models. Journal of hydrology, 198(1), pp.69-97.

Ringius, L., Downing, T.E., Hulme, M., Waughray, D. and Selrod, R., 1996. Climate change in Africa: issues and regional strategy. CICERO, University of Oslo, Oslo, p.154.

Rungo, M. and Olesen, K.W., 2003, October. Combined 1-and 2-dimensional flood modeling. In Proceedings of the 4th Iranian Hydraulic Conference, Shiraz, Iran, October (pp. 21-23).

Sanyal, J. and Lu, X.X., 2006. GIS-based flood hazard mapping at different administrative scales: A case study in Gangetic West Bengal, India.Singapore Journal of Tropical Geography, 27(2), pp.207-220.

Setegn, S.G., Dargahi, B., Srinivasan, R. and Melesse, A.M., 2010. Modeling of Sediment Yield from Anjeni-Gauged Watershed, Ethiopia Using SWAT Model. JAWRA Journal of the American Water Resources Association, 46(3), pp.514-526.

Shrestha, S. and Lohpaisankrit, W., 2016. Flood hazard assessment under climate change scenarios in the Yang River Basin, Thailand. International Journal of Sustainable Built Environment.

Sutcliffe, J. V.; Parks, Y. P. 1999.The Hydrology of the Nile. IAHS Special Publication No. 5, IAHS Press, International Association of Hydrological Sciences, Wallingford, England, 179 pp.

Tarekegn, T.H., Haile, A.T., Rientjes, T., Reggiani, P. and Alkema, D., 2010. Assessment of an ASTER-generated DEM for 2D hydrodynamic flood modeling. International Journal of Applied Earth Observation and Geo information, 12(6), pp.457-465.

Tekleab, S., Uhlenbrook, S., Mohamed, Y., Savenije, H.H.G., Temesgen, M. and Wenninger, J., 2011. Water balance modeling of Upper Blue Nile catchments using a top-down approach. Hydrology and Earth System Sciences, 15(7), p.2179.

Tu, V.T. and Tingsanchali, T., 2010. Flood hazard and risk assessment of Hoang Long River basin, Vietnam. In Proceeding of International MIKE by DHI Conference.

Tuteja, N.K. and Shaikh, M., 2009, July. Hydraulic modelling of the spatio-temporal flood inundation patterns of the Koondrook Perricoota forest wetlands-the living Murray. In 18th World IMACS/MODSIM Congress (pp. 13-17).

United Nation Office for the Coordination of Humanitarian Affairs. Focus on Ethiopia: a monthly focus on humanitarian trends and activities in Ethiopia. Addis Ababa; 2006.

Validation of satellite rainfall products over east Africa ‘s complex topography. International Journal of Remote Sensing, 28 (7): pp. 1503–1526.

Van Griensven, A. and Bauwens, W., 2003. Multiobjective autocalibration for semidistributed water quality models. Water Resources Research, 39(12).

Vent Chow. ‘Hand book of Applied Hydrology’. NewYork :Mc Graw Hill,1988

Wöhling, T., Lennartz, F. and Zappa, M., 2006. Technical Note: Updating procedure for flood forecasting with conceptual HBV-type models. Hydrology and Earth System Sciences Discussions, 10(6), pp.783-788.

Woubet, G., 2007. Flood Hazard and Risk Assessment in Fogera Woreda using GIS & Remote Sensing (Doctoral dissertation, aau).

APPENDIX:

Appendix A: Monthly Stream Flow Data at three selected stream gauging stations and total out from Abelti Catchment

2000

Date	Wabe at Gibe confluence	Megecha at gibe confluence	Great gibe at Abelti	Outflow from Abelti Catchment
Jan	46.81006808	11.47138412	1115.92487	1174.206322
Feb	30.10817748	7.146637774	635.1795738	672.434389
Mar	25.01951542	6.65422719	453.1352622	484.8090048
Apr	52.73174213	7.327114051	1210.078538	1270.137394
May	93.0713895	10.84194526	3172.520762	3276.434097
Jun	157.9713544	9.941791971	4451.999088	4619.912235
Jul	2461.401559	84.16656022	9131.432533	11677.00065
Aug	3540.656071	333.7407427	11734.9783	15609.37511
Sep	1611.724113	190.5461852	11976.75645	13779.02675
Oct	707.7623982	193.9184812	10797.02303	11698.70391
Nov	164.7354119	35.59895802	5350.356295	5550.690664
Dec	98.26001299	22.76445463	2506.216278	2627.240746

2001

Date	Wabe at Gibe confluence	Megecha at gibe confluence	Great gibe at Abelti	Outflow from Abelti Catchment
Jan	49.52672846	12.36596715	3383.330626	3445.223321
Feb	36.08399731	8.778722628	3069.150861	3114.013581
Mar	89.56024392	15.14329653	3628.841713	3733.545253
Apr	61.33883862	14.06266697	3437.928658	3513.330163
May	339.3763777	119.831792	5421.467113	5880.675283
Jun	1107.878887	251.6685985	9368.788437	10728.33592
Jul	3666.66059	481.466146	16083.59593	20231.72266
Aug	4519.94602	598.8871314	14697.68284	19816.51599
Sep	1781.313902	253.1235493	10613.80294	12648.2404
Oct	280.2804238	61.8632573	7317.74213	7659.885811
Nov	97.47281665	22.27545164	4353.398147	4473.146416
Dec	57.55488161	15.04526004	7297.082737	7369.682879

2002

Date	Wabe at Gibe confluence	Megecha at gibe confluence	Great gibe at Abelti	Outflow from Abelti Catchment
Jan	79.93672866	17.95850365	1654.759394	1752.654627
Feb	40.61350006	10.16460219	938.8573375	989.6354398
Mar	74.04851921	18.28046442	1254.570296	1346.899279
Apr	56.80933587	13.08564416	1590.032599	1659.927579
May	73.54038189	21.9824562	1236.800775	1332.323613
Jun	411.8244726	68.27684945	4411.927362	4892.028684
Jul	1396.129153	181.0143641	8447.152768	10024.29629
Aug	2687.746538	262.9542815	10912.00055	13862.70137
Sep	834.3760572	89.33915165	8606.384883	9530.100092
Oct	147.8315158	20.79603127	3466.582285	3635.209832
Nov	55.2526447	9.067665636	1966.763928	2031.084239
Dec	46.61431026	7.897220442	2084.615492	2139.127023

2003

Date	Wabe at Gibe confluence	Megecha at gibe confluence	Great gibe at Abelti	Outflow from Abelti Catchment
Jan	40.2376034	6.971208332	1786.95472	1834.163532
Feb	28.89093869	5.14511534	848.7072587	882.7433127
Mar	45.14612661	7.538671811	1528.537056	1581.221854
Apr	134.1836555	28.14969518	1633.651277	1795.984628
May	70.73729651	14.24091515	1012.024838	1097.003049
Jun	184.4163616	24.14594343	3642.167185	3850.72949
Jul	3032.08142	226.9845684	11511.65028	14770.71627
Aug	3707.410496	405.4199042	14074.13856	18186.96896
Sep	1137.605962	200.4345027	13216.499	14554.53946
Oct	281.4612184	61.07673723	5731.423	6073.960956
Nov	122.3403074	15.60005748	1563.986	1701.926365
Dec	53.43459601	10.04094252	902.237	965.7125385

Appendix B: Daily Precipitation Temperatures and Solar Radiation Data (2000 - 2012) Input

Station	Jimma	Mean Monthly precipitation										
Year	Jan.	Feb.	Mar.	Apr.	May.	Jun.	Jul.	Aug.	Sep.	Oct.	Nov.	Dec.
2000	3.94	3.95	4.16	3.75	3.69	3.49	3.42	3.36	3.61	3.69	3.63	3.66
2001	3.62	3.86	3.72	3.93	3.79	3.47	3.36	3.46	3.75	3.8	3.73	3.82
2002	3.7	3.91	3.89	3.96	3.81	3.55	3.45	3.51	3.56	3.73	3.65	3.57
2003	3.69	3.84	3.96	3.72	3.94	3.62	3.44	3.47	3.64	3.66	3.68	3.86
2004	3.8	3.83	3.94	3.83	3.61	3.48	3.44	3.52	3.59	3.53	3.61	3.66
2005	3.72	4.04	3.9	3.91	3.65	3.49	3.41	3.54	3.58	3.65	3.44	3.69
2006	3.78	3.77	3.85	3.78	3.66	3.61	3.47	3.44	3.61	3.59	3.39	3.29
2007	3.43	3.63	4.01	3.86	3.68	3.51	3.49	3.48	3.66	3.82	3.87	4.01
2008	4.05	4	3.98	3.97	3.76	3.61	3.43	3.53	3.58	3.33	3.21	3.25
2009	3.39	3.66	3.71	3.83	3.82	3.64	3.41	3.41	3.61	3.57	3.58	3.21
2010	3.44	3.54	3.81	3.86	3.58	3.55	3.45	3.47	3.58	3.55	3.38	3.65
2011	3.62	4.14	3.9	4.08	3.92	3.61	3.47	3.45	3.68	3.6	3.4	3.4
2012	3.69	3.48	3.97	3.83	3.85	3.55	3.38	3.45	3.54	3.44	3.67	3.68

Appendix C: Average Daily Dew Point Temperature and Wind for Period (2000 -2012)

Station	Jimma	Average Monthly Maximum Temperature										
Year	Jan	Feb	Mar	Apr	May	Jun	Jul	Aug	Sep	Oct	Nov	Dec
2000	31.0	32.6	33.4	29.7	28.5	26.9	25.8	25.4	27.3	27.2	28.2	28.8
2001	29.0	31.5	29.8	30.2	28.9	26.7	25.4	25.6	28.1	28.2	28.7	29.7
2002	28.8	31.3	30.0	30.7	29.3	26.3	25.8	25.6	26.9	27.8	28.3	27.7
2003	28.0	30.8	30.0	29.3	30.8	27.3	24.7	25.2	26.7	28.1	28.8	28.6
2004	29.8	30.2	30.4	29.4	28.4	26.1	25.1	25.3	26.4	27.1	28.2	27.9
2005	28.4	31.7	30.7	29.4	27.8	25.6	25.2	26.0	26.3	27.4	27.5	29.4
2006	30.3	31.2	29.9	28.9	27.5	27.3	25.6	24.7	26.0	27.7	27.8	27.7
2007	28.0	28.8	30.6	29.0	28.0	26.7	25.5	25.2	26.6	28.3	30.0	30.7
2008	31.4	31.4	32.6	30.2	28.4	27.0	24.8	25.7	25.8	26.9	26.6	28.3
2009	28.4	29.8	30.6	29.2	29.1	27.5	25.0	25.0	26.4	26.9	28.6	26.9
2010	28.5	28.6	29.1	29.4	27.8	26.9	25.1	25.1	26.2	26.2	28.5	26.5
2011	29.5	31.3	30.0	30.3	28.3	26.4	26.0	24.8	26.4	27.9	27.6	28.1
2012	30.3	31.7	31.6	29.5	29.1	26.3	24.9	24.9	25.9	27.9	28.0	28.0

Appendix D: Average Minimum Monthly Temperature

Station	Jimma	Average minimum Monthly Temperature										
Year	Jan	Feb	Mar	Apr	May	Jun	Jul	Aug	Sep	Oct	Nov	Dec
2000	11.3	10.1	12.1	12.1	13.4	13.1	13.4	12.8	13.2	13.4	11.2	10.6
2001	10.0	10.3	11.0	13.6	14.0	13.1	13.1	13.7	13.8	13.7	11.9	11.4
2002	11.0	10.9	12.7	13.3	13.8	13.8	13.7	14.3	13.0	13.2	11.3	10.8
2003	11.7	10.8	13.4	12.2	13.7	14.1	14.3	14.2	13.7	12.0	11.2	12.9
2004	11.0	11.2	12.7	13.3	12.4	13.7	14.3	14.7	13.8	11.9	11.1	11.5
2005	11.6	12.0	12.1	14.0	13.6	14.3	13.9	14.3	13.8	12.8	9.8	10.3
2006	10.3	9.7	12.3	13.3	13.9	14.0	14.3	14.5	14.4	11.9	9.0	7.7
2007	8.8	10.6	13.3	14.0	13.6	13.5	14.5	14.4	14.4	13.7	11.9	12.4
2008	12.0	11.8	11.0	14.0	14.1	14.2	14.5	14.4	14.3	9.8	8.3	6.8
2009	8.1	9.9	10.2	13.5	14.1	14.0	14.1	13.9	14.1	12.4	10.3	7.7
2010	8.6	9.8	12.7	13.6	12.7	13.8	14.4	14.4	14.0	12.8	8.2	12.7
2011	9.5	13.3	12.7	15.1	16.0	14.9	14.9	14.4	14.8	11.7	9.4	8.5
2012	9.4	6.1	11.9	13.2	14.4	14.3	13.8	14.3	13.8	10.0	11.8	11.6

Appendix E: River cross section profile

X	Y
-300	1249.508
-280	1239.904
-260	1230.64
-240	1223.529
-220	1215.92
-200	1211.484
-180	1205.84
-160	1200.34
-140	1194.206
-120	1186.059
-100	1177.837
-80	1170.128
-60	1160.863
-40	1151.433
-20	1144.679
0	1140.584
20	1141.735
40	1147.125
60	1156.219
80	1168.77
100	1182.382
120	1194.331
140	1204.619
160	1213.082
180	1221.759
200	1228.837
220	1233.75
240	1237.875
260	1239.897
280	1240.433
300	1240.282
320	1239.828
340	1238.076
360	1236.723
380	1236.295
400	1236.891
420	1237.097
440	1238.201
460	1238.88
480	1241.596
500	1244.404

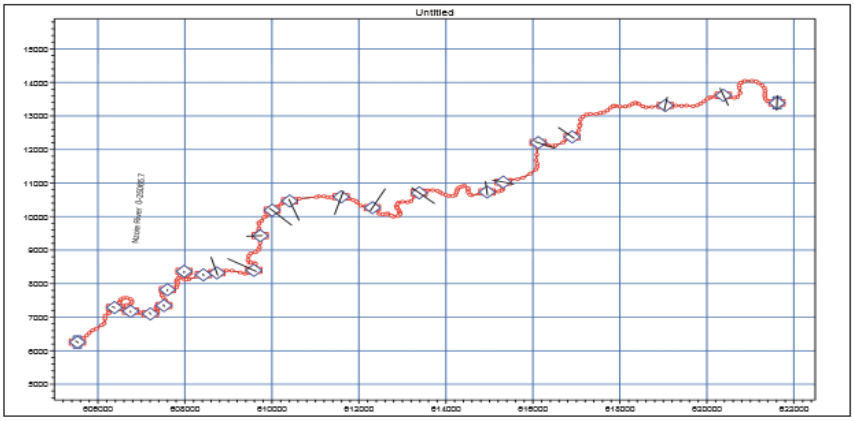

River Network defined by XT coordinate data point

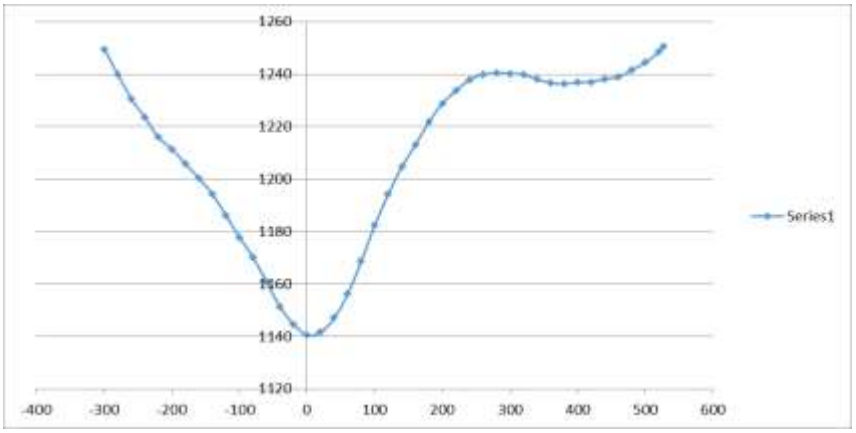

Microsoft Excel plotting River cross section on upper Gibe River

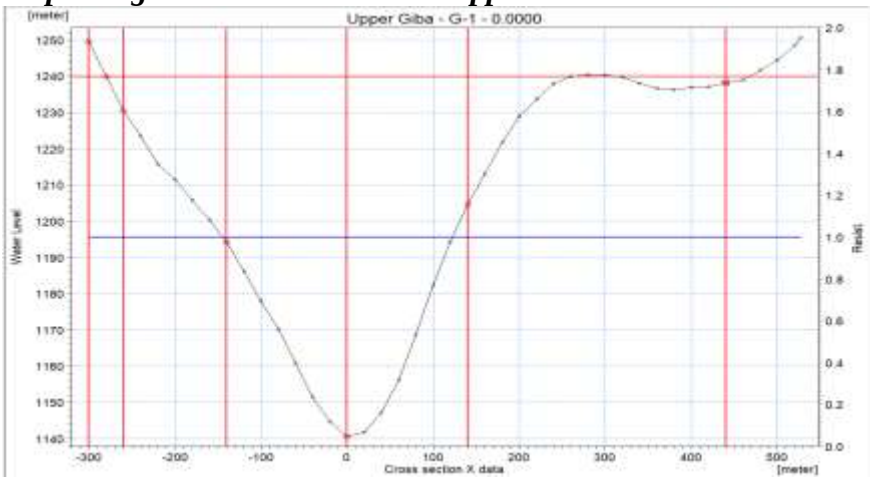

Mike11 plotting River cross section on upper Giba Rive

Appendix F: Graph between EI, RSME and SEE against the non-sensitive model parameter.

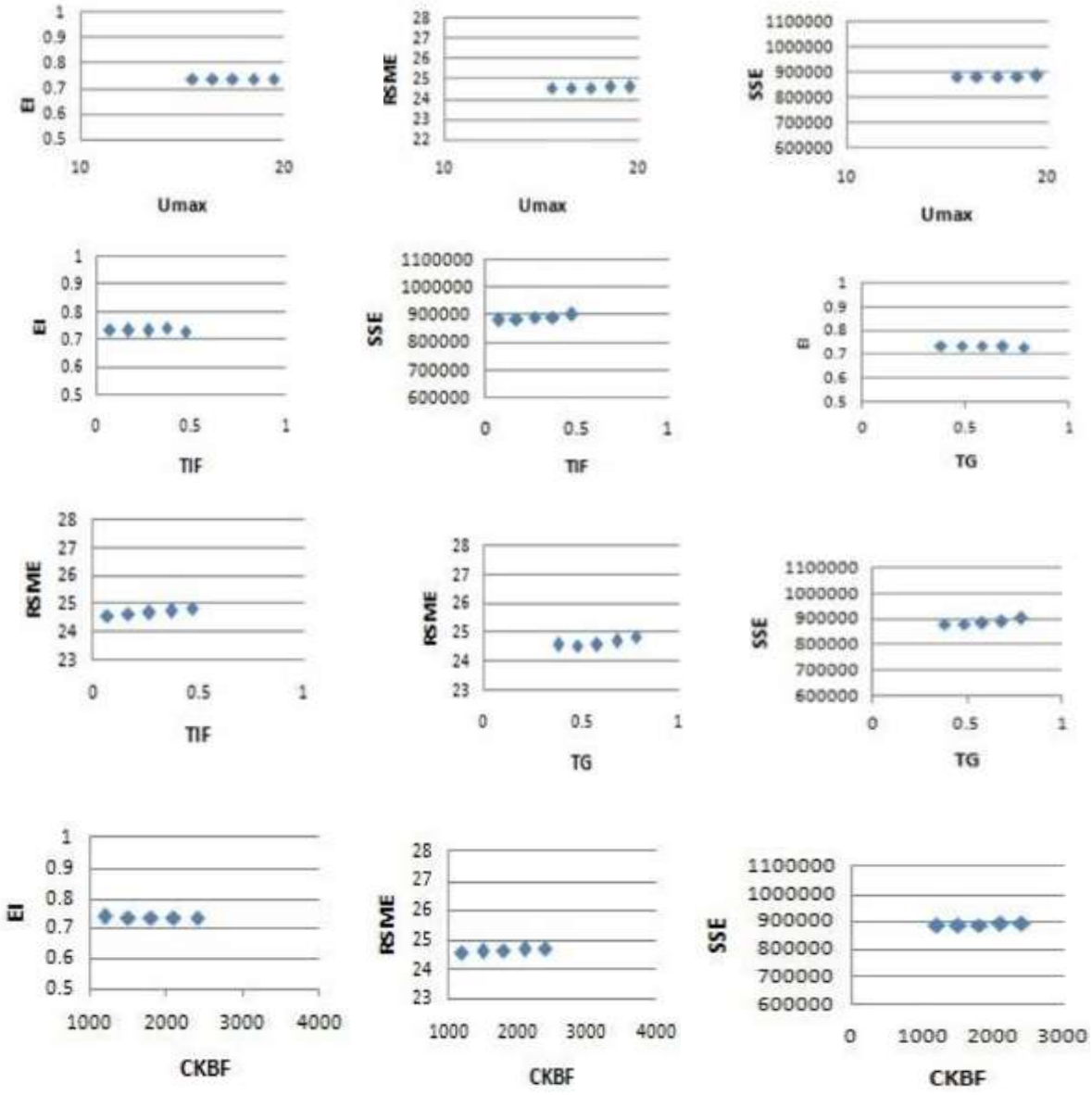

Appendix G: Model Sensitivity Analysis illustrates the final values of parameters that has been adjusted in the calibration process (Auto calibration)

Trial	WBL	RMSE	Agg_Obj	Umax	Lmax	CQOF	CKIF	CK1	TOF	TIF
1	31.544	75.489	91.167	10.000	100.000	0.500	1000.000	10.000	0.000	0.000	0.000
2	30.384	88.005	101.195	10.518	266.857	0.820	856.339	29.703	0.478	0.569	0.129
3	30.488	73.783	89.161	14.650	220.699	0.488	691.261	10.407	0.181	0.750	0.893
4	30.699	59.601	77.970	12.788	250.325	0.219	248.201	25.487	0.305	0.428	0.562
5	31.282	85.522	99.499	11.640	162.046	0.760	838.964	32.032	0.641	0.814	0.632
6	28.697	52.881	71.597	12.573	128.903	0.236	937.409	17.400	0.081	0.671	0.114
7	31.470	68.780	85.650	17.944	157.145	0.493	596.803	33.030	0.902	0.094	0.295
8	30.675	72.477	88.191	19.326	246.904	0.547	335.486	28.085	0.981	0.822	0.986
9	31.891	93.719	106.919	10.420	175.525	0.924	250.022	40.179	0.027	0.082	0.814
10	30.787	58.441	77.144	18.454	132.881	0.320	796.219	26.102	0.621	0.942	0.178
11	31.664	59.309	78.374	18.409	130.846	0.242	684.547	27.233	0.562	0.285	0.549
12	30.832	70.842	86.943	19.657	228.104	0.563	446.921	38.687	0.142	0.601	0.470
13	29.481	50.952	70.726	13.014	103.930	0.172	457.168	11.826	0.734	0.844	0.027
14	30.343	82.569	96.483	15.371	262.296	0.689	621.973	23.415	0.237	0.471	0.730
15	31.094	94.932	107.606	13.166	226.782	0.899	494.059	31.533	0.853	0.073	0.828
16	30.124	55.497	74.495	12.060	155.061	0.256	569.121	16.945	0.378	0.398	0.942
17	30.402	101.216	112.880	10.721	296.268	0.910	942.388	20.601	0.925	0.058	0.762
18	30.080	73.597	88.779	15.563	208.446	0.545	977.713	18.994	0.596	0.581	0.779
19	31.478	84.472	98.699	16.736	192.037	0.604	866.560	11.062	0.790	0.136	0.170
20	29.873	53.482	72.835	17.324	182.124	0.207	317.433	27.413	0.087	0.634	0.504
21	31.494	79.762	94.708	18.268	147.968	0.708	399.542	35.920	0.105	0.065	0.894
22	30.651	54.948	74.441	13.937	166.837	0.256	879.688	47.841	0.318	0.409	0.189
23	31.802	79.693	94.816	18.556	106.921	0.708	883.016	38.667	0.430	0.129	0.206
24	30.264	66.013	82.712	18.619	192.349	0.499	572.215	35.278	0.288	0.102	0.232
25	31.782	87.848	101.757	15.785	133.402	0.864	703.280	43.669	0.218	0.389	0.207
26	29.487	67.314	83.293	13.563	251.163	0.486	986.595	25.711	0.838	0.082	0.799
27	30.412	62.318	79.886	10.720	130.316	0.422	400.963	34.843	0.938	0.191	0.713
28	30.457	54.101	73.687	13.035	142.203	0.244	664.511	30.960	0.140	0.627	0.020
29	29.179	70.146	85.422	10.650	289.569	0.507	588.643	18.675	0.087	0.025	0.266
30	30.058	99.804	111.462	10.909	294.605	0.813	565.380	10.989	0.435	0.331	0.695
31	31.031	104.037	115.690	14.460	229.621	0.914	808.059	16.869	0.961	0.475	0.765
32	30.566	67.905	84.409	17.505	124.335	0.534	626.757	38.404	0.588	0.700	0.685
33	30.985	103.494	115.182	14.470	250.662	0.952	500.363	17.087	0.512	0.620	0.377
34	31.218	79.596	94.419	19.710	113.402	0.708	899.221	36.496	0.193	0.090	0.363
35	29.984	76.652	91.276	15.159	214.360	0.686	817.404	41.894	0.776	0.954	0.981
36	31.751	99.414	111.880	10.732	176.275	0.955	316.987	29.907	0.289	0.114	0.656
37	32.102	77.794	93.391	10.727	104.120	0.678	324.749	40.840	0.729	0.307	0.011
38	29.416	63.366	80.093	11.134	297.268	0.480	685.008	47.024	0.927	0.054	0.613

Appendix H: **Rainfall Runoff Summary on the case of Asendabo with total water balance and Error.**

Rainfall Runoff Summary

Continuity Balance

	Volume [m^3]
(1) Start volume	0.000
(2) Total inflow	16,718,863,773.9
- Net rainfall	16,718,863,773.9
- Added inflow	0.000
(3) Total loss	125,945.7
(4) Runoff discharge	15,527,699,221.5
Catchment Discharge	0.000
(5) End volume	1,191,313,600.6

(1+2) - (3+4+5) [m^3]	% of total inflow
-274,993.8	0.0

Rainfall Runoff Results Summary

Catchments - rainfall runoff per catchment

Catchment ID	Minimum [m^3/s]	Maximum [m^3/s]	Time of minimum	Time of maximum	Accumulated flow [m^3]
ASENDABO	0.00000	162.8	1/2/2006 3:00:00 PM	10/21/2007 3:00:00 PM	15,527,699,221.5
Total runoff					15,527,699,221.5

Catchments - continuity balance per catchment

Catchment ID	Start volume (1) [m^3]	Total inflow (2) [m^3]	Total losses (3) [m^3]	Total runoff (4) [m^3]	End volume (5) [m^3]	Balance [m^3]	% of total inflow
ASENDABO	0.000	16,718,863,773.9	125,945.7	15,527,699,221.5	1,191,313,600.6	-274,993.8	0.0
Total	**0.000**	**16,718,863,773.9**	**125,945.7**	**15,527,699,221.5**	**1,191,313,600.6**	**-274,993.8**	**0.0**

Note: Balance is (1+2)-(3+4+5)

Appendix I: Thiessen polygon area ratio of the Great Gibe watershed

S.No	Station	Thiessenpoly area ratio	Latitude	Longitude	Elevation(m)	Type
1	Asendabo	0.11	7.77	37.53	1764	Recording
2	Bako	0.17	7.5	36.52	1650	Recording
3	Jimma	0.21	7.4	36.5	1725	Recording
4	Limu Genet	0.13	8.05	36.57	1690	Recording
5	Sekoru	0.11	7.34	37.5	2100	Recording
6	Shebe	0.06	7.55	37.25	1813	Recording
7	Woliso	0.1	8.33	37.59	1960	Recording
8	Wolkite	0.1	8.27	37.75	1550	Recording

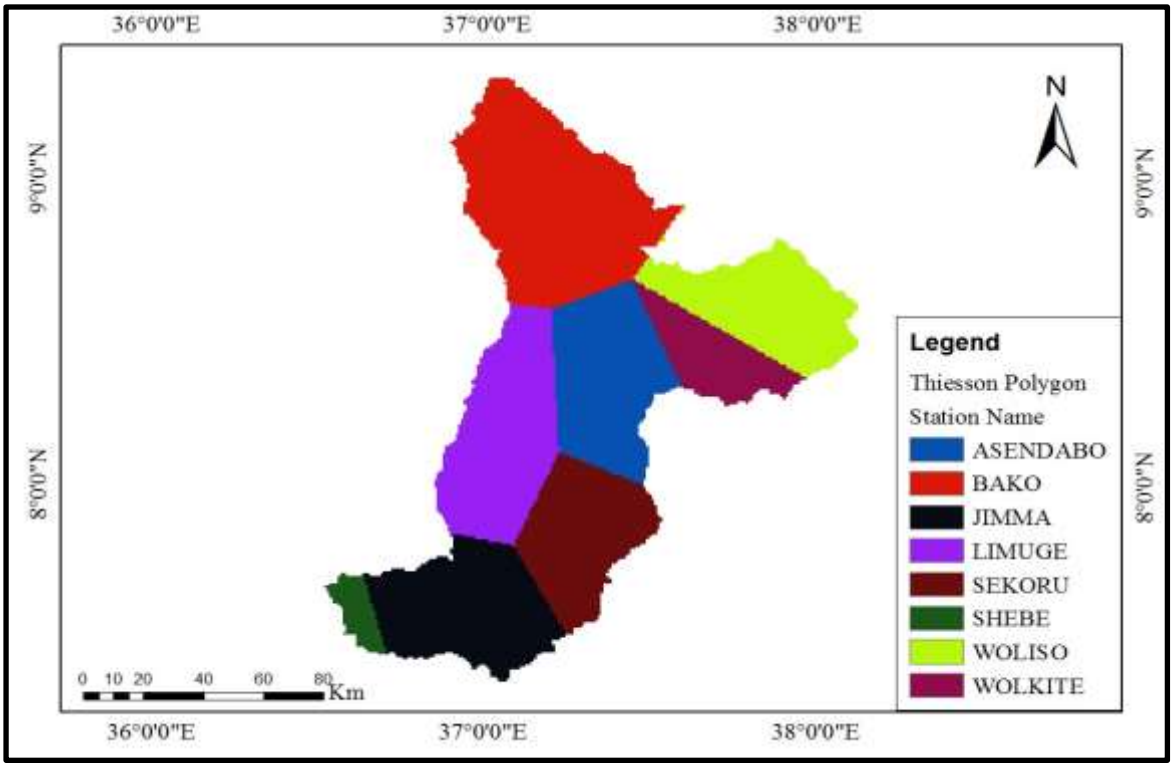

Appendix J: TRMM rainfall and Gauge Discharge Time series data generated by the model(dfs0).

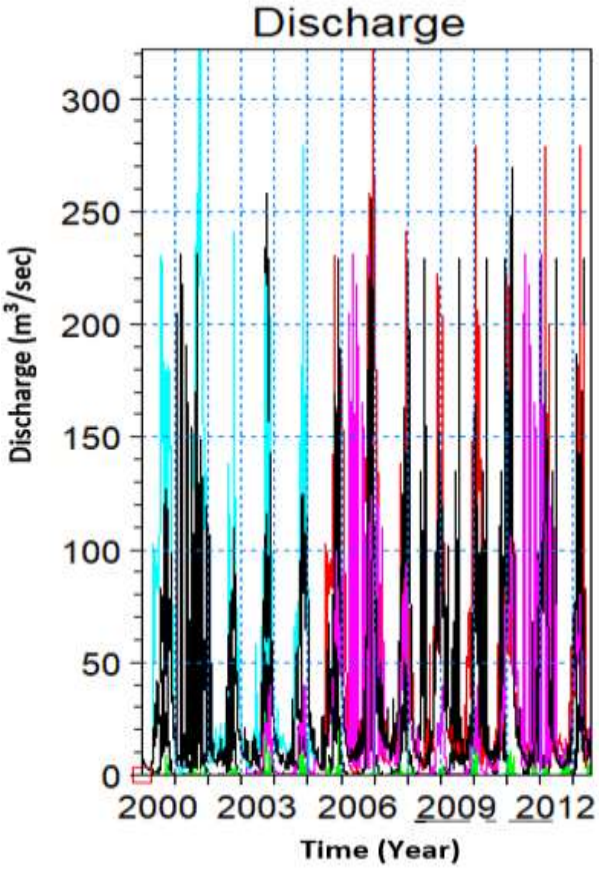

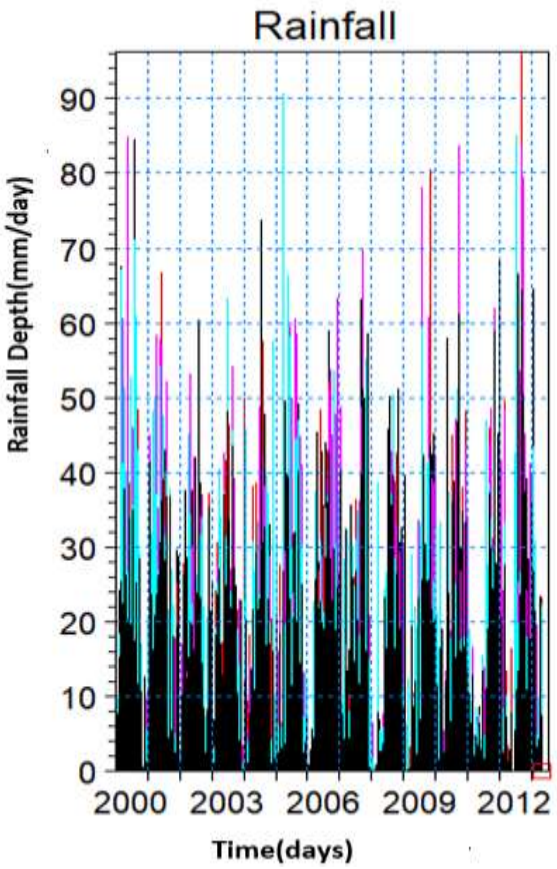

Appendix J: Model Plot Hydrographs comparing simulated and observed discharge against TRMM3B42_7 rainfalls at daily time scale for calibration (Jan.2000–Dec.2005) and validation (Jan.2006–Dec.2012)

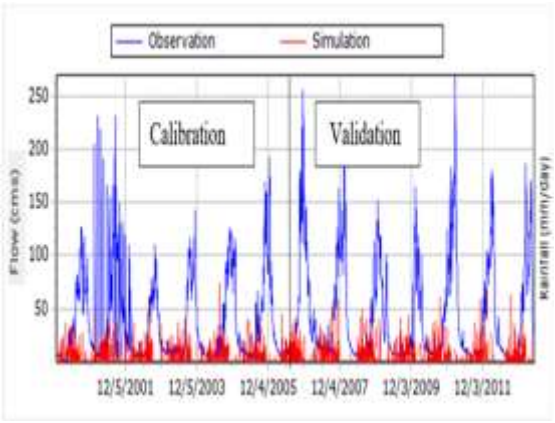

(a)

Hydrograph on simulated discharge vs rainfall at Limugenet (RR03)

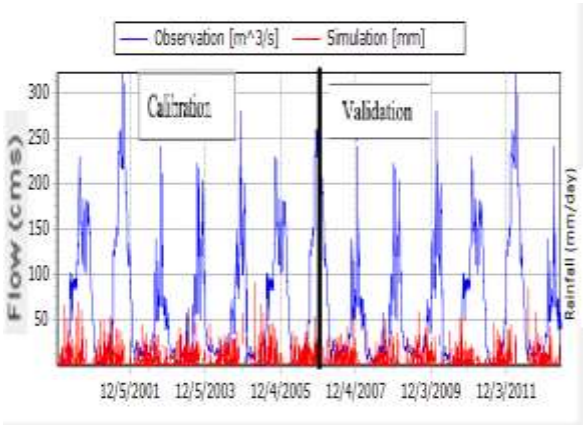

(b)

Hydrograph on simulated discharge vs rainfall at Sekoru (RR04)

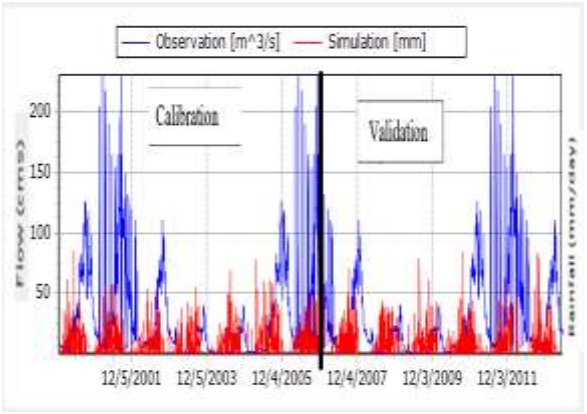

(c)

Hydrograph on simulated discharge vs rainfall at Shebe (RR05)

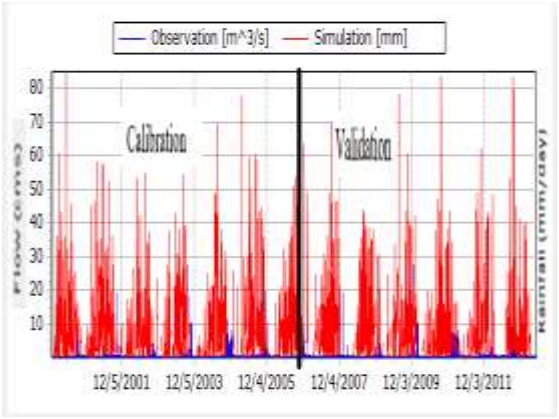

(d)

Hydrograph on simulated discharge vs rainfall at Welkite (RR006)

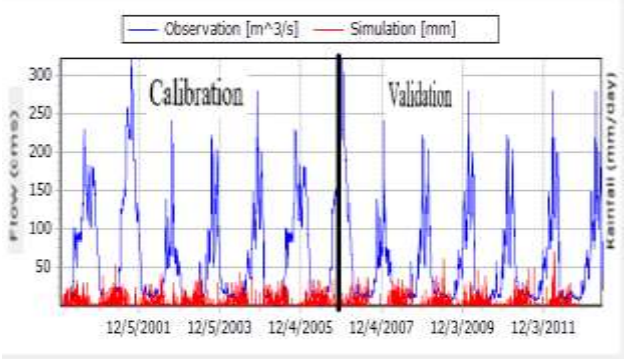

(e)

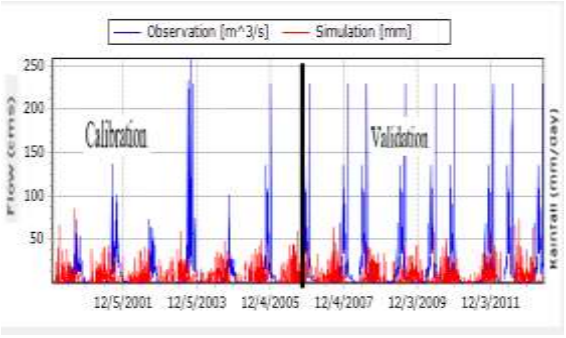

(f)